



**NAVAL
POSTGRADUATE
SCHOOL**

MONTEREY, CALIFORNIA

THESIS

**UNMANNED AERIAL VEHICLE-MOUNTED HIGH
SENSITIVITY RF RECEIVER TO DETECT IMPROVISED
EXPLOSIVE DEVICES**

by

Christopher M. Griffith

September 2007

Thesis Advisor:
Second Reader:

Lonnie A. Wilson
Ray A. Elliott

Approved for public release; distribution is unlimited

THIS PAGE INTENTIONALLY LEFT BLANK

REPORT DOCUMENTATION PAGE

Form Approved OMB No. 0704-0188

Public reporting burden for this collection of information is estimated to average 1 hour per response, including the time for reviewing instruction, searching existing data sources, gathering and maintaining the data needed, and completing and reviewing the collection of information. Send comments regarding this burden estimate or any other aspect of this collection of information, including suggestions for reducing this burden, to Washington headquarters Services, Directorate for Information Operations and Reports, 1215 Jefferson Davis Highway, Suite 1204, Arlington, VA 22202-4302, and to the Office of Management and Budget, Paperwork Reduction Project (0704-0188) Washington DC 20503.

1. AGENCY USE ONLY (Leave blank)	2. REPORT DATE September 2007	3. REPORT TYPE AND DATES COVERED Master's Thesis	
4. TITLE AND SUBTITLE Unmanned Aerial Vehicle-mounted High Sensitivity RF Receiver to Detect Improvised Explosive Devices.		5. FUNDING NUMBERS	
6. AUTHOR(S) Capt Christopher Michael Griffith			
7. PERFORMING ORGANIZATION NAME(S) AND ADDRESS(ES) Naval Postgraduate School Monterey, CA 93943-5000		8. PERFORMING ORGANIZATION REPORT NUMBER	
9. SPONSORING /MONITORING AGENCY NAME(S) AND ADDRESS(ES) N/A		10. SPONSORING/MONITORING AGENCY REPORT NUMBER	
11. SUPPLEMENTARY NOTES The views expressed in this thesis are those of the author and do not reflect the official policy or position of the Department of Defense or the U.S. Government.			
12a. DISTRIBUTION / AVAILABILITY STATEMENT Approved for public release; Distribution is unlimited		12b. DISTRIBUTION CODE	
13. ABSTRACT (maximum 200 words) Improvised Explosive Devices (IEDs) are increasing in complexity and lethality. A RF system is needed to detect the presence of RF IEDs. This thesis describes the evolution of a proven ground based RF detection system. It is designed to collect unintended radio frequency emissions from the IED's RF triggers and receivers. Modification of the ground based version allowed placing this RF system into an airborne platform. The detection range and corresponding time to react to a possible threat is dramatically improved. Increased time provides greater protection for the front line troops that are primary targets of RF IEDs, hence reducing the casualties of U.S. troops. Field testing and technical feasibility demonstrations are conducted using a NPS owned TERN UAV at McMillan Airfield located at Camp Roberts, CA. The research conducted for this thesis primarily deals with the implementation and testing of this RF system onto UAVs. Several additional benefits make this RF system useable over a wide range of applications.			
14. SUBJECT TERMS Improvised Explosive Devices, IEDs, Unmanned Aerial Vehicles, UAVs, Unintended RF Emissions, Remote Detection		15. NUMBER OF PAGES 164	
			16. PRICE CODE
17. SECURITY CLASSIFICATION OF REPORT Unclassified	18. SECURITY CLASSIFICATION OF THIS PAGE Unclassified	19. SECURITY CLASSIFICATION OF ABSTRACT Unclassified	20. LIMITATION OF ABSTRACT UU

NSN 7540-01-280-5500

Standard Form 298 (Rev. 2-89)
Prescribed by ANSI Std. Z39-18

THIS PAGE INTENTIONALLY LEFT BLANK

Approved for public release; distribution is unlimited

**UNMANNED AERIAL VEHICLE-MOUNTED HIGH SENSITIVITY RF RECEIVER
TO DETECT IMPROVISED EXPLOSIVE DEVICES**

Christopher M Griffith
Captain, United States Marine Corps
B.S., University Of Tennessee, 1996

Submitted in partial fulfillment of the
requirements for the degree of

MASTER OF SCIENCE IN INFORMATION WARFARE SYSTEMS ENGINEERING

from the

**NAVAL POSTGRADUATE SCHOOL
September 2007**

Author: Christopher M. Griffith

Approved by: Dr. Lonnie A. Wilson
Thesis Advisor

Mr. Ray A. Elliott
Second Reader

Dr. Dan C. Boger
Chairman, Department of Information Sciences

THIS PAGE INTENTIONALLY LEFT BLANK

ABSTRACT

Improvised Explosive Devices (IEDs) are increasing in complexity and lethality. A RF system is needed to detect the presence of RF IEDs. This thesis describes the evolution of a proven ground-based RF detection system. It is designed to collect unintended radio frequency emissions from the IED's RF triggers and receivers. Modification of the ground-based version allowed placing this RF system into an airborne platform. The detection range and corresponding time to react to a possible threat is dramatically improved. Increased time provides greater protection for the front line troops that are primary targets of RF IEDs, hence reducing the casualties of U.S. troops. Field testing and technical feasibility demonstrations are conducted using a NPS-owned TERN UAV at McMillan Airfield located at Camp Roberts, CA. The research conducted for this thesis primarily deals with the implementation and testing of this RF system onto UAVs. Several additional benefits make this RF system useable over a wide range of applications.

THIS PAGE INTENTIONALLY LEFT BLANK

TABLE OF CONTENTS

I.	BACKGROUND	1
A.	WHY IEDS	1
B.	THE IED PROBLEM	3
C.	LOCATING IEDS	7
D.	THE HIGH SENSITIVITY RF RECEIVER	9
E.	CONCLUSION	10
II.	SYSTEM OVERVIEW	11
A.	OVERVIEW	11
B.	ANTENNA	12
C.	PREAMPLIFIER	13
D.	RECEIVER	14
E.	PICOSCOPE	16
F.	SINGLE BOARD COMPUTER	17
G.	CONCLUSION	18
III.	ANTENNA MODELING	19
A.	ANTENNA BACKGROUND	19
B.	ANTENNA THEORY	19
C.	ANTENNA SELECTION	20
D.	ANTENNA TESTING	22
E.	CONCLUSION	30
IV.	TESTING	31
A.	CAMP ROBERTS	31
B.	THE TERN UAV	33
C.	SIMULATED THREAT SYSTEM	35
D.	COHERENT INTEGRATION	38
E.	ANTENNA MOUNTING	40
F.	LOSSES	43
G.	TESTING SCENARIOS	45
H.	CONCLUSION	47
V.	RESULTS	49
A.	CONDITIONS	49
B.	DATA FORMAT	53
C.	SOURCES OF VARIABILITY	56
D.	IED ANALYSIS METHOD	61
E.	SINGLE IED ANALYSIS	64
1.	Area of Interest 1	65
2.	Area of Interest 2	67
3.	Area of Interest 3	69
4.	Single IED Alternate Flight Profiles	71
5.	Single IED Conclusion	73
F.	MULTIPLE IED ANALYSIS	73

1.	Area of Interest 1	75
2.	Area of Interest 2	77
3.	Area of Interest 3	82
4.	Multiple IEDs Conclusion	85
G.	POWER SPECTRAL FILTERING	86
H.	CONCLUSION	89
VI.	FUTURE DEVELOPMENT	91
A.	SCAN EAGLE	91
B.	TROOP PORTABLE UNIT	93
C.	ACTIVE DETECTION	96
D.	JAMMER INCORPORATION	98
E.	CONCLUSION	99
APPENDIX A.	ANTENNA LAB VOLT RESULTS	101
APPENDIX B.	TERN DATA	105
LIST OF REFERENCES	145	
INITIAL DISTRIBUTION LIST	147	

LIST OF FIGURES

Figure 1.	DoD Casualties by reason Oct 2001 through Aug 2007. (From Defense Manpower Data Center).....	4
Figure 2.	Common initiating device. (From Kevin Kelly).....	6
Figure 3.	Typical IED emplacement as a roadside bomb. (From Lt Doug Thorlakson).....	8
Figure 4.	Component block diagram for High Sensitivity RF Receiver.....	12
Figure 5.	LPY41 log periodic antenna. (From Ramsey Electronics)	13
Figure 6.	LN1000A Amplifier.....	14
Figure 7.	ICOM PCR1000 Receiver. (From ICOM America).....	15
Figure 8.	Pico Scope 3205. (From Picotech).....	16
Figure 9.	Single Board Computer.....	18
Figure 10.	Equation for power spectral density of a transmitted signal.....	21
Figure 11.	GNEC display of LPY41 antenna.....	23
Figure 12.	E-plane and H-plane for the LPY41 Antenna.....	26
Figure 13.	E and H plane for LPY41 antenna compared to known Dipole antenna.....	27
Figure 14.	Excel plot of tabulated data.....	28
Figure 15.	Equation for Directivity as a function of the principle plane beamwidths in degrees.....	29
Figure 16.	3-Dimensional antenna pattern for LPY41.....	30
Figure 17.	McMillan overhead picture. (From McMillan Homepage).....	32
Figure 18.	TPC showing area surrounding McMillan Airfield. (From McMillan Homepage).....	33
Figure 19.	Motorola radios models T4500 and FV-200. (from Motorola).....	35
Figure 20.	Frequency vs. Time Plot for each Handset.....	36
Figure 21.	Temperature vs. Time Plot for each Handset.....	37
Figure 22.	Equation for the signal to noise ratio improvement for n-pulses coherently integrated..	38
Figure 23.	Antenna geometry.....	41
Figure 24.	Determining Free Space Loss in dB.....	43
Figure 25.	The four testing scenarios.....	46
Figure 26.	Final TERN configuration on test day.....	50
Figure 27.	TERN in flight during testing.....	51
Figure 28.	TERN internal circuit systems.....	53
Figure 29.	Frequency plotted versus Time.....	55
Figure 30.	Power Spectral Density plotted versus Frequency.....	56
Figure 31.	Basic Signal Equation.....	56

Figure 32.	Signal Equation with Doppler frequency.....	57
Figure 33.	Geometry for Doppler frequency Shift.....	57
Figure 34.	Equation for Doppler Frequency.....	58
Figure 35.	Simplified block diagram of the ICOM local oscillators.....	60
Figure 36.	Sample single pass with all factors.....	62
Figure 37.	Sample single pass plot with only two factors...	63
Figure 38.	Ground Station Display.....	64
Figure 39.	Single Pass Plot with one IED.....	65
Figure 40.	PSD-Plots for data records 300 to 303.....	66
Figure 41.	PSD-Plots for data records 304 to 307.....	67
Figure 42.	PSD-Plots for data records 328 to 331.....	68
Figure 43.	PSD-Plots for data records 332 to 335.....	69
Figure 44.	PSD-Plots for data records 336 to 339.....	70
Figure 45.	PSD-Plots for data records 340 to 343.....	70
Figure 46.	PSD-Plots for data records 344 to 347.....	71
Figure 47.	Single Pass Plot with 4 IEDs.....	74
Figure 48.	PSD-Plots for data records 701 to 704.....	75
Figure 49.	PSD-Plots for data records 705 to 708.....	76
Figure 50.	PSD-Plots for data records 709 to 712.....	77
Figure 51.	PSD-Plots for data records 728 to 731.....	78
Figure 52.	PSD-Plots for data records 732 to 735.....	79
Figure 53.	PSD-Plots for data records 736 to 739.....	79
Figure 54.	PSD-Plots for data records 740 to 743.....	80
Figure 55.	PSD-Plots for data records 744 to 747.....	81
Figure 56.	PSD-Plots for data records 748 to 751.....	82
Figure 57.	PSD-Plots for data records 768 to 771.....	82
Figure 58.	PSD-Plots for data records 772 to 775.....	83
Figure 59.	PSD-Plots for data records 776 to 779.....	84
Figure 60.	PSD-Plots for data records 780 to 783.....	85
Figure 61.	Unfiltered Power Spectral Density Plot.....	87
Figure 62.	Filtered Power Spectral Density Plot.....	88
Figure 63.	Scan Eagle UAV. (From Boeing)	93
Figure 64.	CrossMatch PIV system. (from CrossMatch Technologies).....	94
Figure 65.	Characteristics of common Artillery rounds (from the USMC FAC Handbook)	95
Figure 66.	Standard Radar block diagram.....	97

LIST OF TABLES

Table 1.	YP41 dimensions.....	22
Table 2.	Example of tabulated data from LPY-41 and Reference Dipole.....	25
Table 3.	McMillan Aeronautical Information.....	32
Table 4.	Comparison of TERN and Scan Eagle UAV.....	34
Table 5.	Tabulated Antenna Angle and Ranges.....	42
Table 6.	Free Space Loss in dB of a signal as a function of Range and Frequency.....	44
Table 7.	Loss in Decibel and effect on detection range.....	45
Table 8.	Testing conditions.....	49
Table 9.	Simulated IED center frequencies.....	51
Table 10.	Sample of collected data.....	54
Table 11.	Family Radio Services channels.....	59
Table 12.	Table of Frequencies for four IED pass.....	74

THIS PAGE INTENTIONALLY LEFT BLANK

ACKNOWLEDGMENTS

Freedom is never more than one generation away from extinction. We didn't pass it to our children in the bloodstream. It must be fought for, protected, and handed on for them to do the same.

—Ronald Reagan, 40th President of the United States

I would like to thank Professor Wilson for his guidance during this thesis process. I would like to thank LtCol Ray Elliott USAF(ret) for his help throughout my two years at the Naval Postgraduate School in Monterey. Knowing there is light at the end of the tunnel helped immensely. Additionally I would like to thank Jim Horning and David Rigmaiden for their help in successfully testing the High Sensitivity RF Receiver. Lastly, I thank the Mike D for running all those long miles with me that kept me sane.

THIS PAGE INTENTIONALLY LEFT BLANK

I. BACKGROUND

A. WHY IEDS

Improvised Explosive Devices (IEDs) can come in almost any size. They are made from homemade explosive compounds whose construction can be found on the Internet. IEDs can also be military explosives such as artillery shells that are using improvised detonators. IEDs can be detonated by using many methods. The form of an IED is only limited by the imagination and skill of the person making it. The question to ask is: Why are artillery shells being used against U.S. troops in the form of an IED and not as a projectile fired from artillery as it is intended? The answer to this question gives insight into the new form of combat that U.S. troops will be fighting for the foreseeable future, and a glimpse into the dangers that they face.

In the ever-evolving world of combat, the United States has taken and maintained a commanding lead in third-generation warfare or maneuver warfare. Now the U.S. is leaping into the fourth-generation of warfare with information dominance. No country is currently able to attain parity with the United States, and so the rules of combat have changed. Few adversaries are willing to attack the United States head-on and suffer the inevitable casualties. In his article, "Chaos as Strategy,"¹ P. H. Liotta states,

¹ Liotta, P.H., Chaos as Strategy, *Parameters*, Vol.XXXII, No. 2, Summer 2002, pp. 47-56.

Adversaries who do not practice a similar process of decision making [U.S. method] – balancing resources and constraints, means and ends – will increasingly look for innovative ways to “attack” without attacking directly the brick wall of American military predominance. The chaos strategist thus targets the American national security decision-making process and, potentially, the American people, rather than American military force, in order to prevail. Such a strategist seeks to induce decision paralysis.

This strategy attacks at the perceived Achilles’ heel of the U.S., that our public is unwilling to take casualties. While this strategy will not defeat the U.S. in any traditional way, the goal is making the cost, in terms of blood and treasure for the U.S. involvement in their area, higher than the U.S. public is willing to pay. This would than force the U.S. government to leave their area. This strategy relies on time being an advantage to our enemies; the longer the enemies can last, the greater chance they have for success – as long as they continue to cause U.S. casualties. This can be seen in the U.S. involvement in Somalia, where U.S. forces are withdrawn five months after the October 3, 1993, firefight in Mogadishu where 19 U.S. Servicemen lost their lives. The international press showed U.S. servicemen’s bodies being dragged in the streets of a foreign city. If the enemies of the U.S. cannot face our military might directly, they must do so indirectly, and so they will make an IED out of artillery shells, instead of launching them as projectiles from artillery pieces that would be located and destroyed.

B. THE IED PROBLEM

IEDs are not a new phenomenon, as seen in such attacks as the one on the Marine barracks in Beirut, Lebanon, which used a truck bomb and killed 241 U.S. Marines in 1983. From the U.S. Department of Defense manpower chart shown in Figure 1, the number of U.S. servicemen who have been killed or wounded in Operations Iraqi and Enduring Freedom due to explosive devices is over 21,000². This is almost seven times the number caused by gunshot, the second largest number.

² DoD personnel and Procurement Statistics, Defense Manpower Data Center, Casualty Reasons, October 7, 2001, through August 4, 2007, online at [http://siadapp.dmdc.osd.mil/personnel/CASUALTY/gwot_reason.pdf], June 2007.

CASUALTY REASON	GLOBAL WAR ON TERRORISM BY REASON						TOTALS
	OEF	OEF	OEF	OIF	OIF	OIF	
	HOSTILE	NON-HOSTILE	HOSTILE	HOSTILE	NON-HOSTILE	HOSTILE	
	DEATHS	DEATHS	WIA	DEATHS	DEATHS	WIA	
MEDICAL, CANCER			1			6	7
MEDICAL, HEART RELATED			8		1	38	49
MEDICAL, OTHER				1		3	3
MEDICAL, OTHER MEDICAL			1				1
MEDICAL, RESPIRATORY FAILURE			1		1	12	14
MEDICAL, STROKE			1			7	8
OTHER, BURNS/SMOKE INHALATION				6	18	6	76
OTHER, DEHYDRATION						2	2
OTHER, DROWNING			4		15	36	57
OTHER, DRUG AND/OR ALCOHOL OVERDOSE			1			6	7
OTHER, ELECTROCUTION					2	12	20
OTHER, EXPOSURE TO ELEMENTS						1	1
OTHER, FALL/JUMP	2	4	2	2	6	32	48
OTHER, FRACTURE OR BROKEN BONE				1		21	22
OTHER, LACERATION				4		79	83
OTHER, LOSS OF LIMB(S)	1				1	3	5
OTHER, MILITARY EXERCISE						1	1
OTHER, PARACHUTE ACCIDENT						8	8
OTHER PHYSICAL TRAINING -- MILITARY RELATED						1	1
OTHER, STAB WOUNDS				2		1	4
TRANSPORTATION, AIRCRAFT CRASH -- CREW (MC)	26	87	14	93	85	41	346
TRANSPORTATION, AUTOMOBILE ACCIDENT (PRIVATE)						2	2
TRANSPORTATION, PEDESTRIAN						2	2
TRANSPORTATION, VEHICLE CRASH (MC)	2	25	1	17	193	94	332
WEAPONRY, ARTILLERY/MORTAR/ROCKET	8		48	177	4	2,284	2,521
WEAPONRY, EXPLOSIVE DEVICE	94	12	801	1,898	15	18,803	21,623
WEAPONRY, GRENADE	1					70	71
WEAPONRY, GUNSHOT	77	22	333	613	146	2,119	3,310
WEAPONRY, NUCLEAR, CHEMICAL OR BIOLOGICAL AGENTS						14	14
WEAPONRY, OTHER						4	4
WEAPONRY, ROCKET PROPELLED GRENADE	5		72	27		413	517
NOT REPORTED/UNKNOWN/MISCELLANEOUS	21	14	188	148	68	3,189	3,624
TOTALS	237	181	1,472	3,013	647	27,279	32,829

OEF=OPERATION ENDURING FREEDOM; OIF=OPERATION IRAQI FREEDOM
 WIA=WOUNDED IN ACTION
 MC=MILITARY CONTROL
 DATA ARE SUBJECT TO CHANGE

Prepared by: Defense Manpower Data Center
Statistical Information Analysis Division

Figure 1. DoD Casualties by reason Oct 2001 through Aug 2007. (From Defense Manpower Data Center)

This disturbing trend only backs up the belief that attacking America is best done by IED and not the AK-47. From an article posted on GlobalSecurity.Org, an IED can be almost anything with any type of material and initiator. Generally, IEDs share a common set of components and consist of an initiation system or fuze, explosive fill, detonator, power supply for the detonator and a container. Improvised devices are characterized by varying employment techniques. In most of the techniques shown below, an IED can easily be

engineered to replace a mine or explosive device using one of the several following techniques:³

Coupling is a method of linking one mine or explosive device to another, usually with detonating cord. When the first device is detonated, it also detonates the linked explosive. This technique is often used to defeat countermine equipment, such as mine rollers.

Rolling is a method by which a clearing vehicle will pass over the initial, unfuzed device and set off the second fuzed device. This in turn detonates the over-passed device underneath the clearing vehicle. When the linked devices are directional fragmentation mines, they can create a large, lethal engagement area.

Boosting is a method by which buried mines, UXOs, or other explosive devices are stacked on top of one another. The device buried deepest from the surface is fuzed. Fuzing only the deepest ordnance helps mask no- and low-metal explosive hazards placed near the surface. This reduces the probability of detection by metal detectors, and it increases the force of the blast.

A common method used is called daisy chaining. AP mines may be used in daisy chains linked with other explosive hazards. Enemy forces may link the mines together with trip wire or detonating cord. When the initial mine is detonated, the other mines are detonated. This may also create large, lethal engagement areas.

³ Information derived from GlobalSecurity.org at [<http://www.globalsecurity.org/military/intro/ied.htm>], June 2007.

Testing will take into account a few of the above mentioned techniques. The most important component of an IED, and the focus for this thesis, is the initiation system or triggers. Triggering methods for IEDs may include using a cell phone, a garage door opener, or a child's remote-control toy, or may even be as simple as running over a rubber hose to produce enough air pressure to activate a switch for a mine. At other times, the insurgent may remain concealed and trigger an IED manually⁴. A picture of a common initiating device is shown below in Figure 2. Without the initiating device, the IED is rendered useless and is no longer a threat. There are two methods for effectively dealing with IEDs, either cut the signal, which causes detonation, or locate the IED and dispose of it before it detonates.



Figure 2. Common initiating device. (From Kevin Kelly)

⁴ Congressional Research Service Report for Congress found at [<http://www.history.navy.mil/library/online/ied.htm>], June 2007.

The first method is ideal for the subset of IEDs which are called Remote Control IEDs (RCIEDs) or RF IEDs. The Joint Improvised Explosive Device Defeat Organization has received \$6.7 billion in taxpayer dollars since 2003. This sum is for the sole purpose of eliminating the threat of improvised explosive devices⁵. Their primary means of accomplishing this task has been the development of high tech systems that preemptively suppress detonation signals. While these systems are having some successes, they do little to remove the threat. However, the second method of locating the IED and destroying it does. But first, you must locate it.

C. LOCATING IEDS

Locating an IED may sound easy in principle. Normally they are right next to the road. In practice, it is much more difficult. Many IEDs are buried next to the road with only the emitter or a command wire exposed, as shown in the picture below (Figure 3). This becomes somewhat easier when dealing with RCIEDs since they have Radio Frequency (RF) emission that can be detected.

⁵ Boston Globe Article found at
[http://www.boston.com/news/nation/washington/articles/2007/02/06/president_requests_boost_for_ied_fund/] August 2008.



Figure 3. Typical IED emplacement as a roadside bomb.
(From Lt Doug Thorlakson)

But even this becomes problematic since the only time the enemy will be communicating with the IED is when they intend to detonate it. At this time, it may be too late. However, the systems used generally are commercially developed, which gives them both advantages and disadvantages. Their advantages include ease of procurement, variety and low cost. However, they are designed for commercial use and not intended for military application. Therefore, they are designed for low cost manufacture and have little need or thought to shielding the equipment from unintended RF emissions as in military equipment. This disadvantage becomes our advantage when trying to locate a trigger for an IED, as the unintended emissions from the trigger will give the location of the IED away. Sounds easy, but it is not.

D. THE HIGH SENSITIVITY RF RECEIVER

Unintended RF emissions of the triggering systems involved for detonating IEDs are extremely weak compared to the RF transmitted emissions used in their normal operation. This makes them extremely difficult to differentiate from the general noise that is constantly present (the noise floor). One option for finding these low power signals is increasing the time which a receiver listens for a signal. This increased time allows for digital signal processing to pull the signal out of the noise. This works because the signal remains constant while the noise is random. The noise does not coherently integrate and increase in strength while the signals of interest will. This allows the signal to cross the threshold of signal detection. This process requires a greater number of samples to be taken over a longer integration period thereby increasing the strength of the real signal at a greater rate than the signal strength of the noise. A second process is to increase the sensitivity of the entire system. This increases the systems ability to discern the unintended emissions from the noise.

In 2005, Professor Lonnie Wilson from the Naval Postgraduate School developed a RF system which combines both techniques into an innovative detection system named the High Sensitivity RF Receiver. A prototype of this system was tested from a ground based vehicle with success against potential RF IEDs. After demonstrating the system's effectiveness in detecting the initiator of an IED system, the next logical step is to determine ways of increasing detection range. Because the system requires line of sight

with the IED, the easiest way to improve detection range is to package the system for employment on an Unmanned Arial Vehicle (UAV).

E. CONCLUSION

If the U.S. pulled its troops from both Iraq and Afghanistan, the threat of IEDs will continue to haunt our forces for the foreseeable future. The reasons for using IEDs will not change. In fact, as U.S. Military might increases, so will our enemies use of IEDs. It is imperative that new and innovative ways of dealing with this threat are found and demonstrated. The High Sensitivity RF Receiver is such a way and its implementation into UAV operations will enhance our nation's military capabilities.

II. SYSTEM OVERVIEW

A. OVERVIEW

The High Sensitivity RF Receiver is designed to locate signals in background noise. It finds high value signals with inherently low powered. With the signal strengths current threats are emitting, an optimal RF system is one specifically designed and built from the ground up to locate and identify them. It would also have a high cost of designing, making this system cost prohibitive at this early stage of development. In an effort to overcome this obstacle, commercially available equipment is modified and packaged to construct the front-end payload of the Tern UAV. This RF system is the one used for testing. The High Sensitivity RF Receiver is composed of five main subsystems which are shown below in Figure 4. The elements in blue are unique to the High Sensitivity RF Receiver while those in red are components of both the TERN and the system.

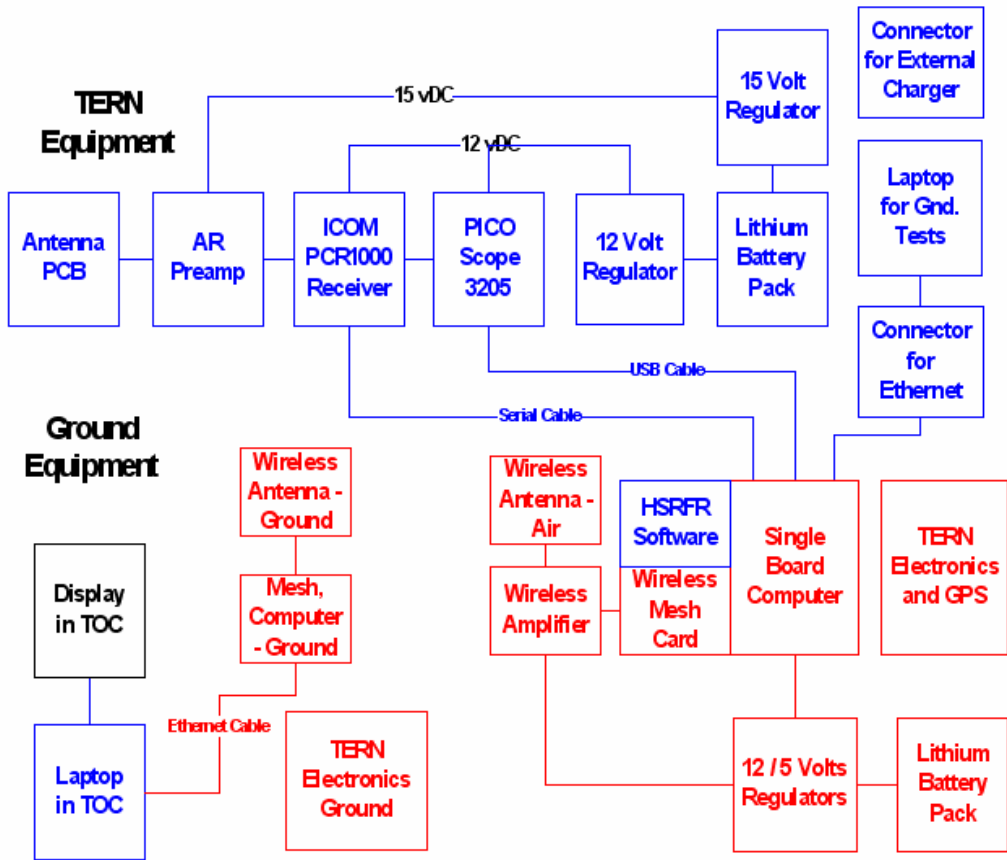


Figure 4. Component block diagram for High Sensitivity RF Receiver.

B. ANTENNA

The target signal first enters the system through the antenna. The antenna chosen for this system is a log periodic antenna. One of the most important factors in detecting the threat signal is selecting a reasonably high gain antenna, capable of being fitted onto a UAV. This proved challenging since the initial concept of the High Sensitivity RF Receiver involves a vehicle base for mounting. This ground version uses a standard Yagi antenna which provides gain and directivity, but is impractical for use on a UAV. The Ramsey Electronics Model LPY41 is chosen

for mounting on the UAV. It is shown below in Figure 5. Because little technical information is available on the characteristics of the LPY41, testing is conducted in order to obtain the required information. The Antenna will be discussed further in Chapter III.



Figure 5. LPY41 log periodic antenna. (From Ramsey Electronics)

C. PREAMPLIFIER

After the signal passes through the Antenna, it enters the preamplifier. When dealing with unintentional signals which may be as low as -160dB, it is essential to have a low noise, yet high gain amplifier in order to ensure the signal is processed. The Amplifier Research Model LN1000A amplifier is selected for this system. The LN1000A, show in Figure 6, requires a +15VDC power fed from the UAV package's lithium battery pack. The power is converted from the battery pack by a 15 volt regulator to the preamplifier. The Amplifier contains two connection ports, RF IN and RF

OUT allowing the signal to enter from the antenna and proceed to the next stage of the system. The LN1000A operates over a range of 10kHz to 1000kHz providing an advertised gain of 30dB. It is important to note that this preamplifier is designed for laboratory use with broadband applications. By designing a preamplifier for the expressed purpose of implementation into the High Sensitivity RF Receiver system, this gain can be improved with the added benefit of decreasing the noise inherent in any broadband amplifier. This shows one possible increase in sensitivity at an increase in cost. If the system is produced in numbers, this cost would be reduced to an acceptable limit.

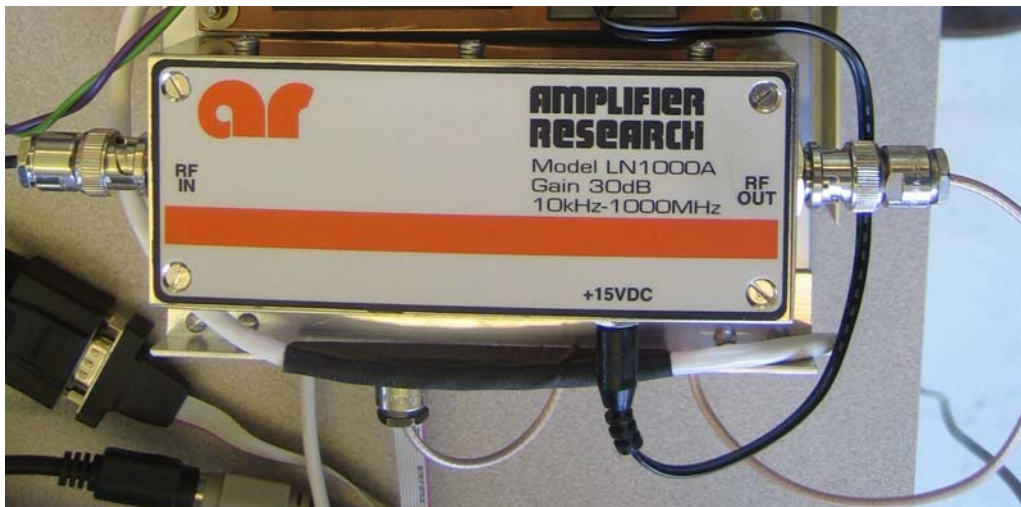


Figure 6. LN1000A Amplifier.

D. RECEIVER

After the signal is amplified by the preamplifier, it passes into the RF receiver. The receiver chosen for the High Sensitivity RF Receiver is the ICOM PCR 1000 receiver.

It is shown below in Figure 7. The receiver is modified slightly for our application. The PCR 1000 is a wideband radio receiver controlled from a personal computer (PC). It has a frequency range from 100 kHz to 1.3 GHz and a power requirement of 12VDC. The ICOM receiver covers the AM (Amplitude Modulated), FM (Frequency Modulated), WFM (Wideband Frequency Modulated), SSB (Single Side Band) and CW (Continuous Wave) modes allowing the process of nearly all threat signals. One modification to the PCR 1000 is the power cord connection to the receiver. The connection is such that it easily disconnected. This occurrence in dynamic flight is a possibility and would effectively disable the system. To solve this, the power cord is hard wired to the internal circuit board. The "off the shelf" model only weighs 2 lbs 3 oz. This weight can be reduced if required. The PCR 1000 is controlled by a PC. The High Sensitivity RF Receiver system used a single board computer onboard the TERN for this purpose.



Figure 7. ICOM PCR1000 Receiver. (From ICOM America)

E. PICOSCOPE

After the analog signal passes through the receiver, it enters into an Analog to Digital (A/D) converter. The output from the A/D converter is a digital data stream. This allows the signal to be processed by the onboard computer. For the High Sensitivity RF Receiver, the Pico Scope 3205 is used. It is shown below in Figure 8. The Pico Scope 3205 is produced by Pico Technology Limited. It has a 100 MHz bandwidth with dual channels. For the High Sensitivity RF Receiver, only one channel is used by the systems single antenna receiver channel. The extra channel provides additional capabilities that are not used in the present UAV configuration. In a future model, it could be developed or removed to reduce weight. The Pico Scope has a maximum effective sampling rate is 5GS/s. During field testing, it is used at a significantly lower sampling rate.



Figure 8. Pico Scope 3205. (From Picotech)

F. SINGLE BOARD COMPUTER

Now that the signal is in a digital format, it passes into the onboard computer. There are two processing options when dealing with the signal at this time. The signal is processed onboard the UAV, or it is passed to a ground station through a wireless mesh network for processing. The first choice allows the required downlink bandwidth to be reduced, yet requires more processor power in the UAV package. This equates to more weight. The second option requires less weight; yet requires more bandwidth in the downlink signal.

Sampling rates are such that the bandwidth requirement is low enough to allow almost all the processing to be done by the ground station. The onboard computer used in the High Sensitivity RF Receiver is a simple single board computer with all required programs stored in flash memory. The single board computer is a required part of the TERN UAV yet has enough processor capabilities to run both systems. Shown below in Figure 6 is the single board computer used for testing. The flash memory contained all the code used to control the system as well as run windows XP. The single board computer controlled the Pico Scope and ICOM receiver for the High Sensitivity RF Receiver in addition to the systems required for the TERN UAV. A MESH network card provided connectivity with the ground station for data transfer and flight control inputs either manual or automated. This MESH network card allowed the ground station to remote log onto the onboard payload.

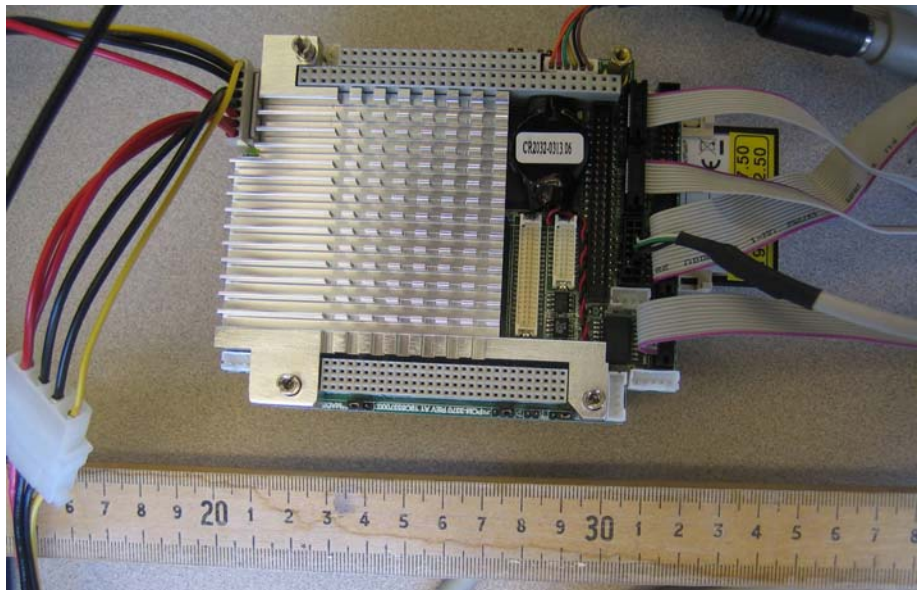


Figure 9. Single Board Computer.

G. CONCLUSION

The High Sensitivity RF Receiver is composed of five main sub-systems: the antenna, preamplifier, ICOM receiver, PICO Scope A/D converter and the single board computer with network capabilities. This system is modified for packaging as the front-end payload of the TERN UAV and has an overall weight of only 7 lbs. The system is composed of commercially available, off the shelf equipment requiring only slight modification. The majority of modifications dealt with "toughening" the system to handle the shock and vibration of use in an UAV.

III. ANTENNA MODELING

A. ANTENNA BACKGROUND

The antenna is the ears of the High Sensitivity RF Receiver. As such, it is critical to pick the correct antenna to meet the needs of the RF system. Several factors go into picking the correct antenna such as weight, gain, material, shape, and even cost. Any or all of these factors cause the system to fail if not chosen correctly. At the least they can decrease performance below an acceptable level. There are always tradeoffs in system's design, while an antenna with high gain is desirable; the increased cost in weight is not. Increasing one antenna parameter usually requires a decrease from another. There is no perfect antenna for all occasions.

B. ANTENNA THEORY

There are many antenna design types, such as electronically small, resonant, broadband or aperture antennas. When choosing the proper type, parameters such as gain, directivity, radiation pattern and bandwidth need to be discussed. The first parameter discussed is the radiation pattern. This is simply the angular variation of radiation around the antenna. This pattern is three dimensional and viewed as a balloon that surrounds the antenna. In the simplest case of a theoretical point radiator, the shape is similar to a circular balloon.

The directivity (D) of an antenna expresses how much greater the peak radiated power density is for an antenna

than it would be if all the radiated power is distributed uniformly around the antenna [point radiator]. This mathematically is the ratio of power density in the direction of the pattern maximum to the average power density at the same distance from the antenna. This is conceptually explained by use of a simple balloon, if the balloon is stretched in one direction, than directivity would be the ratio of the length of the stretched balloon to that of the balloon un-stretched. Gain (G) is the directivity reduced by the losses on the antenna.

Electronically small antennas are simple in structure. Their properties are not sensitive to construction details and are ideal for use in cars for AM reception. Electronically small antennas properties include low directivity, and they are inefficient due to ohmic losses. Resonant antennas are specific to a selected narrow frequency band. While they result in low to moderate gain, they are designed to work in a simple structure where the frequency is known and stable. When dealing with broadband antennas, the pattern and gain remain acceptable and are nearly consistent over a wide frequency range. A log periodic dipole is a good example of this type of antenna. The last type of antenna is the aperture antenna which has a physical aperture through which the electromagnetic waves flow such as a horn antenna. These antennas yield high gain but only moderate bandwidth.

C. ANTENNA SELECTION

For the High Sensitivity RF Receiver, the broadband antenna is chosen to provide usability over a large frequency bandwidth with moderate gain. Because threat

capabilities are increasing almost daily, choosing a specific frequency to operate over would limit the future usability of the system. The trade off is in gain. A high gain system such as a horn antenna would allow for reception at a greater range. The equation in Figure 10 equates the power spatial density of a signal as a function of range⁶.

$$P_d = \frac{G \cdot P_t}{4 \cdot \pi \cdot R^2}$$

Figure 10. Equation for power special density of a transmitted signal.

In this equation, P_t is the transmitted power, R is the range between the transmitter and the antenna, and G is the gain of the antenna. For signal detection by the High Sensitivity RF Receiver, it must be greater than a minimum power density level which the system is capable of determining from background noise. Because this is set, the maximum range is improved by increasing the transmitted power or the gain of the RF system. Because the threat system is inherently low powered while in a receive mode, the only way to increase the detection range or sensitivity of the system is to increase the effective gain of the antenna and receiver.

A horn antenna has the highest gain and it is at the cost of bandwidth and size. Most horn antennas are made of heavy materials and require larger sizes for lower

6 Radar Basics
[http://www.alphalpha.org/radar/intro_e.html#L%27Equazione%20Radar] July 2007

frequencies. This is ideal for ground based systems that can handle the larger size requirement. They are not ideal for UAVs. For example, the SAS-570 Double Ridge Guide Horn Antenna from A.H. Systems Inc has a frequency range of 170 MHz to 3 GHz comparable to that of the LPY41. The SAS-570 is 28x38 inches at the opening and 36 inches long weighing in at 22.5 lbs and only has a gain of 10dB. This is compared to the LPY41's weight of 0.29 lbs and gain of 7.49dB. While the increased gain would be desired, the size and weight make this type of antenna unusable.

D. ANTENNA TESTING

Because little information is available for the Ramsey Electronics Model LPY41 Antenna, testing is conducted to determine the antenna's parameters. The first approach is testing a model of the antenna through use of a computer program. The program used is GNEC version 1.6 which is supplied through the Naval Postgraduate School for scholastic use. Antenna measurements are tabulated as shown in Table 1 below and placed into GNEC for analysis.

Antenna Element	Width (cm)	Length (cm)	Spacing (cm)
1	0.60	28.20	-
2	0.50	25.00	3.50
3	0.40	22.60	3.20
4	0.30	20.00	2.90
5	0.20	17.80	2.60
6	0.15	15.80	2.40
7	0.15	14.00	2.00
8	0.15	12.60	1.80
9	0.15	11.60	1.60
10	0.15	10.20	1.40

Table 1. YP41 dimensions.

After these measurements are placed into GNEC, the program displays a simulation of the antenna as shown below in Figure 11. The program's input code is altered on several occasions in an attempt to correctly measure the antenna.

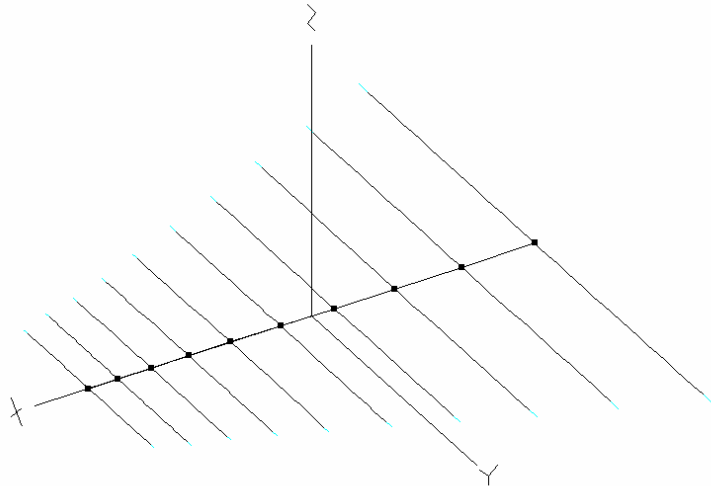


Figure 11. GNEC display of LPY41 antenna.

Several inconsistencies are found in the results after testing several variations in the model and consulting with Naval Postgraduate Professors familiar with the program. Because the antenna is a logarithmic periodic array, the shape of its radiation pattern is somewhat known and comparing the results from GNEC program is not matching the expected pattern. The geometry of the LPY41 is set as a log-periodic dipole array, which is a series-fed array of parallel wire dipoles of successively decreasing length and spacing between the dipoles. This system works by creating a zone or active region that the incoming electro-magnetic wave will resonate with at the dipole antenna which is

closest to its wavelength⁷. The element directly behind acts as a reflector while the one in front acts as a director giving the shape of the antenna pattern an elongated view in the direction of the antenna. As the frequency of the incoming wave is increased, the active region moves forward on the antenna as the wavelength decreases in size. Correspondingly, the active zone moves to the larger elements in the back of the antenna as the frequency decreases and the wavelength increases. While the shape of the antenna pattern is understood, each antenna pattern is individual and only testing can truly measure them. Understanding the pattern is important, yet understanding the gain is crucial to the success of the system.

Because of these ambiguities, the antenna is tested in a laboratory to discover the actual antenna pattern. The results are compared with what GNEC is showing and the expected pattern for an antenna of this type. In the laboratory, the antenna is tested using the Lab-Volt Antenna Training and Measuring System, which is a powerful antenna measuring system and is designed for low-power safe operation. Testing can be conducted both in the 1 GHz and 10 GHz bands (specifically at 915 MHz and 10.5 GHz), allowing measurement of antenna characteristics in either of these bands. The Data Acquisition Interface controls the Antenna Position and acquires the received antenna signal⁸. The LPY41 is tested using the 915 MHz frequency and compared

⁷ W.L. Stutzman, and G.A. Thiele, , *Antenna Theory and Design* , 2nd ed, John Wiley and Sons, Inc.,1998.

⁸ LabVolt training pamphlet found at
[<http://www.itp101.com/files/dsa8092.pdf>] July 2007.

to a known dipole antenna to measure overall gain. Due to the signal strength received, 8dB of attenuation is needed for plotting the results in the Lab Volt software. This attenuation is taken out when the raw data is tabulated.

During the testing of the LPY-41, an anomaly kept showing in the results. The expected shape of the antenna pattern is displayed yet a marked decrease in gain on one side of the main lobe kept appearing. After several runs of the testing system, the anomaly is found to be the position of the feed cable. The feed cable attenuates the signal on the side where the cable is positioned. This is corrected by careful placement of the feed cable to limit the interference yet is noteworthy for implementation on the UAV package.

The collected data is tabulated and an example is shown in Table 2 below. The complete table is located in Appendix A.

Results from Lab Volt Antenna Training and Measuring System							
Angle	LPY41		Dipole	Angle	LPY41		Dipole
	E	H	E		E	H	E
0	5.45	5.4	-0.12	180	-15.38	-17.5	-0.51
1	5.43	5.4	-0.11	181	-15.38	-17.5	-0.51
2	5.42	5.37	-0.12	182	-15.6	-17.17	-0.49
3	5.43	5.38	-0.13	183	-15.38	-17.17	-0.51
4	5.42	5.37	-0.13	184	-15.38	-17.17	-0.49
5	5.43	5.35	-0.12	185	-15.38	-17.17	-0.5
6	5.41	5.34	-0.13	186	-15.38	-17.17	-0.49
7	5.37	5.35	-0.16	187	-15.18	-16.87	-0.51
8	5.37	5.34	-0.19	188	-15.38	-17.17	-0.52
9	5.34	5.34	-0.22	189	-14.98	-16.58	-0.54
10	5.28	5.32	-0.27	190	-14.98	-16.58	-0.58

Table 2. Example of tabulated data from LPY-41 and Reference Dipole.

Figure 12 shows both the E-plane (vertical) and H-plane (horizontal) of the LPY-41. The E-plane and H-plane must not be confused with the electrical and magnetic fields associated with RF emissions. They are simply the software's labeling for the primary planes (vertical and horizontal) the RF energy travels through.

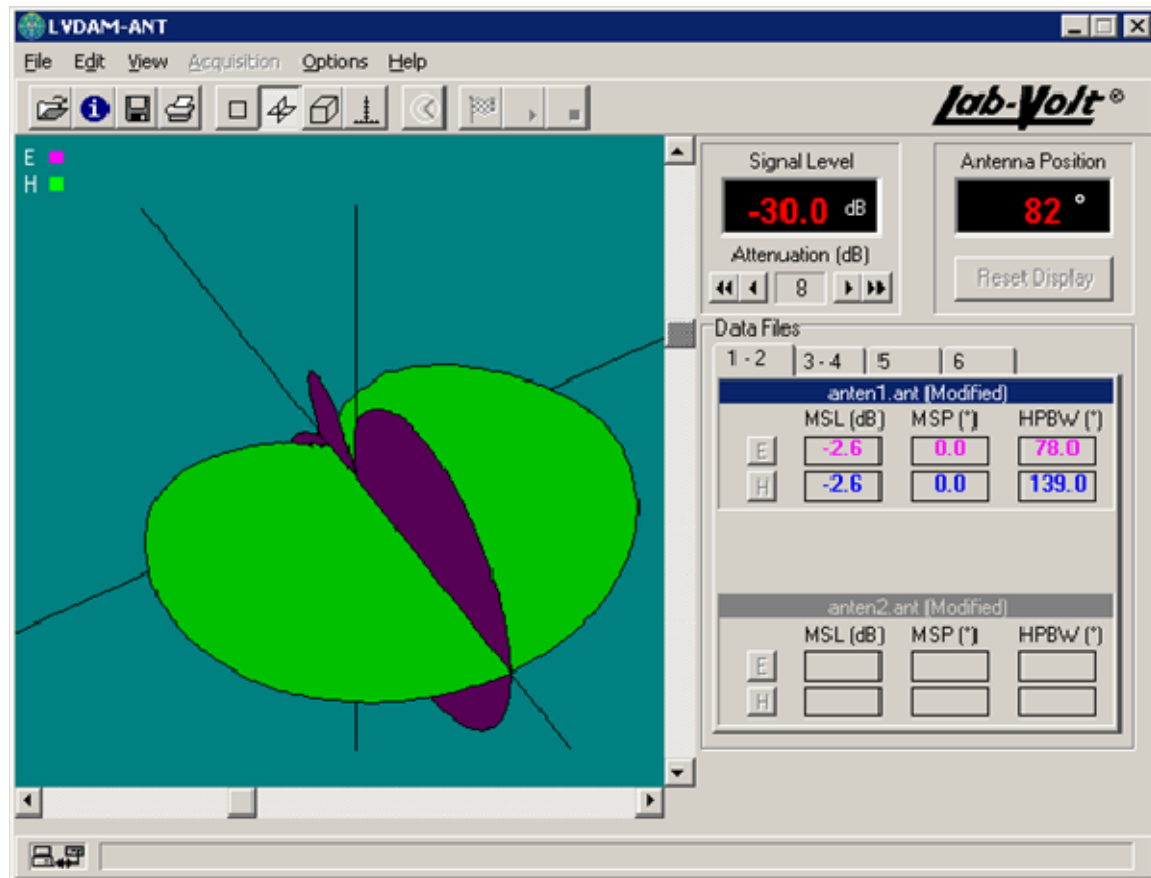


Figure 12. E-plane and H-plane for the LPY41 Antenna.

Figure 13 shows both planes as well (magenta and blue correspondingly for the LPY-41) but also depicts the pattern of the reference dipole antenna (teal) all of which is displayed in a Cartesian plot.

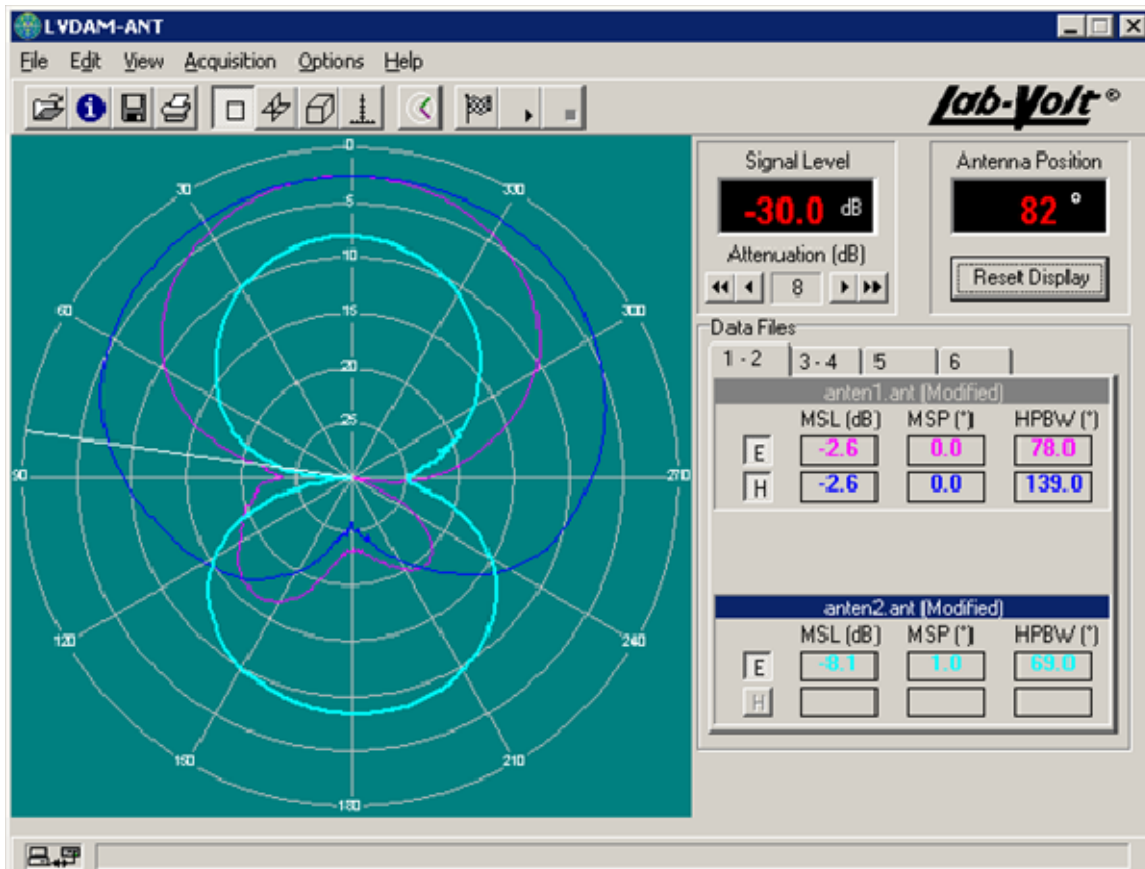


Figure 13. E and H plane for LPY41 antenna compared to known Dipole antenna.

Figure 14 shows the same information but in the form of an excel plot of the tabulated data. The Dipole antenna is verified to have a gain of 2.16dB and only the E-plane is shown. In dipole antennas, the E-plane and H-plane mirror each other. Because of this, only one plane needs to be measured.

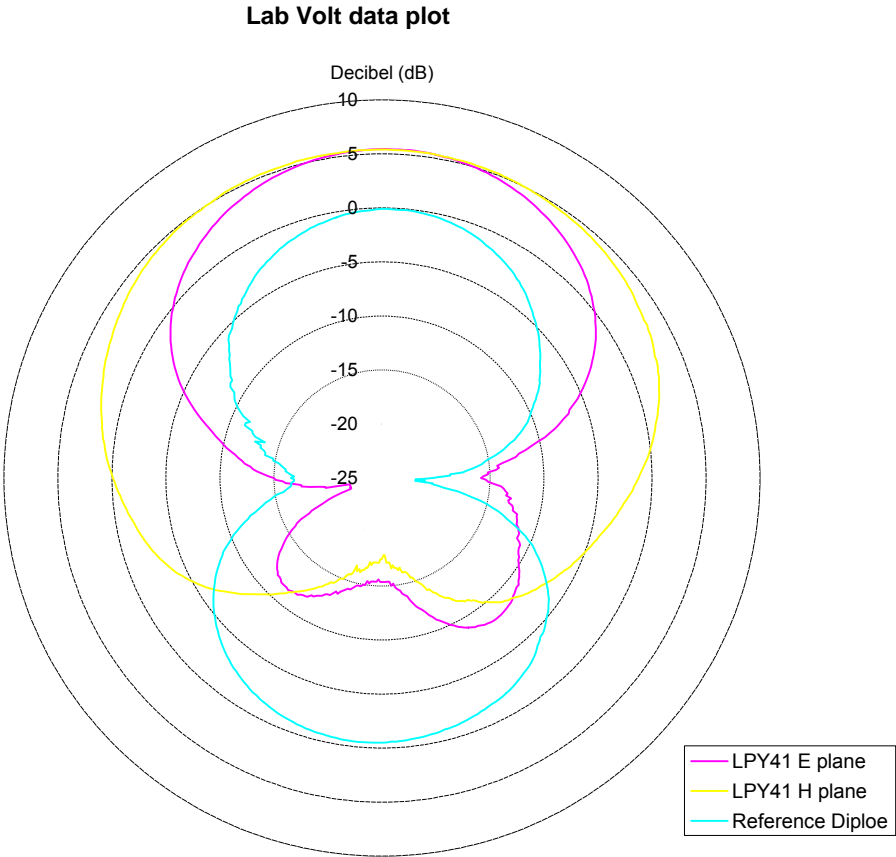


Figure 14. Excel plot of tabulated data.

This allows for a direct measurement of gain from the plots of the LPY41 pattern. Knowing the maximum gain for the reference dipole is 2.16 dB and that there is a difference of 5.33dB between the maximum of the LPY41 and the reference dipole, the maximum gain of the LPY41 is determined as 7.49dB. This maximum is directly off the front of the antenna as expected. Both plots show the primary beam radiating out of the front part of the antenna with its maximum gain of 7.49dB as well as a corkscrewing backlobe.

From Figure 13, a rough directivity measurement is found to back up the number received from the Lab Volt software. Directivity is measured from the equation in Figure 15⁹.

$$D = \frac{41,253}{HP_{E^\circ} \cdot HP_{H^\circ}}$$

Figure 15. Equation for Directivity as a function of the principle plane beamwidths in degrees.

With a rough estimate of the half power beamwidths of both principle planes (the E-plane and H-plane and is defined correspondingly in the equation as HP_{E° and HP_{H°) from the plot as 70° and 90° respectively, the directivity (D) is computed as 6.54dB which is close to the 6.2dB calculated from the analysis software as shown in the upper right corner of Figure 16.

⁹ W.L. Stutzman, and G.A. Thiele, *Antenna Theory and Design*, 2nd ed, John Wiley and Sons, Inc., 1998.

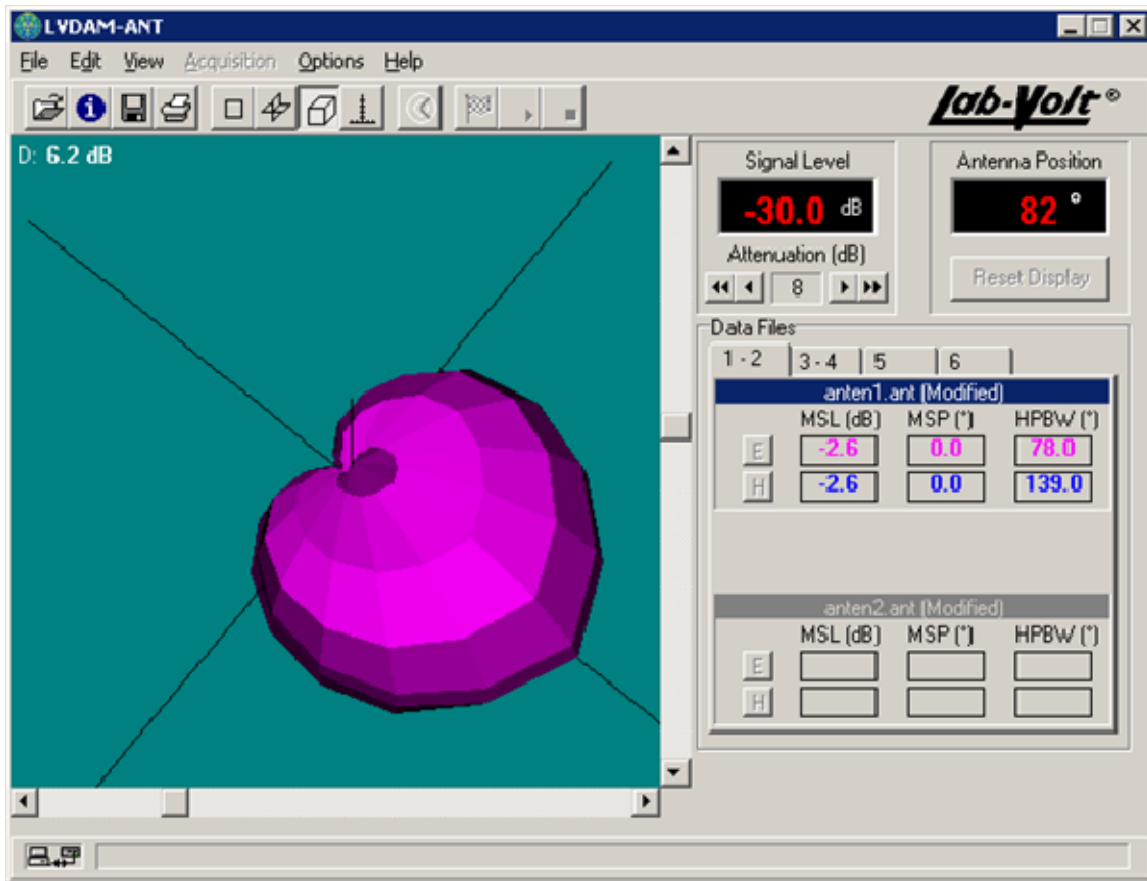


Figure 16. 3-Dimensional antenna pattern for LPY41.

E. CONCLUSION

The antenna choice is one of the most important decisions in constructing the High Sensitivity RF Receiver because it is the front end part of the system. When dealing with signal strengths below the noise floor, any increase or decrease in signal strength due to the antenna becomes important to the processing of that signal. The LPY-41 measurements reveal a heart shaped mainlobe with corkscrewing backlobe. The Gain of the antenna is measured at 7.49dB with a directivity of 6.2dB.

IV. TESTING

A. CAMP ROBERTS

Field testing is conducted at McMillan Airfield located onboard Camp Roberts. Camp Roberts is primarily a U.S. Army National Guard and U.S. Army Reserve training facility¹⁰. Camp Roberts is located approximately 100 miles south of the Naval Postgraduate School (NPS) in Monterey California. Located near the southwestern boarder of Camp Roberts is McMillan Airfield which is 3500' long, 65' wide with 10' shoulders and lays on a heading of 281 degrees and at an elevation of 920'. The airfield originally was a dirt assault strip used by the Army and Air Force for tactical C130 training¹¹. Recently a NPS initiative called the Center for Interdisciplinary Remotely-Piloted Aircraft Studies or CIRPAS has improved the strip to make it acceptable for UAV flight operations¹². The airstrip is paved and marked with centerline and limit line markings. Wind socks are located on the north side of the runway at either ends.

¹⁰ Camp Roberts homepage found at
[<http://www.globalsecurity.org/military/facility/camp-roberts.htm>]
August 2007.

¹¹ McMillan homepage found at
[<http://www.globalsecurity.org/military/facility/mcmillan.htm>] August 2007.

¹² CIRPAS homepage found at
[<http://www.cirpas.org/Facilities/McMillan%20Faciltiy%20003.htm>] August 2007.

FAA Identifier: CA62
Lat/Long: 35-43-08.8860N / 120-46-04.6290W
35-43.148100N / 120-46.077150W
35.7191350 / -120.7679525
(estimated)
Elevation: 920 ft. / 280 m (estimated)
Variation: 15E (1985)
From city: 5 miles SW of CAMP ROBERTS, CA
Time zone: UTC -7 (UTC -8 during Standard Time)
Zip code: 93451
Table 3. McMillan Aeronautical Information.

Table 3 contains the aeronautical Federal Aviation Administration information effective as of 15 March 2007. Figure 17 below shows an overhead picture of the airfield.



Figure 17. McMillan overhead picture. (From McMillan Homepage)

Currently the airfield is daytime operations only and non-instrumented. Facilities include a 40 x 70' hangar, office spaces and a conference room. The runway is a B-II category airstrip, adequate for a maximum 12,500 lbs. aircraft. Figure 18 below shows the Tactical Pilotage Chart (TPC) which provides coverage at a scale of 1:500,000 for the area surrounding McMillan Airfield. McMillan is at the southern portion of restricted area 2504 as seen from the chart. This makes it ideal for testing purposes as airspace deconfliction is easily arranged internally.

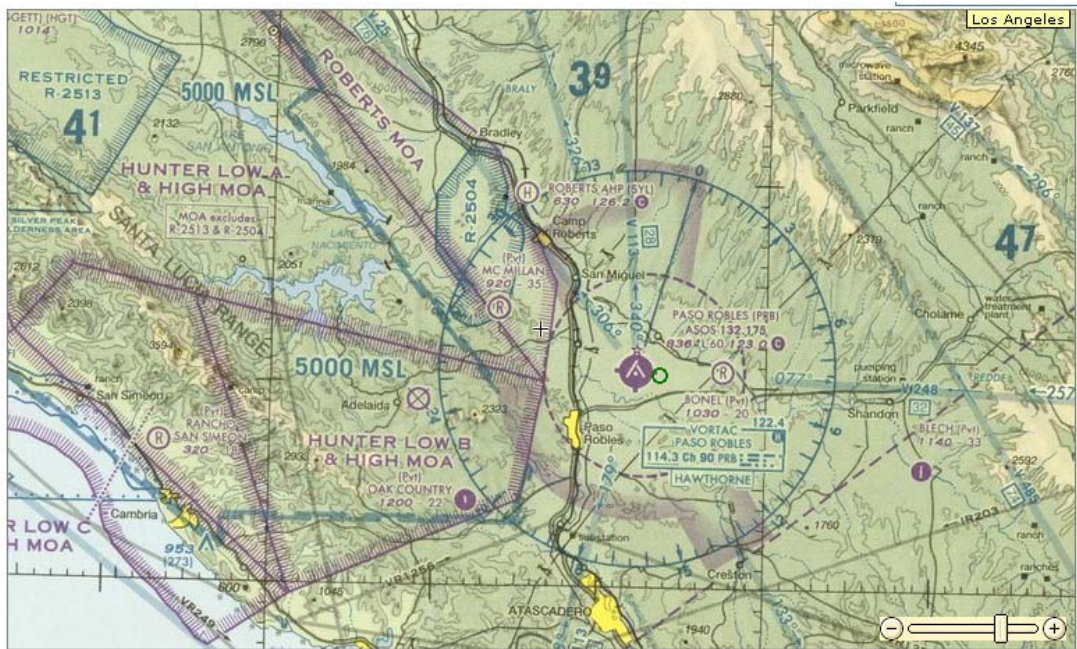


Figure 18. TPC showing area surrounding McMillan Airfield. (From McMillan Homepage)

B. THE TERN UAV

The TERN UAV is the chosen platform for testing the High Sensitivity RF Receiver. The TERN has several desirable attributes that make it ideal among the possible

test platforms¹³. The second possible platform is the Scan Eagle UAV. Both systems are compared in Table 4 below.

	SCAN EAGLE	TERN
Max Takeoff Weight	37.9 lb / 18 kg	120 lb / 55 kg
Payload	13.2 lb / 6 kg	25 lb / 12 kg
Endurance	15 hours	2-4 hours
Max Level Speed	70 knots / 36 m/s	101 knots / 52 m/s
Cruise Speed	49 knots / 25 m/s	58 knots / 30 m/s
Wing Span	10.2 ft / 3.1 m	11ft / 3.4 m
Fuselage Diameter	7.0 in / 0.2 m	9.5 in / 0.24 m
Length	3.9 ft / 1.2 m	8 ft / 2.4 m
Propulsion	1.5 hp	9.5 hp

Table 4. Comparison of TERN and Scan Eagle UAV.

Payload capacity is the first and most important attribute compared. The TERN has the largest payload at over 25 lbs (not including the internal navigational equipment that is removed from the NPS TERN) as compared to that of 13.2 lbs for the Scan Eagle. The TERN is designed as a test bed and as such has great adaptability with different payloads. The Scan Eagle is designed for long loiter surveillance missions and has issues when integrating a payload such as High Sensitivity RF Receiver at around 7 lbs. Additionally, the TERN's size allows for stable flight after the Antenna is attached to the outside. This would prove problematic for the Scan Eagle. The one downside of the TERN is that it is a test bed platform. The TERN is no longer used outside of academic purposes. The Scan Eagle is presently used in support of forward deployed troops in

¹³ NASA web site found at
[<http://www.aeroconcepts.com/Tern/VehiclePage.html>] August 2007.

combat zones. The High Sensitivity RF Receiver can be streamlined to work as a Scan Eagle payload with additional time and money.

C. SIMULATED THREAT SYSTEM

For testing purposes, the simulated threat is the Motorola Talkabout T4500 and Talkabout FV-200 Two-Way Radios. Both models used are displayed below in Figure 19 and are part of the Family Radio Service (FRS).



Figure 19. Motorola radios models T4500 and FV-200.
(from Motorola)

It is important to understand the unintentional emissions of the systems and how they change with time and temperature. To better understand this, the frequencies of 4 hand held systems are tested using the High Sensitivity RF Receiver. This is done in Monterey prior to field testing. Each unit is tested in an identical method with the major difference being the time of day that the unit is tested. Each unit is tested one after the other. Each unit is placed next to a concrete walkway directly in the path of the High Sensitivity RF Receiver's antenna beam. The distance between is approximately 20 ft. In-between is a

glass window. The frequency and power received by the system is recorded every min for 50 minutes for the first two units. The data is recorded for 30 minutes for the last two units. Every five minutes, external temperature measurements are recorded by use of a Fluke 52 K/J Thermometer. The Fluke's probe is attached to the rear external housing of the unit. The data is tabulated and plotted below in Figures 20 and 21. Each handset is given a 4 letter/numbers identifier that corresponded to the last 4 letter/numbers of its serial number.

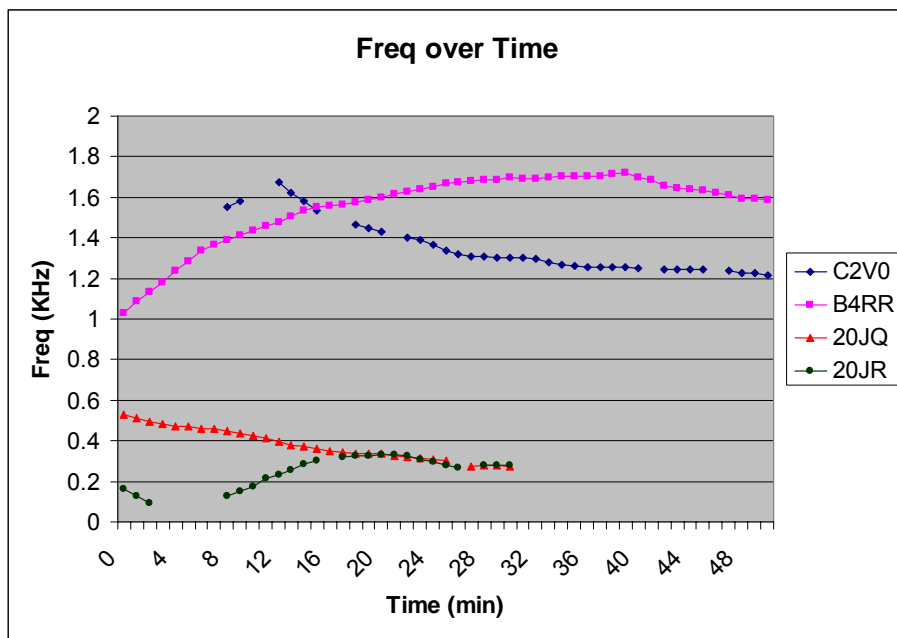


Figure 20. Frequency vs. Time Plot for each Handset.

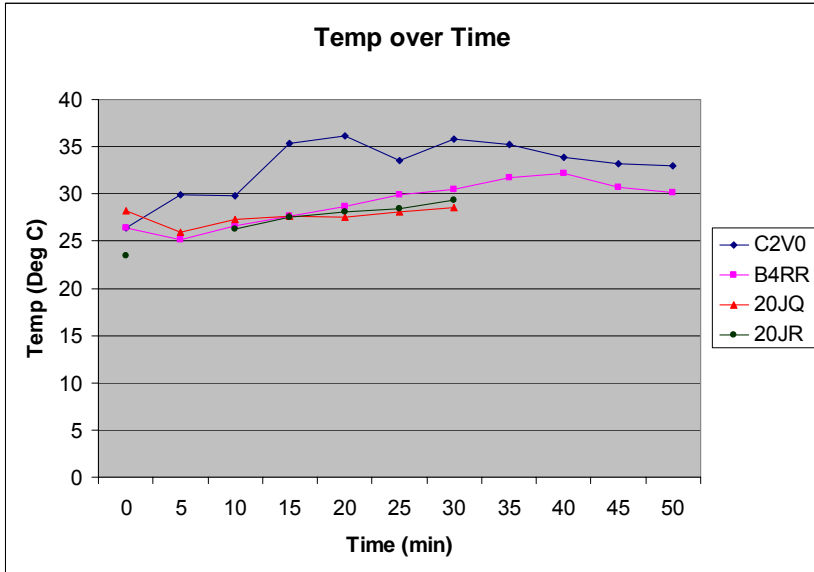


Figure 21. Temperature vs. Time Plot for each Handset.

These plots reveal some interesting results. As each handset is turned on, the internal components heat up slightly changing the frequency of the handset and contain positive or negative variations. After a short time, we expect the handset to reach a steady state power level and the frequency should stabilize. In general, this did not occur. Any variation could be a factor of the increasing temperature of the unit, however while the temperature increased in all cases, the drift of the handset's frequency did not occur in the same direction. The overall temperature coefficient may be varying from positive to negative in sign or vice versa. Sufficient assessments are not completed to make any detailed determination. As seen in Figure 20, the drift of a handset did not occur in any set direction either. Handsets would increase, decrease or some combinations of the two with no corresponding change in an outside stimulus. This shows the lack of tight quality

control in these types of commercial equipment. Additionally, this becomes a limitation in the integration time available for the High Sensitivity RF Receiver. As described in the next chapter, one of the fundamental equations for this system requires a constant signal for integration to reduce the effects of background noise. This integration allows the signal to be retrieved from below the noise floor.

D. COHERENT INTEGRATION

The primary strength of the High Sensitivity RF Receiver is the coherent integration processing that is accomplished in the system. Coherent integration is defined as the time-domain integration of measurements in coherent radar over a sequence of pulses or over an observation interval, prior to estimating the signal properties, to improve the signal-to-noise ratio while minimizing signal processing¹⁴. In the following equation¹⁵ shown in Figure 22, the number of pulses received and integrated will increase the signal to noise ratio of the system significantly.

$$\left(\frac{S}{N}\right)_n = n \left(\frac{S}{N}\right)_1$$

Figure 22. Equation for the signal to noise ratio improvement for n-pulses coherently integrated.

¹⁴ Glossary of terms found at
[<http://amsglossary.allenpress.com/glossary/browse?s=c&p=62>] August 2007.

¹⁵ Skolnik, M.L., *Introduction to Radar Systems*, 3rd ed, McGraw-Hill, Inc., 2001.

In this equation $(S/N)_n$ represents the signal to noise ratio of the system after coherent integration of n pulses. Ideally, there are no losses for true coherent integration and this number is simply the signal to noise ratio of one pulse or $(S/N)_1$ multiplied by the number of pulses received.

The Simulated IEDs are unintentionally emitting a continuous wave signal. This signal emits at a wide band frequency and occasionally poll at a narrow band frequency. In this situation the RF signals received are not pulses from the emitter but CW signals from the receiver and digital samples from the Picoscope A/D converter. The Picoscope A/D converter packatizes the digital data stream it receives from the receiver to be processed by the ground station computer. These packets become individual records which are received at 12,207 samples per second. This number is a software setting and can be changed. These packets contain the number of samples processed as individual pulses. This number is a function of sampling rate and is also software setting. The standard numbers are 4, 8, 16, 32, 64 or 128K samples per second.

Each setting gathers samples until the size is reached, and the data passes down to the ground station for processing as a data record. Increasing the sampling size also increases the time between receiving packets from the TERN at the ground station. For example if each packet transmitted to the ground station is 16K (16,384) samples long, the time it takes to fill a packet is the data rate (16k) divided by the sampling rate (12,207 SPS). In this example, the time is 1.34 seconds. This means every 1.34 seconds, a packet is sent to the ground station for

processing. This leads the tradeoff between the systems ability to increase the signal to noise ratio and the time between signals displayed to the operator. The TERN has the simulated IED in the antenna beam for a few seconds. This means the system only have a few chances at discovering and displaying it. By increasing the data samples, the system might miss a fleeting signal.

E. ANTENNA MOUNTING

The position of the antenna on the outside of the UAV becomes particularly important. The position has a dramatic impact on threat detectability. If the antenna is positioned at too great of an angle, the main beam is pushed in front of the UAV yet is above possible threats. The system could possibly miss the threat entirely depending on the altitude of the UAV.

Two questions must be answered in determining the position of the antenna. The first is the expected detection range. These tests are conducted to determine this range. Because of this, an educated guess is made. The second question is the altitude of the aircraft. Once an expected detection range is determined, the altitude of the aircraft must be known to determine the antenna position by simple geometry. This is not an easy matter since the TERN is unmanned and its ability to maintain an altitude in dynamic flight is limited. This is especially true when the aircraft is flown manually as is done in field testing. The altitude is gauged visually by the TERN's ground stationed pilot. The targeted altitude is 500 feet.

Knowing the answer to these questions, analysis of antenna position is conducted. Additional beamwidth numbers needed are the 3dB point or the position on the antenna pattern that the signal strength is 3dB less than the maximum, the Angle of Attack (AOA) of the TERN in flight and the cruising speed of the TERN. Given the maximum antenna pattern gain, it is simple matter of looking for a gain 3dB less. By looking at Table 2 in Chapter III, the 3dB point is around 40 degrees left or right of the main beam. The AOA of the TERN, or the position of the TERN fuselage during flight is determined to be 10 degrees. The cruise speed of the TERN is 50 - 60 knots. Given no winds the planning speed is taken as 60 knots which equates to 90.7 feet per second of flight.

Several cases are looked at in determining the antenna position. Two cases are computed and compared. The first positions the center of the antenna pattern, the greatest point of gain, on a point ahead of the UAVs position on the ground. The second requires a greater angle and places the upper 3dB point on that same position. Figure 24 below shows the geometry for both cases. From this geometry, a key definition is drawn out. What is detection range?

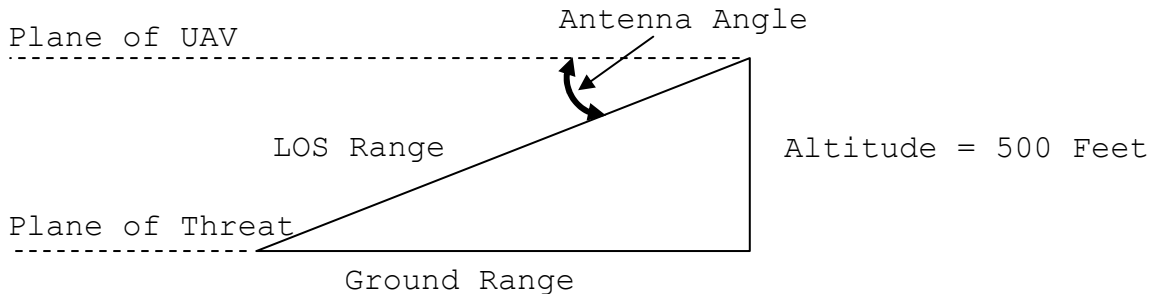


Figure 23. Antenna geometry.

The figure shows two possible definitions for detection range, the first deals with Line Of Sight (LOS) range, or the distance from the antenna to the threat. The second deals with ground range, or the distance between the threat and the position of the UAV on the ground. The second definition has more meaning to the serviceman on the ground. This is because it tells how far away they are from the threat. However, this range is not a constant, it changes with altitude. The first definition is more applicable since it is independent of any other controlled factor.

Several cases are analyzed to determine the Antenna Angle, LOS range and where the antenna beam impacts the ground. The last is determined by finding where the 3dB points, both upper and lower, impacted on the ground. In a few cases these ranges are theoretically infinite (INF). Once this condition is achieved, further analysis is stopped. It should be noted that these ranges are theoretical and based upon the geometry of the aircraft. Additionally, the Antenna Angle does not take into account the AOA of the UAV which is added to the chosen angle. Table 5 below shows the results of this analysis. The antenna angle chosen is close to 32 degrees.

Ground Range (ft)	Line of Sight Range (ft)	Antenna Angle (deg)	3db Point (ft)	
			Min	Max
1000	1118.03	26.57	270.74	INF
800	943.40	32.01	212.18	INF
600	781.02	39.81	135.79	5947.41
400	640.31	51.34	31.98	1705.42
200	538.52	68.20	0	764.12
0	500.00	90.00	0	350.10

Table 5. Tabulated Antenna Angle and Ranges.

F. LOSSES

Several losses affect the transmission of a signal from the simulated IED to the High Sensitivity RF Receiver. Some, such as Fresnel Zone Loss are dependent on the ground shape over which the signal travels and the height of the receiver and transmitter. Others such as ground wave propagation loss are dependent on the distance that the signal travels, and over what ground soil types it travels. Other losses occur when passing through the Ionosphere or heavy atmospheric occurrences such as squall lines. All of these losses are additive to the basic Line of Sight Loss (LOS) and mostly occur over long ranges. With the geometry involved during the testing of the High Sensitivity RF Receiver, relatively negligible distances and the transmitter being in direct line of sight to the antenna, only LOS loss has a significant impact.

Many losses affect the transmission of the RF signal. Basic LOS loss occurs as the RF signal passes through the atmosphere. Line of Sight loss or LB in the below equation shown in Figure 24 is dependent on two factors, the first is the range of the transmitter from the antenna and the second is the frequency of the transmission.

$$L_B = 37 + 20\log_{10}(Freqz_{MHz}) + 20\log_{10}(Range_{mile})$$

Figure 24. Determining Free Space Loss in dB.

This loss is looked at over the frequency range of the LPY-41 Antenna (400-1000 MHZ) and from a range of 500 to 4000 feet line of sight and tabulated below.

RANGE (ft)	Frequency (MHz)			
	400	600	800	1000
4000	86.63	90.15	92.65	94.59
2000	80.61	84.13	86.63	88.57
3000	84.13	87.65	90.15	92.09
1000	74.59	78.11	80.61	82.55
900	73.67	77.20	79.69	81.63
800	72.65	76.17	78.67	80.61
700	71.49	75.01	77.51	79.45
600	70.15	73.67	76.17	78.11
500	68.57	72.09	74.59	76.53

Table 6. Free Space Loss in dB of a signal as a function of Range and Frequency.

Two trends are displayed, as range and frequency are increased the losses due to free space increase. Additionally, with the lowest frequency and being directly overhead, the minimum possible loss is 68.57dB. This number shows that even with ideal circumstances, there are large losses. Table 7 below shows the relationship of loss in dB to the range the signal is detected.

Loss in dB	% Range Decrease	Range Multiplier
0.5	6	0.94
1.0	11	0.89
1.5	16	0.84
2.0	21	0.79
3.0	29	0.71
4.0	37	0.63
5.0	44	0.56
6.0	50	0.50
7.0	56	0.44
8.0	60	0.40
9.0	65	0.35
10.0	68	0.32
11.0	72	0.28
12.0	75	0.25
13.0	78	0.22
14.0	80	0.20
15.0	82	0.18
16.0	84	0.16
17.0	86	0.14
18.0	87	0.13
19.0	89	0.11
20.0	90	0.10

Table 7. Loss in Decibel and effect on detection range.

From this table, every 6 dB in loss decreases the detection range by half. With a baseline of 68.57dB of LOS loss, the percent range decrease is over 99.96. This gives an indication of just how difficult the signal is to detect given the original power of the unintended emission is incredibly small.

G. TESTING SCENARIOS

Two sets of test scenarios are developed. The first set of test scenarios consist of four series of tests. Test one is a simulated IED roughly one third of the way down the runway, and it is used for general testing of the system.

The second test is the same simulated IED but also places a simulated triggerman within sight of the simulated IED yet perpendicularly off the runway. This tests the RF system's sensitivity in width. The third test is four simulated IEDs set in a daisy chain several hundred feet apart. This tests the RF system's ability to discriminate in RF by length. The last test buries the transmitter, only revealing the remote trigger's antenna and looks at alternate placement of IEDs. The figure below shows a pictorial location of the simulated IEDs in each of the four test scenarios.

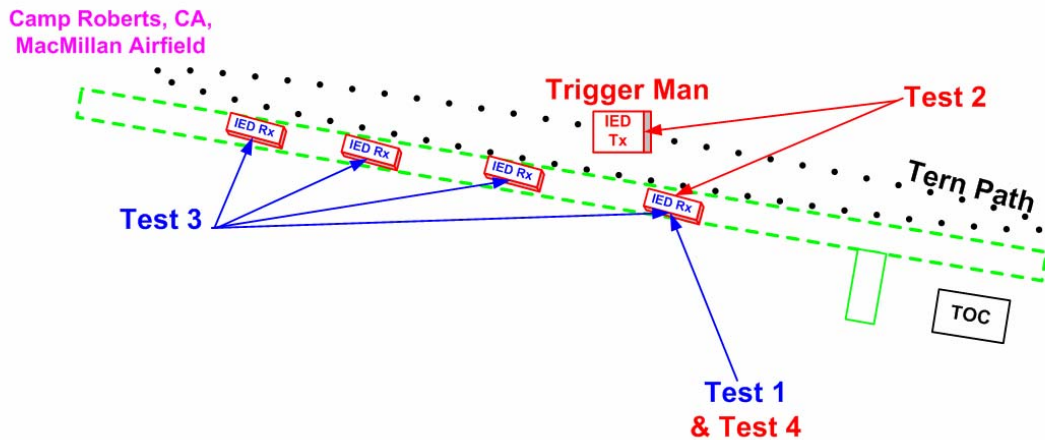


Figure 25. The four testing scenarios.

The second set of test scenarios incorporates only test one and three of the original set. This series is used if the time available for testing is limited. The time needed for each test is approximately 15 minutes per test except during the first. During the first test, the single simulated IED, the TERN UAV is flown at a lower altitude initially in order to test the system. The altitude is incrementally increased to decide the optimal altitude for

detection. This also helps determine the maximum detection range. The time allotted for this test is open ended and determined on the detection capabilities of the High Sensitivity RF Receiver.

H. CONCLUSION

There are many factors that allowed for a successful testing of the High Sensitivity RF Receiver system. The antenna position, the altitude and speed of the TERN UAV all played a part. Additionally the stability of the simulated IED's frequency played a part in the systems ability to perform coherent integration on the signal and pull it out of the background noise. These factors are analyzed to determine optimal configuration of the TERN payload.

THIS PAGE INTENTIONALLY LEFT BLANK

V. RESULTS

A. CONDITIONS

The TERN's propeller sheared its retaining bolts during preflight checks for the initial field testing scheduled on Thursday, May 17, 2006, resulting in a catastrophic failure. During ground test rescheduled for Friday, 3 August 2007, the front wheels' steering actuator broke resulting in cancellation of this test. Final field testing is successfully conducted Wednesday August 22, 2007, during TNT exercises. The test conditions are shown in the below in Table 8.

Time (PDT)	Temp	Dew Point	Humid ity	Sea Level Pressure	Visibility	Wind Dir	Wind Speed	Condi tions
7:53AM	61.0 °F / 16.1 °C	54.0 °F / 12.2 °C	78%	29.82 in / 1009.8 hPa	10.0 miles / 16.1 kilometers	Calm	Calm	Clear
8:53AM	64.9 °F / 18.3 °C	54.0 °F / 12.2 °C	68%	29.82 in / 1009.8 hPa	10.0 miles / 16.1 kilometers	Calm	Calm	Clear
9:53AM	71.1 °F / 21.7 °C	54.0 °F / 12.2 °C	55%	29.80 in / 1008.9 hPa	10.0 miles / 16.1 kilometers	Calm	Calm	Clear
10:53AM	79.0 °F / 26.1 °C	55.0 °F / 12.8 °C	44%	29.78 in / 1008.4 hPa	10.0 miles / 16.1 kilometers	Calm	Calm	Clear

Table 8. Testing conditions.

As seen, the conditions are ideal, calm winds and clear skies. The time window available for testing during the TNT schedule is 8:00 AM to 10:00 AM. Due to aircraft problems during preflight and link issues between the payload and ground station, the TERN is not airborne until slightly

before 9:00 AM. Testing scenario set two is chosen for time requirements. In addition to removing test two and four, a fifth test is added placing a simulated IED #1 in the position of simulated IED #3. Figure 26 below shows the final TERN payload configuration prior to placement of all hatches and the wing section. The High Sensitivity RF Receiver is located in the front bay of the TERN and the LPY-41 Antenna (green in color) is clearly visible on the port side of the UAV.



Figure 26. Final TERN configuration on test day.

The simulated IEDs frequencies are measured prior to the start of testing. The results are presented in Table 9.

Simulated IED #	Center Freq (kHz)	last 4 of serial #	Model Type
1	1.39	0XVZ	FV200
2	2.36	B4RR	T4500
3	0.496	20JQ	FV200
4	1.37	UYHT	FV200

Table 9. Simulated IED center frequencies.

As seen in the Figure 27 below, the antenna position on the TERN UAV is on the port side. Because of this, airframe blocking reduces the signal strength for an emitter that is located on the starboard side of the UAV. For the initial passes of the TERN, the simulated IED is on the south side of the runway (portside of the UAV), yet when the scenario is changed from test 1 to test 3, the simulated IEDs are moved to the north side for safety. A decrease in signal strength is seen and the TERN's flight path is altered to the north to compensate.



Figure 27. TERN in flight during testing.

Since the RF components are essentially off the shelf, the digital drivers used in the operation of the system created some problems. Due to port conflicts, the onboard computer is powered up prior to turning on the GPS system; otherwise the computer does not recognize the port supporting the GPS as in fact receiving data. The boot up process for the system can be refined in a future version of the system. Additionally, the GPS unit used is intended to be a handheld version. When the unit loses signal during startup it pauses for user input. This becomes a factor during pre-test checks but did not affect the actual test. This can easily be solved by replacing the hand held unit with a "puck" unit such as the Garmin GPS 18 unit. This reduces weight and plugs directly into the onboard computer shown in the figure below.



Figure 28. TERN internal circuit systems.

B. DATA FORMAT

Each packet sent to the ground station is not only processed and displayed, but saved as a data file. An example of the data is displayed in Table 10. An additional piece of data that is not calculated is the altitude of the TERN during flight. This data is essential in calculating the detection range of the system. The ground distance is used instead to give a rough estimate of detection range.

Data Record #	Speed (MPH)	Heading (deg Magnetic)	Fc [kHz]	PSD Peak [dB]
499	62.6	254.8	1.668	-9.14
500	62.6	254.8	0.606	-16.52
501	62.6	254.8	1.683	-8.87
502	62.6	254.8	0.936	-16.85
503	62.6	254.8	1.281	-16.47
504	No GPS	No GPS	0.624	-15.97
505	62.9	249.6	1.719	-17.22
506	62.9	249.6	0.534	-16.95
507	No GPS	No GPS	1.412	-17.01

Table 10. Sample of collected data.

The data collected included the system time, latitude and longitude of aircraft, airspeed of aircraft, heading of aircraft and the center frequency of collected emitter. The system centers on the strongest frequency within its bandwidth and records that frequency as the center frequency. The IED location is known. By use of spherical geometry, the distance of the TERN from each IED position is calculated. The elapsed time is generated from the system time and the end of the test. Each time the data file is opened, a time stamp is placed on the file. The last cumulative time stamp is used for tabulating the local time. The program opens the file and appends the data adding each new packet. After appending the file, the program closes the file, forcing the information download to the ground station avoiding any buffer issues. There are 1816 data records recorded over the TERN's 48 minutes flight.

The initial data analysis tried to match up the center frequencies with the IED emitters. Test scenario one contains only simulated IED #1. For the first 15 minutes of the flight, only one simulated IED emitter is active. For

the next 15 minutes, all four emitters are present. The last few minutes has the original emitter present but at the third simulated IED's position. The frequency plot below shows all frequencies associated with power peaks in Fourier Transforms of a data record recorded for the duration of the test versus the time recorded. The amount of data is overwhelming the plot hence reducing its usefulness.

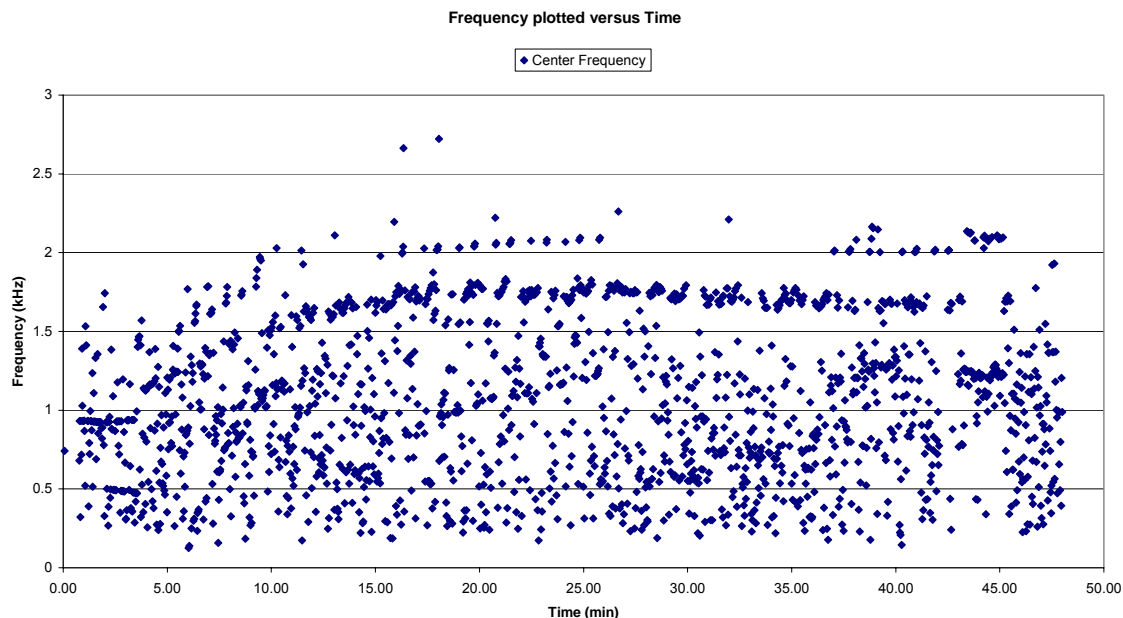


Figure 29. Frequency plotted versus Time.

The data is processed several different ways. The plot below shows the power of the signal plotted versus the frequency. Ideally, the system only receives the target signals. In this case, the plot should show four groupings of signals below their corresponding frequencies. This is clearly not the case. The data received does not directly correlate to the expected frequencies.

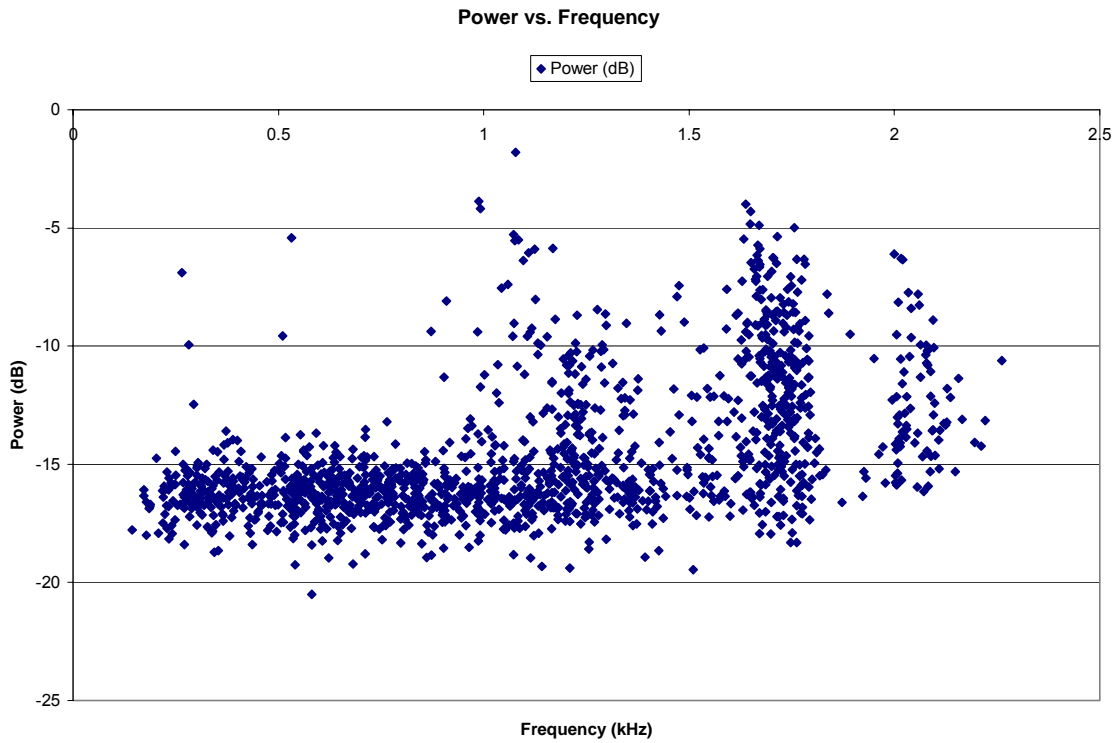


Figure 30. Power Spectral Density plotted versus Frequency.

C. SOURCES OF VARIABILITY

Before continuing, two sources of frequency variability are discussed. Both sources are examples of phenomena that explain the variances seen in the data. The first source of variability is the Doppler frequency shift due to platform motion relative to the simulated IED. The signal is mathematically modeled below as the standard sinusoidal wave formula as it leaves the emitter. This equation holds as long as the emitter and the receiver are stationary.

$$A_1 \cos[2\pi(f_t)t]$$

Figure 31. Basic Signal Equation.

In this equation, f_t is the frequency of the emitter. If either the emitter or the receiver contains a relative motion, the equation is no longer valid. Once there is relative motion, the Doppler frequency shift must be taken into account.

$$A_l \cos[2\pi(f_t \pm f_d)t]$$

Figure 32. Signal Equation with Doppler frequency.

Figure 32 above shows the equation adjusted to take into account the Doppler frequency shift. In this equation, f_d is the frequency of the Doppler shift. As the relative velocity increases, the frequency of the Doppler shift increases. The figure below displays the factors involved in determining the Doppler frequency shift.

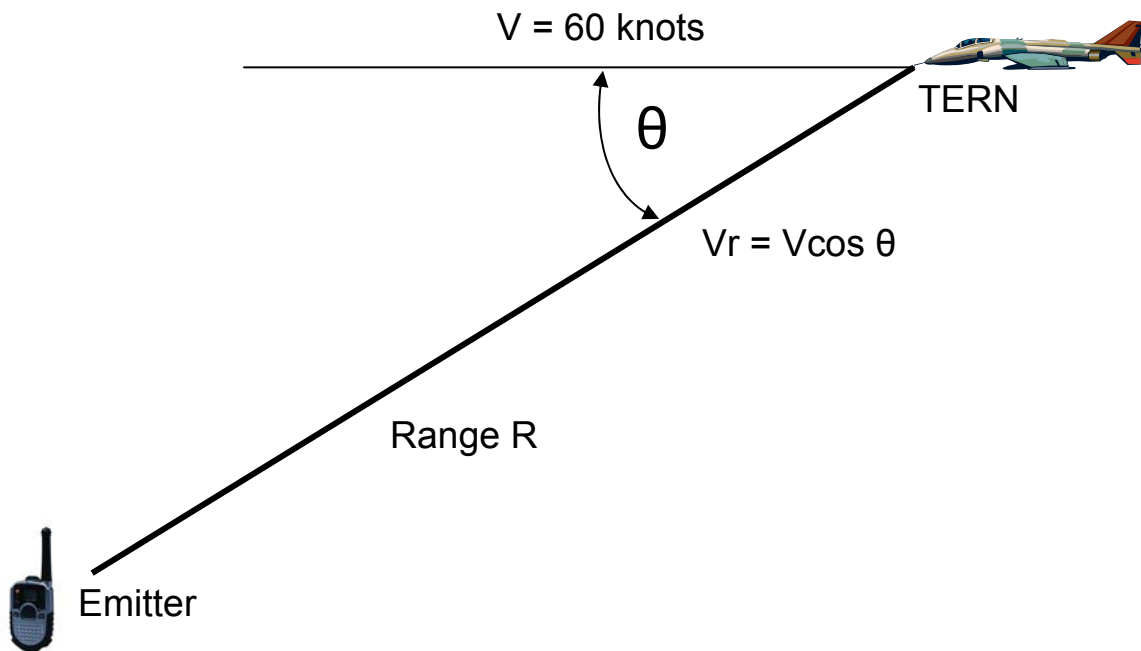


Figure 33. Geometry for Doppler frequency Shift.

The relative velocity, V_r is a function of the angle between the TERN and emitter. It is at a maximum as the TERN is pointed directly at the emitter and zero when it is perpendicular to the emitter. The figure below shows the formula used to determine the Doppler frequency shift.

$$f_d(\text{Hz}) = \frac{1.03V_r(kt)}{\lambda(m)}$$

Figure 34. Equation for Doppler Frequency.

This equation requires the wavelength of the transmitting emitter, λ in meters. The simulated IEDs are Motorola radios and each unit is set to channel one. These units use the Family Radio Service which is one of the Citizens Band Radio Services.¹⁶ The table below shows the frequencies of each channel.¹⁷

CHANNEL	FREQUENCY
01	462.5625
02	462.5875
03	462.6125
04	462.6375
05	462.6625
06	462.6875
07	462.7125

¹⁶ FCC description of FRS
[http://wireless.fcc.gov/services/index.htm?job=service_home&id=family], September 2007.

¹⁷ FCC listing of FRS band plan
[http://wireless.fcc.gov/services/index.htm?job=service_bandplan&id=family], September 2007.

08	467.5625
09	467.5875
10	467.6125
11	467.6375
12	467.6625
13	467.6875
14	467.7125

Table 11. Family Radio Services channels.

With this information, the maximum possible Doppler frequency shift is 95.3 Hz based on a frequency of 462.5625 and a maximum relative velocity of 60 knots. This Doppler frequency shift is carried through the entire system.

The second source of variations is the tolerances of local oscillators of the IED receiver and the ICOM receiver. A local oscillator is defined as

the oscillator in a superheterodyne receiver, whose output is mixed with the incoming modulated radio-frequency carrier signal in the mixer to give the frequency conversions needed to produce the intermediate-frequency signal.¹⁸

The local oscillator drift depends on several factors, such as changes in temperature. The simulated IEDs are tested and the system showed frequency drifts of over 400 Hz. There are four local oscillators being used. One local oscillator within the Simulated IED and three located within

¹⁸ Definition of local oscillator found at [http://www.answers.com/topic/local-oscillator-1?cat=technology], September 2007.

the RF receiver. The below figure is a simplified block diagram of the ICOM PCR1000's local oscillators with its three intermediate frequencies. This figure displays the receiver's triple superheterodyne system which utilizes three intermediate frequencies between the input signal from the antenna and the A/D converter.

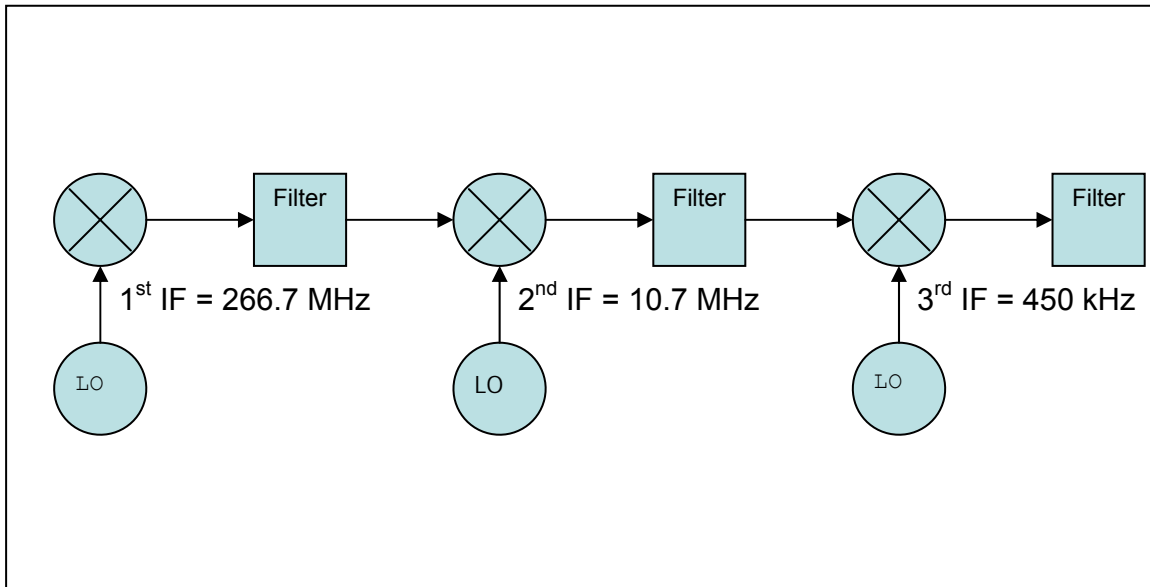


Figure 35. Simplified block diagram of the ICOM local oscillators.

Each of these local oscillators can drift. Exacerbating the issue, all four can change in different directions. For example, of the four simulated IEDs tested, two drifted up in frequency while two drifted down.

These two sources of frequency variability indicate the difficulty of performing detailed signal analysis. The High Sensitivity RF Receiver is intended to perform signal detection. It performs signal analysis but the intended

purpose is to provide the user the ability to determine the presence of a RF IED. Specific signal analysis is not conducted in this thesis.

D. IED ANALYSIS METHOD

The data analyzed is quite large with the number of packets received greater than eighteen hundred. By conducting analysis on chunks of data at a time, relevant understanding is drawn out. The easiest method found is looking at a series of data that corresponds to a complete pass of the TERN. A pass is the completion of a circuit of the TERN's flight path from an arbitrary starting position over the simulated IEDs and circling back to return toward the starting position. Plotting the center frequency, peak power spectral density, heading and distance to the IED allows identification of regions of interest. These regions of interest show areas that indicate possible detection of a signal and are highlighted by a red box over that time period. A sample of this plot is shown below in Figure 36. In this plot, the range data is simulated and the data shown is not real data.

Sample Graph Display

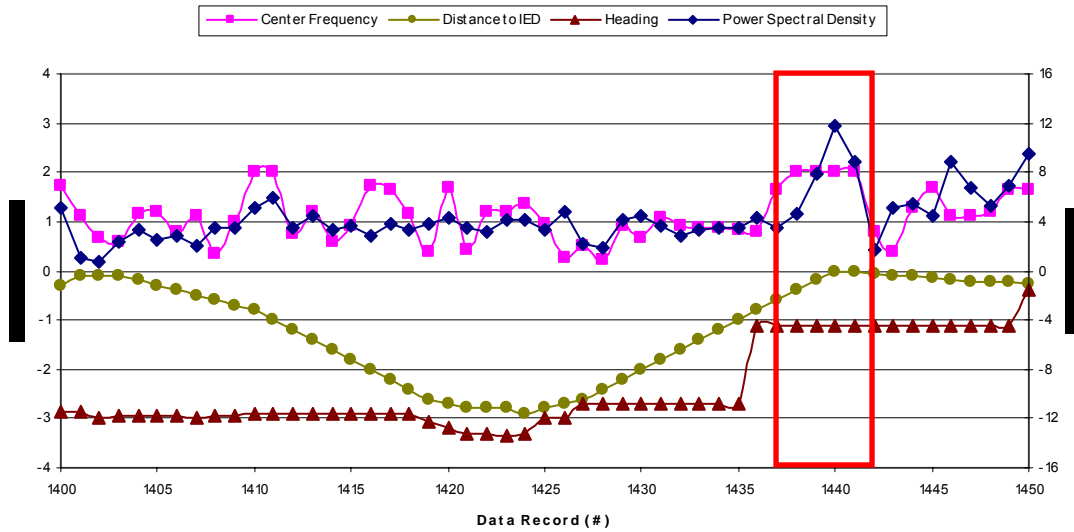


Figure 36. Sample single pass with all factors.

The above plot indicates the process of identifying the areas of interest. These plots are not displayed. Additionally, no range data is provided or discussed to keep the classification of this thesis unclassified. Further analysis is conducted after identifying the areas of interest.

The identification of the areas of interest take into account three factors. The first factor is the power spectral density level. From the plot above, the power spectral density shows one peak. This peak corresponds to either a detected signal or background noise and interference. The second factor is distance from the IED. As the TERN approached the simulated IED, the probability of detection is expected to increase. Lastly, the TERN heading provides a sanity check for the results. In some cases, the peak power spectral densities indicate signal detection, yet

the TERN is in a turn. This situation is not expected to receive a strong signal. The simulated IED may switch from a wideband mode into a narrowband search mode with more power, it could just be noise or it could be other wideband emitters from neighboring electronic facilities. A mix of these three factors is the basis for identifying areas of interest.

Once identified, the plot is reformatted as displayed below. This plot type is displayed for two TERN passes analyzed for this thesis. From this plot, the areas of interest are identified.

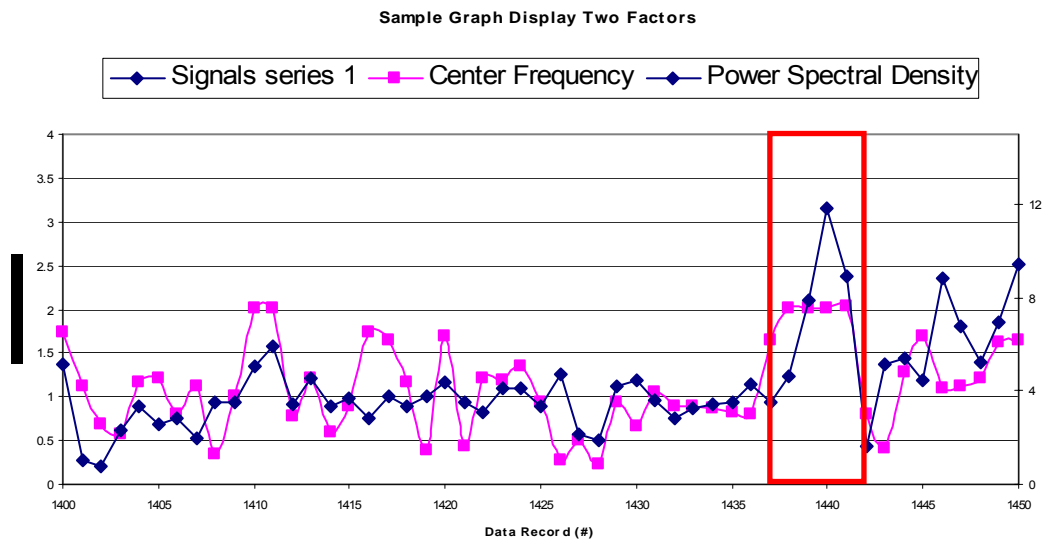


Figure 37. Sample single pass plot with only two factors.

Each area of interest is further broken down to show the computer display of the Fast Fourier Transform (FFT) that is graphed for a display box on the ground station. The ground station display, shown below in Figure 38, provides the time signal and power spectral density.

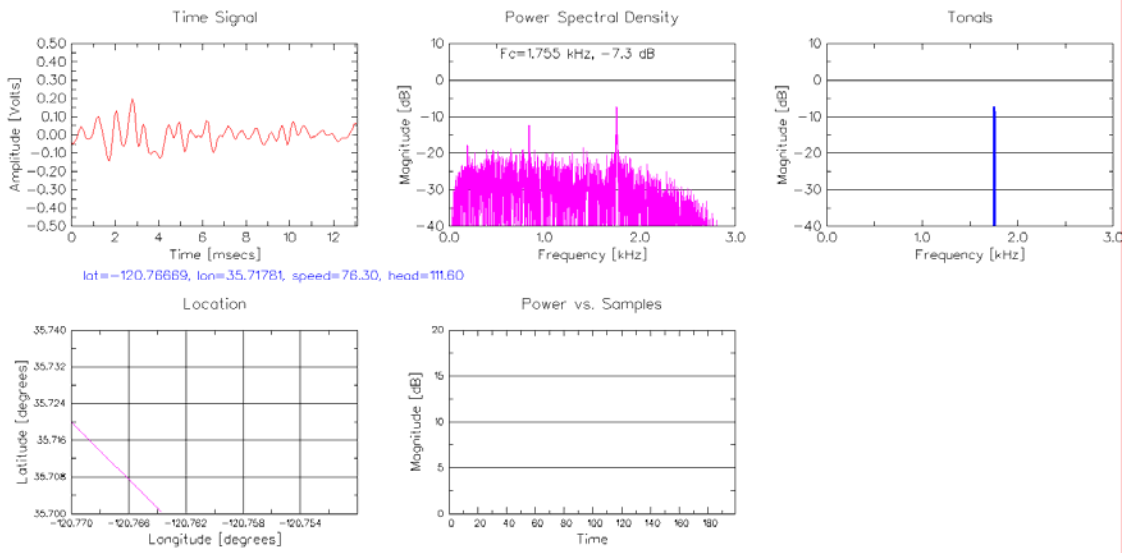


Figure 38. Ground Station Display.

Additionally, the box named Tonals displays a filtered power spectral density peak by removing the noise floor. The location displayed the TERN's position while the power vs data records box is a software option that is not used during testing. By looking specifically at the power spectral density of each data record, signal detection is performed.

E. SINGLE IED ANALYSIS

The first set of data analyzed is a pass locating a single simulated IED. This data is plotted below in Figure 39. Three areas of interest are identified. During this test, the single simulated IED is emitting at a center frequency of 1.39 kHz before being placed.

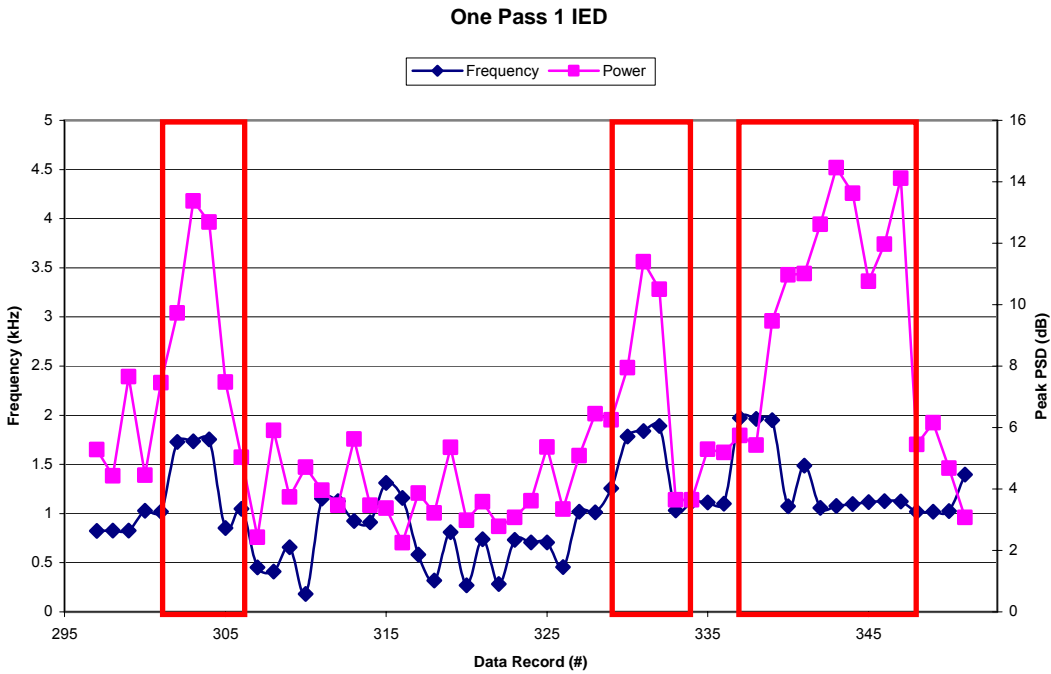


Figure 39. Single Pass Plot with one IED.

However this unit's frequency drifted as the testing took place. At the beginning of this pass, the center frequency is tagged at 1.72 kHz.

1. Area of Interest 1

The Power Spectral Densities (PSD) plots below correspond to data records 300 to 307. The TERN is heading east. From the below Figure 40, the simulated IED #1's Power Spectral Density (PSD) begins to build and by data record 302, the system is locked on the frequency at 1.728 kHz and with a PSD peak of -10.3 dB.

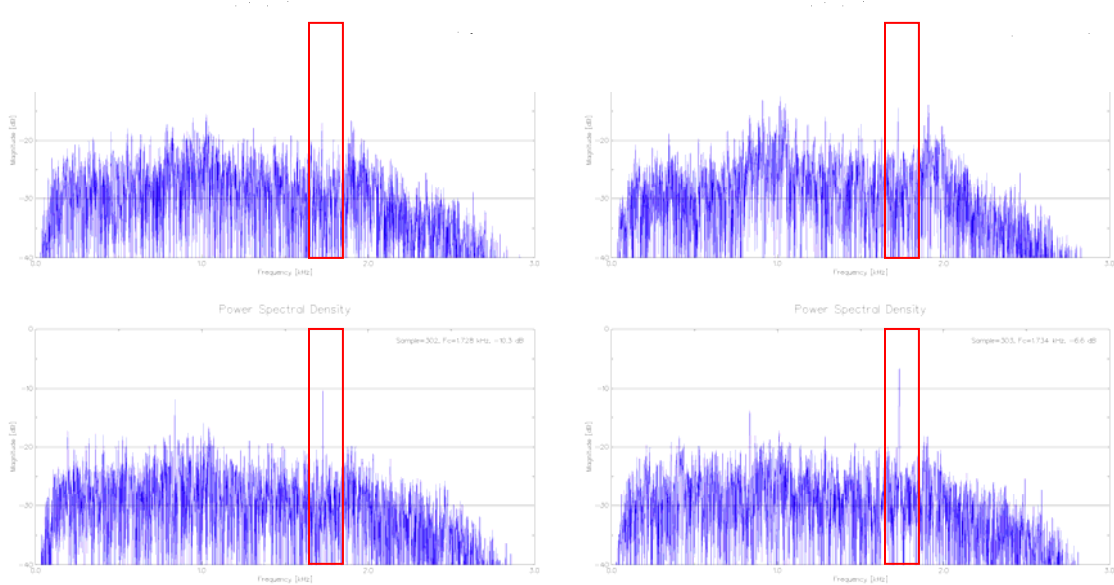


Figure 40. PSD-Plots for data records 300 to 303.

By the next data record, the PSD peak increases to -6.6 dB and reveals a nice narrow peak that is indicative of a good lock on the simulated IED. The noise floor remains around -20 dB. Continuing into the next group of PSD-plots in the below figure. A secondary signal at approximately 0.8 kHz appears to be manifesting as the TERN approaches and over flies the Simulated IED.

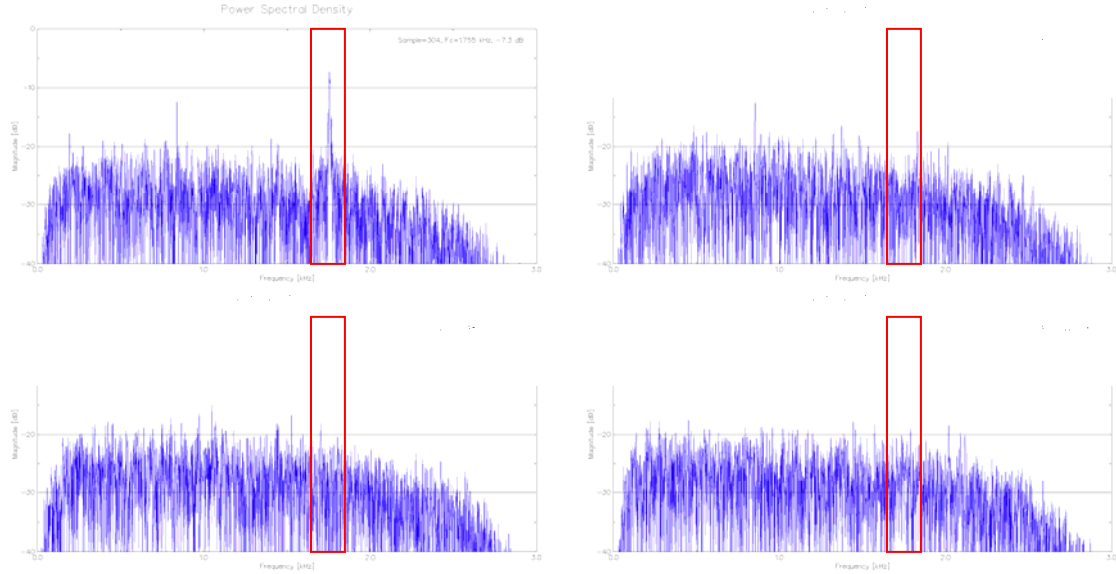


Figure 41. PSD-Plots for data records 304 to 307.

Data record 304 shows the closest plot to the signal. The Automatic Gain Control of the receiver kicked in and the noise floor shifts down about 5dB. This data record also shows considerable noise being averaged in with the simulated IED's signal as the peak begins to broaden out. This is also the time that the greatest change in Doppler frequency happens. This is due to the relative rate of change in the angle between the TERN's flight path and the simulated IED. Both signals disappear as the TERN over flies the Simulated IED. By the last PSD-plot, no signals remain and the system is picking up pure noise again.

2. Area of Interest 2

The below PSD-plots correspond to data records 328 to 335. The TERN is heading west. From the below figure, data

record 330 shows a solid hit for the expected signal at a center frequency of 1.78 kHz.

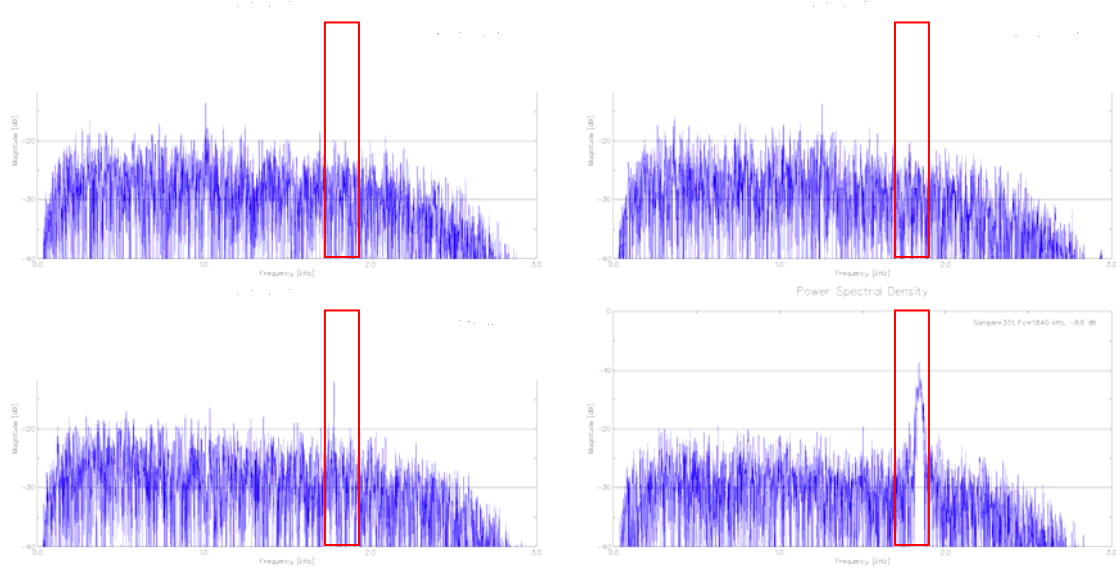


Figure 42. PSD-Plots for data records 328 to 331.

The data records prior to this one show no indications of the simulated IED. By data record 331, the TERN is approaching the closest point to the simulated IED and once again the signal begins to broaden out. In the next set of PSD-plots shown in Figure 43, the system gets one additional hit on the simulated IED before the TERN over flies the signal and receives only noise. Data record 332 shows a center frequency at 1.89 kHz.

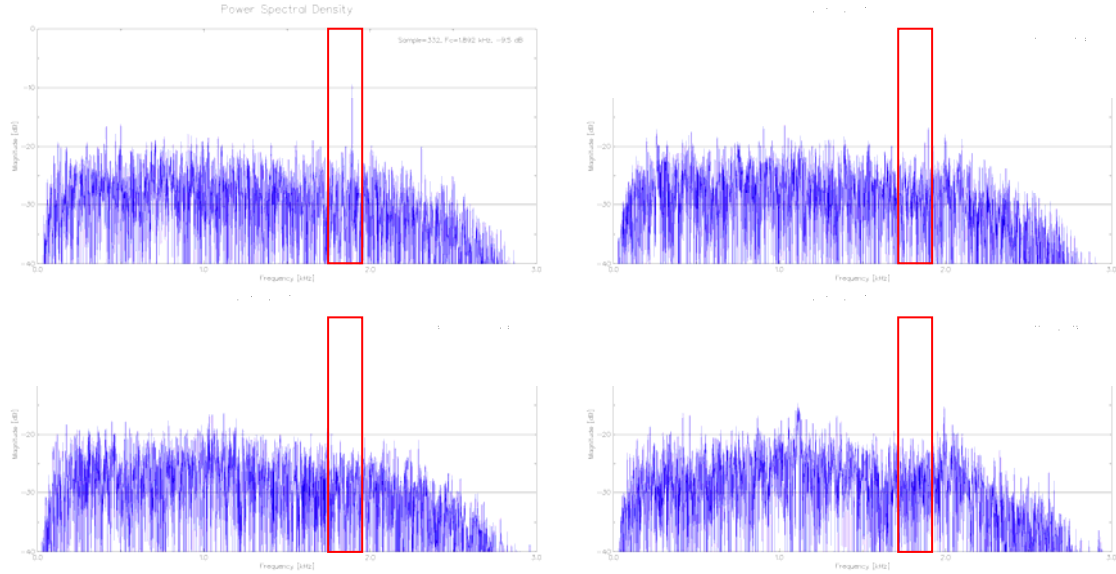


Figure 43. PSD-Plots for data records 332 to 335.

3. Area of Interest 3

The below PSD-plots correspond to data records 336 to 347. The TERN is in a north turn from 280 degrees magnetic to a heading of 100 degrees magnetic. This area of interest is the most intriguing of the single pass single IED plots as it corresponds to a situation that is not expected to see the simulated IED. The TERN is at the end of the runway turning north to make its next run at the simulated IED. The system should receive the normal noise as seen in data record 336 shown below in Figure 44. As the system antenna is turned perpendicular to the runway, wide band signals sources or noise begin to emerge.

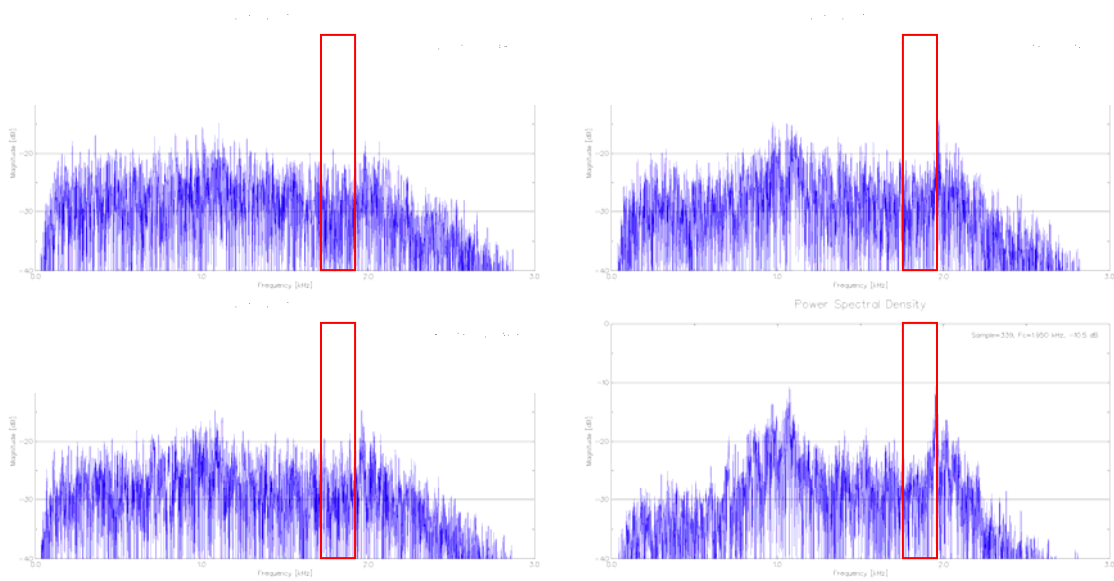


Figure 44. PSD-Plots for data records 336 to 339.

These peaks are seen in data records 337 and 338. By data record 339, both peaks have emerged, one centered at 1.95 kHz the other centered at 1.05 kHz. As data record 340 shows in Figure 45, the signals become so strong that the noise floor is pushed down below -30 dB.

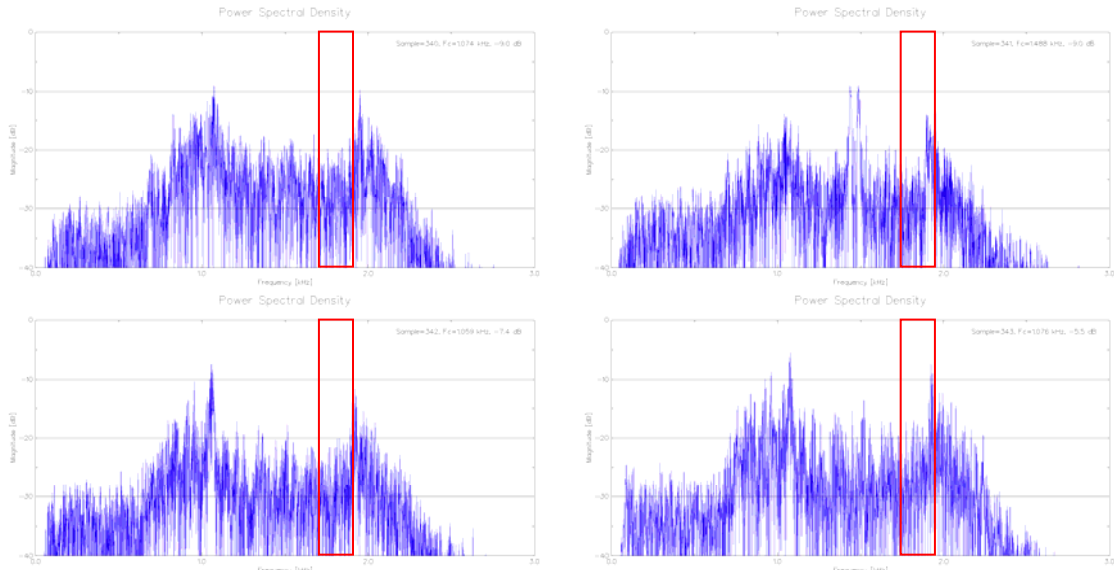


Figure 45. PSD-Plots for data records 340 to 343.

Data record 341 shows a wide band peak around 1.5 kHz which is not seen previously. The peaks continue through data record 346 shown in the below in Figure 46. The noise floor is pushed entirely off the display.

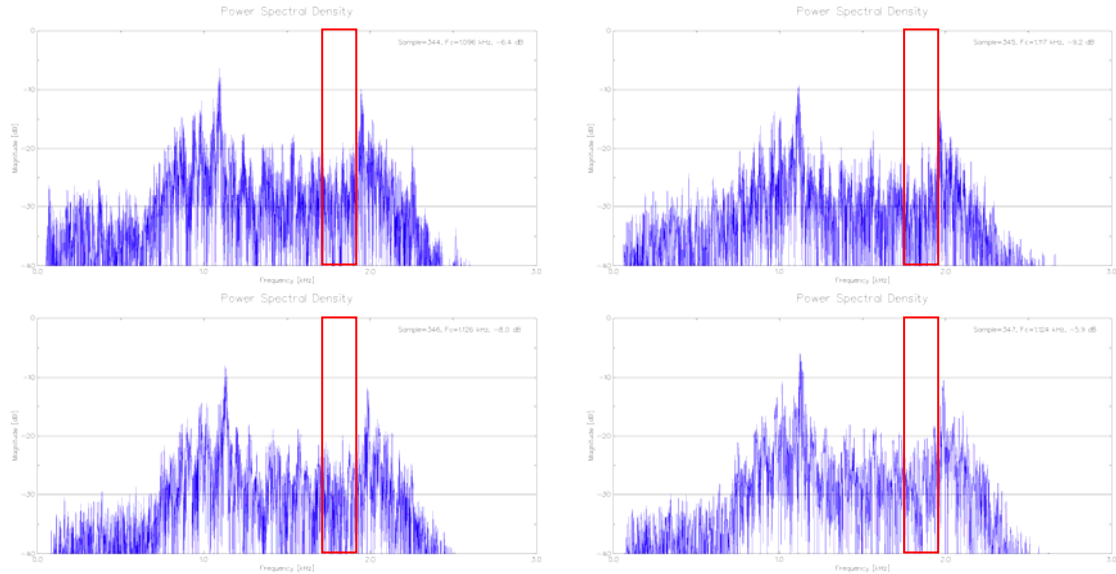


Figure 46. PSD-Plots for data records 344 to 347.

By data record 347, the wide band signal or noise begins to pass as the TERN completes its turn. This signal may be emitting from a government communications installation approximately one and a half miles north of the airfield, which is the direction the antenna is pointing. The PSD spikes shown at that end of the runway in a north turn are consistent throughout the experiment.

4. single IED Alternate Flight Profiles

The fist set of passes are flown at a relatively low altitude to ensure system operability. This is the first time the pilot is able to fly the TERN with the High Sensitivity RF Receiver onboard. Additionally, it is the

first time the RF system is flown on a UAV. The pilot quickly becomes comfortable flying the TERN and the RF system is sending good data records to the ground station. After a few passes, the additional three simulated IEDs are placed for multiple emitter passes. After completion of this series, the first simulated IED is placed at IED #3's position on the runway. The TERN is flown at alternate flight profiles against a single simulated IED in an effort to test limitations.

The first deviation in flight profile is in altitude. The Tern's altitude is incrementally increased after each pass to test the limits in altitude of the RF detection system. After several passes, the TERN's altitude is stabilized as it is currently flying at an altitude that exceeds expectations. The High Sensitivity RF Receiver's maximum height is never reached and follow-on tests need to be conducted to determine it.

The Second alternate deviation in flight profile is in range. The TERN's flight profile is extended in length to give the RF detection system a greater chance at detecting emissions at long ranges. A function of the High Sensitivity RF Receiver that is not tested is the in-flight capability to alter the data record length. This function increases the integration time available for the system to pull the signal out of the noise. Additionally, each data record can be averaged with the ones preceding it in an effort to gain an additional computative gain. Both these gains will be small. However, the system is dealing with long range detection. In this case, a few dB's can be the difference between detection and missing the IED. Both

capabilities are built into the system as a software function but time does not permit testing. The detection ranges determined from these tests are not included in this thesis. However, they are sufficient enough to cover the present needs of war fighters involved in combat today.

5. Single IED Conclusion

The field test performed in detecting a single simulated IED prove very successful. With further testing, full capabilities and limitations of the RF system will be found. Several trends appear. As the TERN approaches the IED, the tonal spike begins to broaden just prior to over flight. Additionally, these passes show the importance of the PSD-plot. Looking at frequency and peak PSD gives a good indication of a possible emitter. However, the truth lies in analyzing the PSD plot to determine the shape of the signal's spectral pattern.

F. MULTIPLE IED ANALYSIS

The second set of data to be analyzed will be a pass locating four simulated IEDs. This data is plotted below in Figure 47.

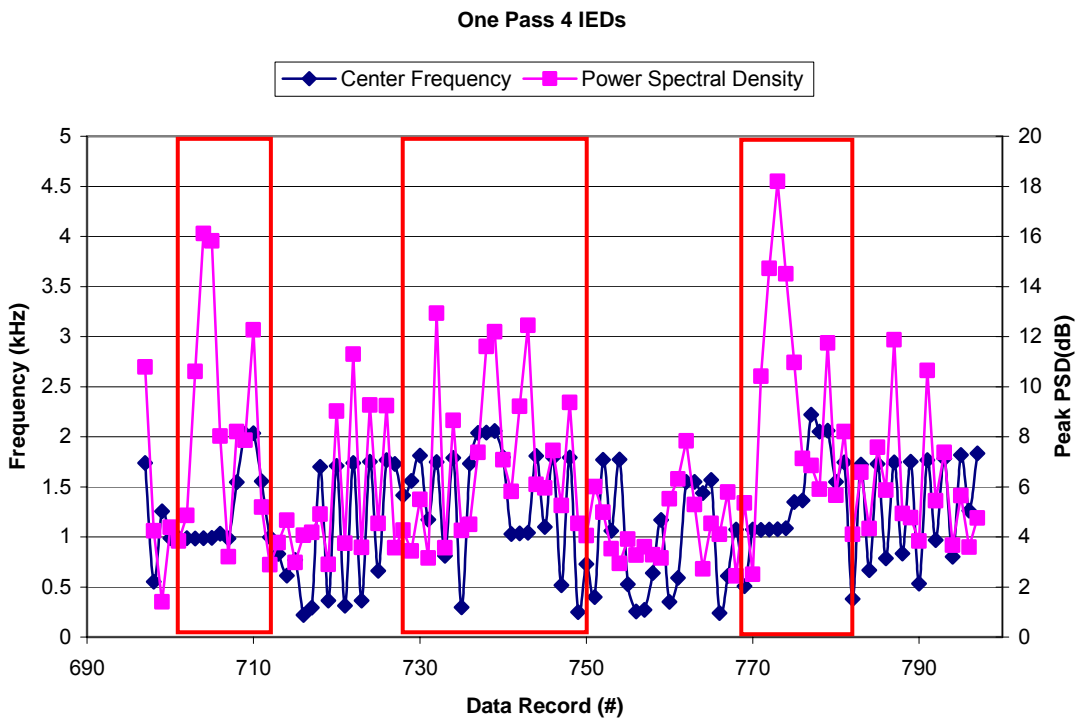


Figure 47. Single Pass Plot with 4 IEDs.

Three areas of interest are identified. Four simulated IEDs are present and had center frequencies as shown in Table 12. As seen, frequencies are drifting. Frequencies are tagged to a simulated IED during post-flight analysis. The most significant drift is seen in Simulated IED #3.

Simulated IED #	Center Freq before test (kHz)	Tagged Center Freq post flight (kHz)	Drift Direction
1	1.39	2.03	Higher
2	2.36	2.75	Higher
3	0.496	1.54	Higher
4	1.37	.98	Lower

Table 12. Table of Frequencies for four IED pass.

1. Area of Interest 1

The below PSD-plots correspond to data records 701 to 712. The TERN is heading east. With an east heading, the first simulated IED intercepted is number four. From data record 701 shown below in Figure 48, a PSD peak at that frequency is beginning to grow. By data record 703, the system is locked on to the simulated IED.

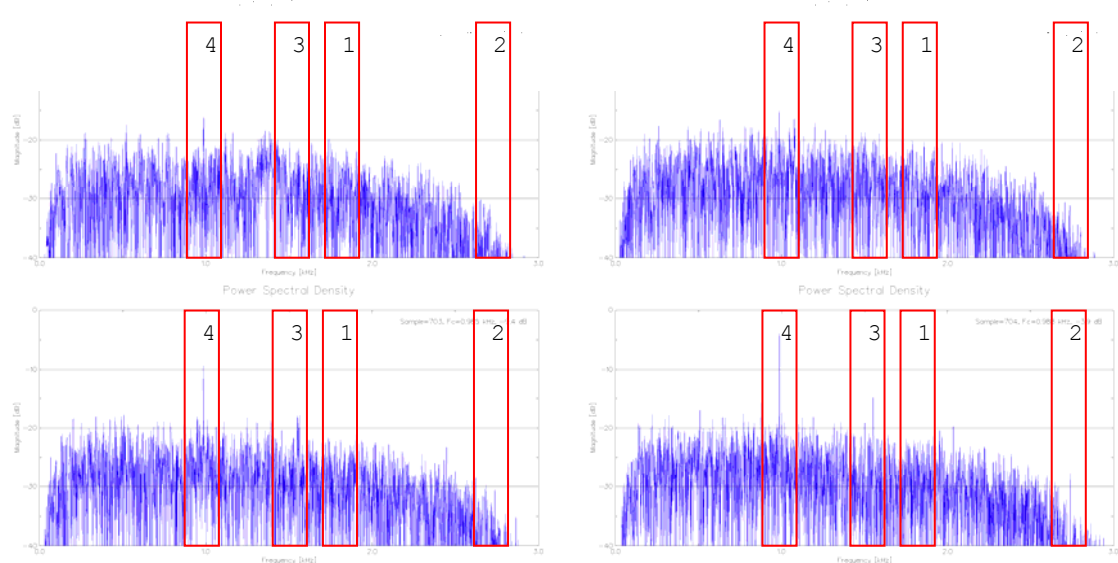


Figure 48. PSD-Plots for data records 701 to 704.

Additionally, the system is starting to pick up simulated IED #3, which is next in line. The next data record clearly shows simulated IEDs #4 and #3. Additionally, it is beginning to pick up simulated IED #2.

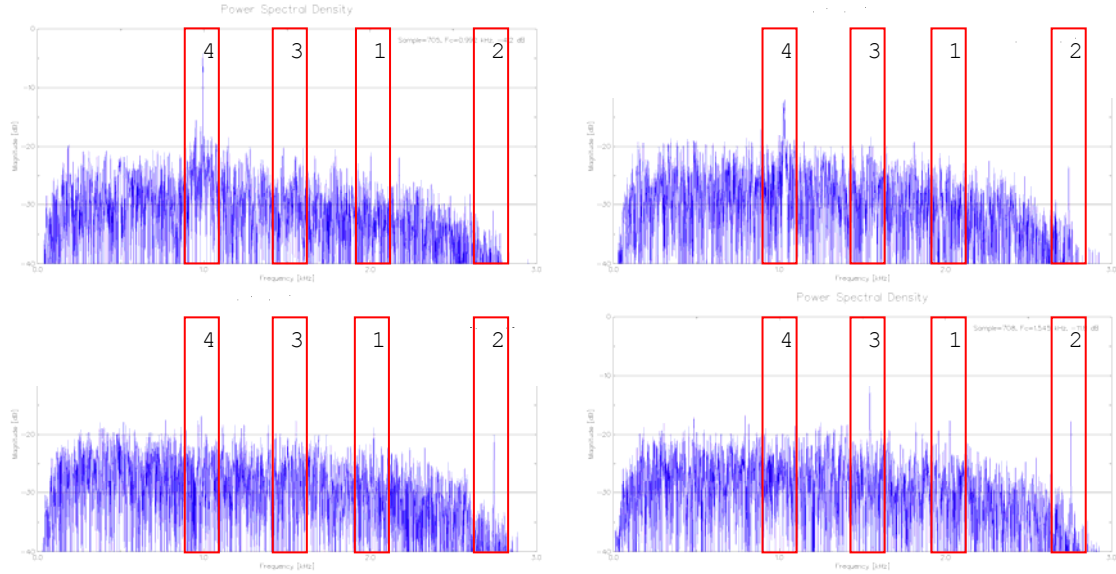


Figure 49. PSD-Plots for data records 705 to 708.

Data record 705 in Figure 49 shows the automatic gain control in the receiver pushing the noise floor and the rest of the signals as the TERN over flies Simulated IED #4. Data record 707 clearly shows simulated IED #2, yet because the signal is at the edge of the bandwidth, the system attenuates the signal. This attenuation is a function of the receiver. By decreasing the bandwidth processed, the amount of noise processed decreases. By increasing the bandwidth looked at, the signal from simulated IED #2 increases and the system locks onto the signal displaying its data. This is the trade off of including more noise in the processing. Data record 708 clearly shows simulated IED #2 being picked up by the system but at a peak PSD of only -16dB which is lower than the other signals. From Figure 50, data record 709 shows simulated IED #1 being locked onto.

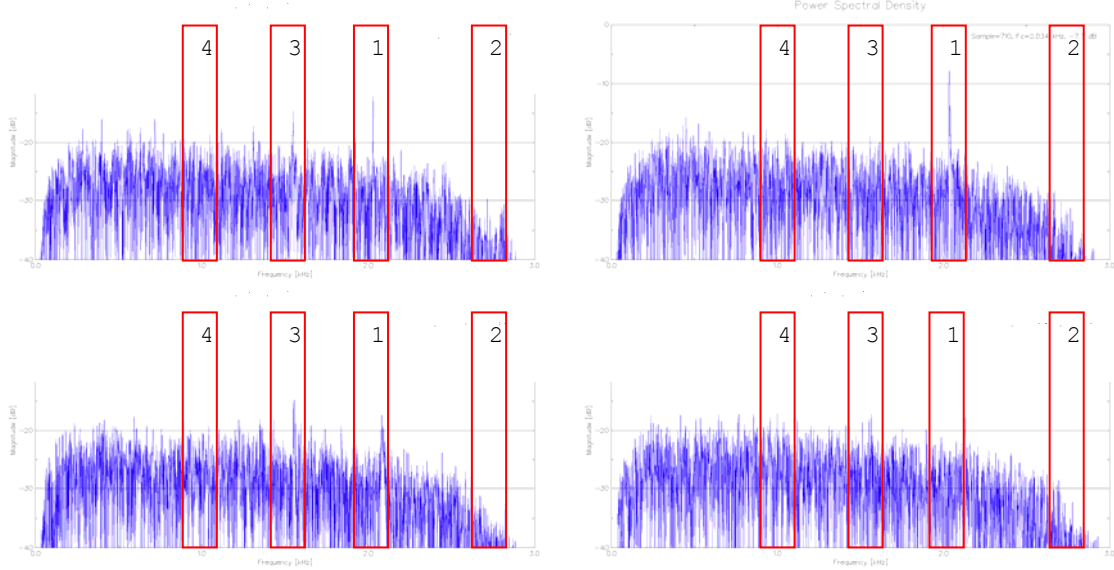


Figure 50. PSD-Plots for data records 709 to 712.

This signal is growing for the past 2 data records and is now the dominate signal. As the TERN continues to pass the simulated IEDs, the signals received begin to disappear. By data record 711, signals are no longer present. Some noise signals peak in the Simulated IED #3 area yet are simply noise spikes.

2. Area of Interest 2

The below PSD-plots correspond to data record 728 to 751. The TERN is heading west. Figure 51 shows 4 PSD-plots that display a standard noise pattern.

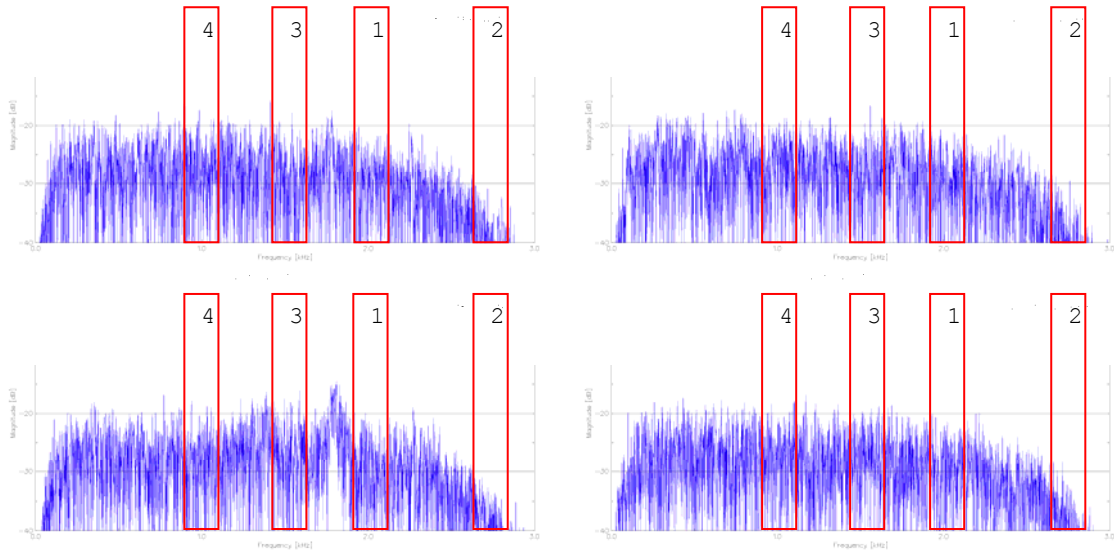


Figure 51. PSD-Plots for data records 728 to 731.

The first simulated IED encountered is number one. No indications are present for any true signal. Data records 729 and 730 show how random noise peaks either narrow or wide may show up as signals with good PSD levels yet are not a real signal. When dealing with a filter that works on PSD, this must be understood. This is further demonstrated in the next Figure 4 data records. These four data records, ending in 735, display two PSD peaks of wide band noise.

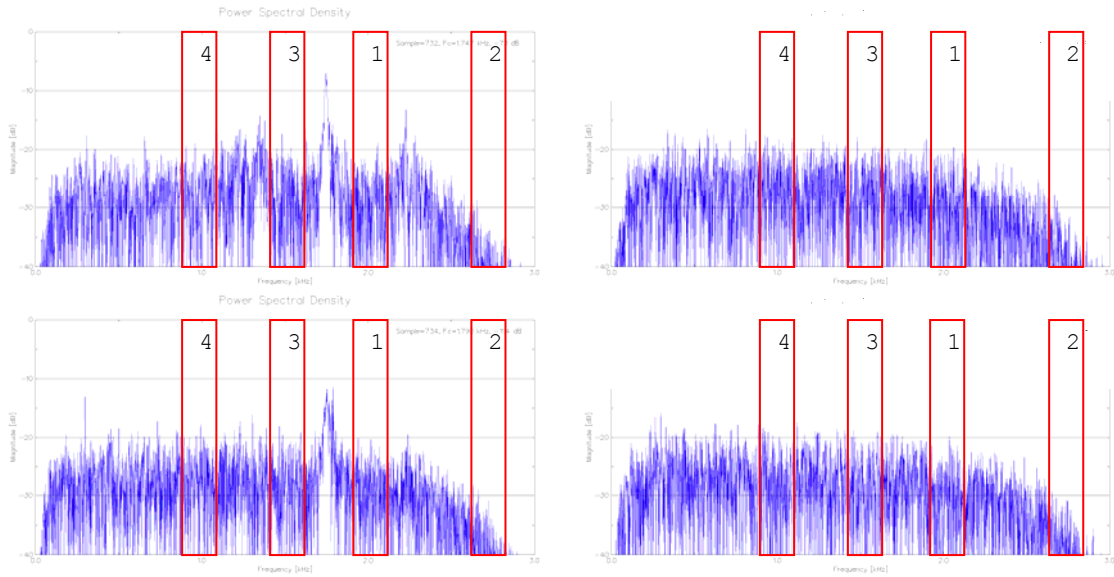


Figure 52. PSD-Plots for data records 732 to 735.

Data record 735 begins to display simulated IED #1. The next four data records in Figure 53 are observed to confirm this. Data record 736 shows a small peak where simulated IED #1 appears, yet the PSD level of -17 dB is not high enough to break out of the noise as it does in data record 737.

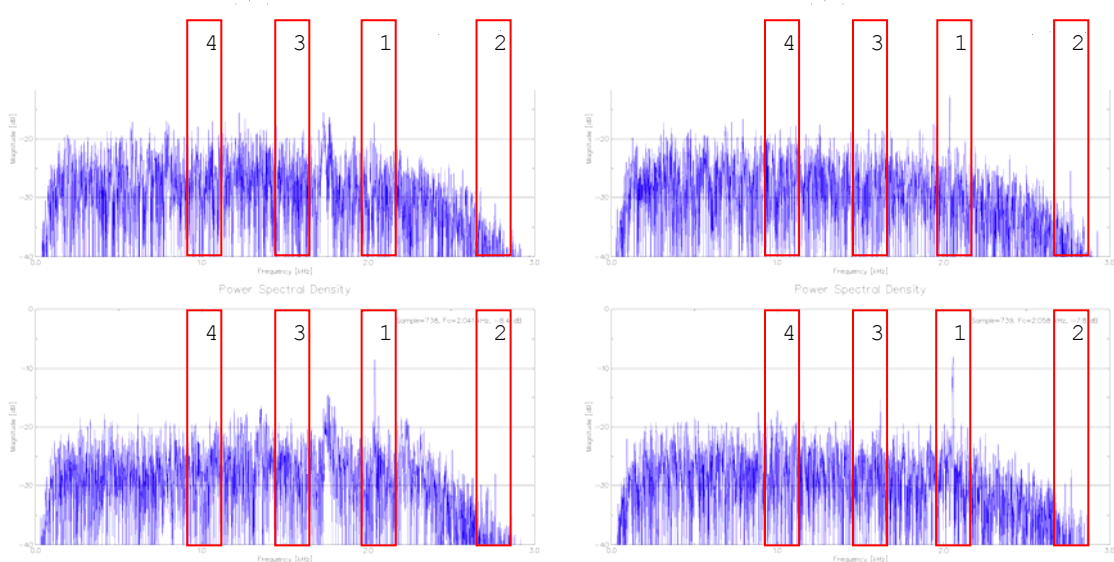


Figure 53. PSD-Plots for data records 736 to 739.

The center freq is displayed as 2.039 kHz with a PSD peak of -12.6 dB. Furthermore, simulated IED #2 begins to break out and by data record 738 is clearly displayed. Data record 739 shows a peak that simulated IED #3 should be at yet does not appear in data record 740 of Figure 54. By data record 741, the TERN passes simulated IED #1 and is about to pass Simulated IED #2.

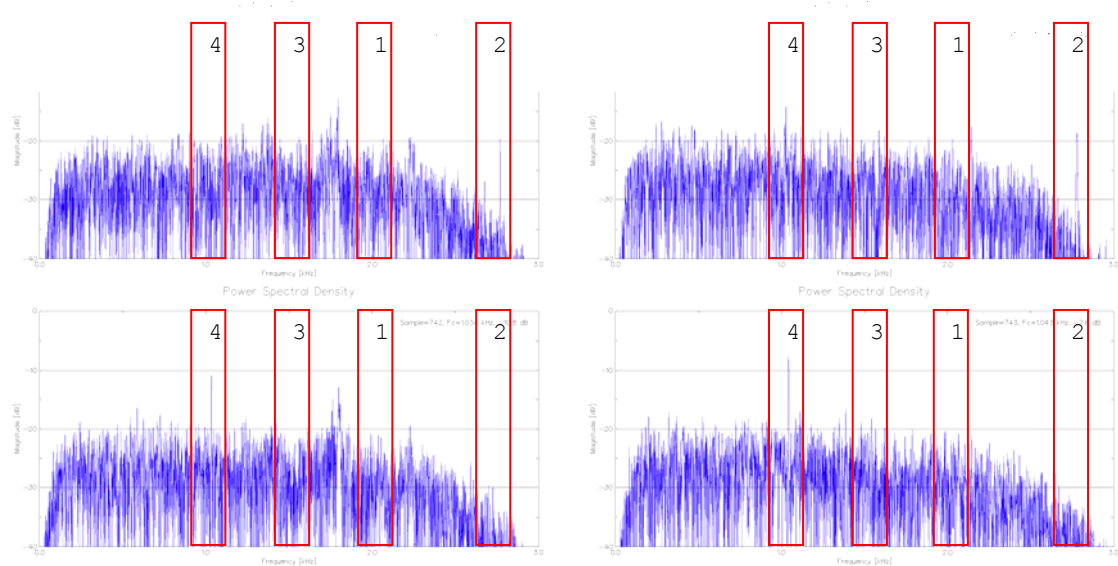


Figure 54. PSD-Plots for data records 740 to 743.

It also shows the beginnings of simulated IED #4. By data record 742, Simulated IED #4 is clearly visible and the system is lock on displaying a center frequency of 1.03 kHz and a peak PSD of -10.8 dB. By data record 744 in Figure 55 below, the TERN is about to pass the last simulated IED in the run.

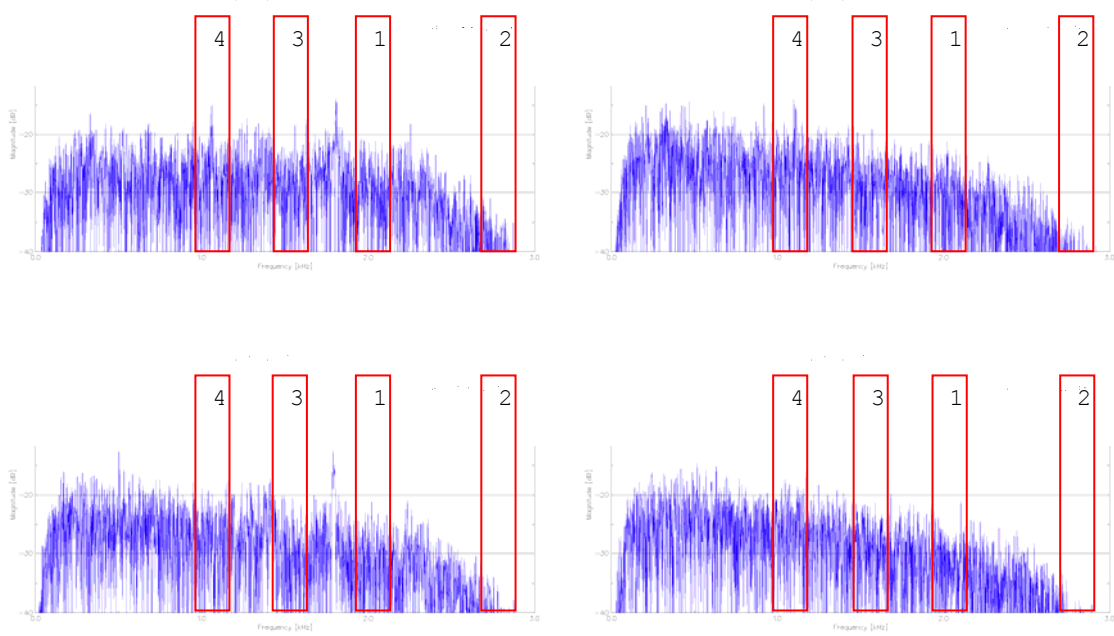


Figure 55. PSD-Plots for data records 744 to 747.

Data record 746 shows no real signal and a noise spike around 1.8 kHz. Further noise spikes are displayed in the next figure. These data records appeared interesting from the original One Pass Four IED plot but simply show noise spikes upon closer examination.

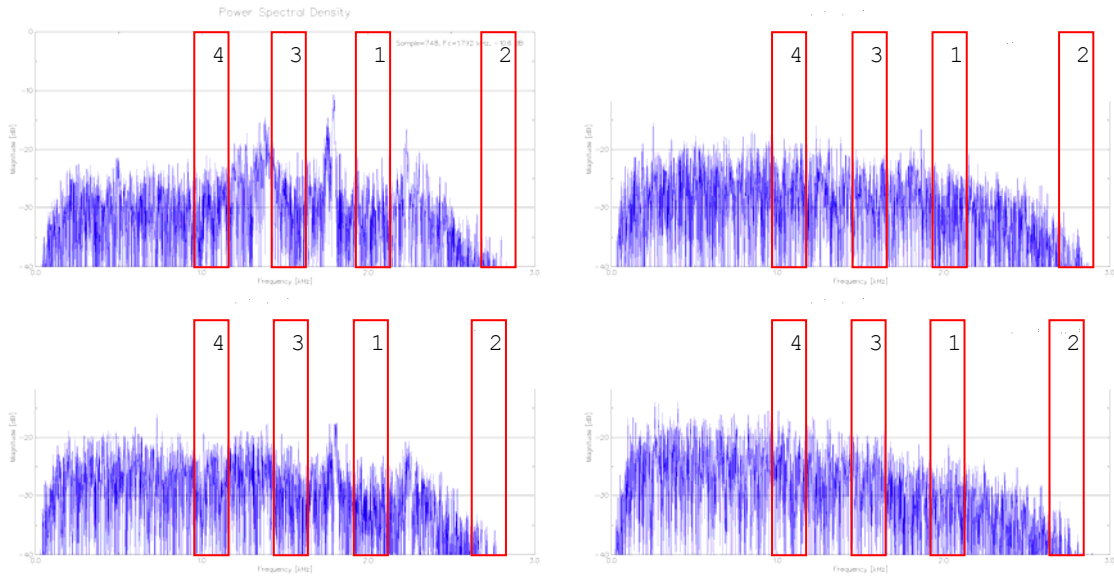


Figure 56. PSD-Plots for data records 748 to 751.

3. Area of Interest 3

The below PSD-plots correspond to data records 768 to 783. The TERN is heading east. From Figure 57, data record 768 shows possible indications of Simulated IED #4, the first of the 4 simulated IEDs for this run.

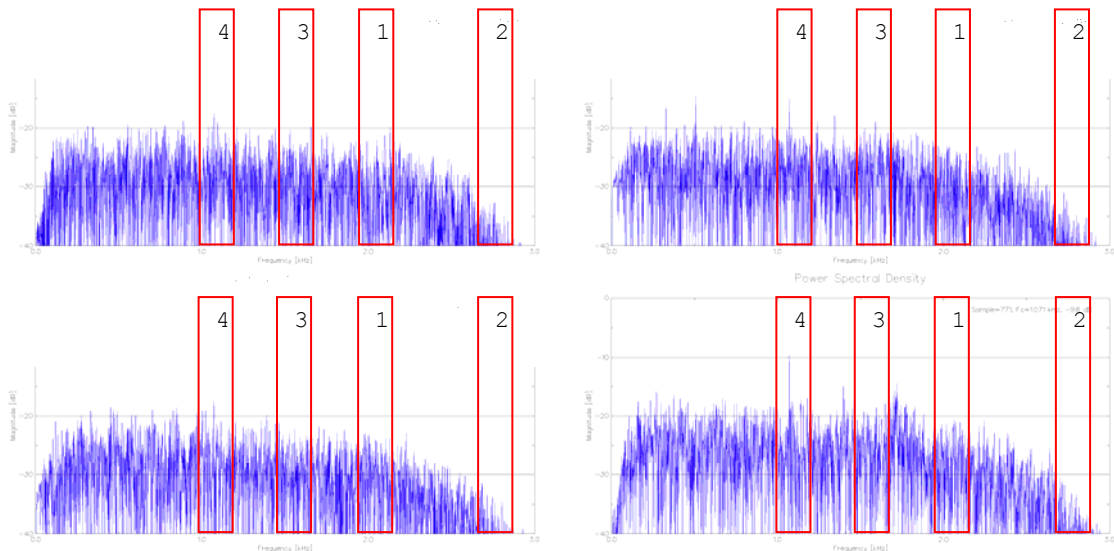


Figure 57. PSD-Plots for data records 768 to 771.

The next data record clearly shows a real signal but a noise spike at 0.507 kHz is locked onto by the system. By data record 771, the system is locked onto the signal displaying its center frequency as 1.071 kHz and a peak PSD level of -9.6 dB. Data record 772 of Figure 58 may display a hit from simulated IED #3, or it may have drifted.

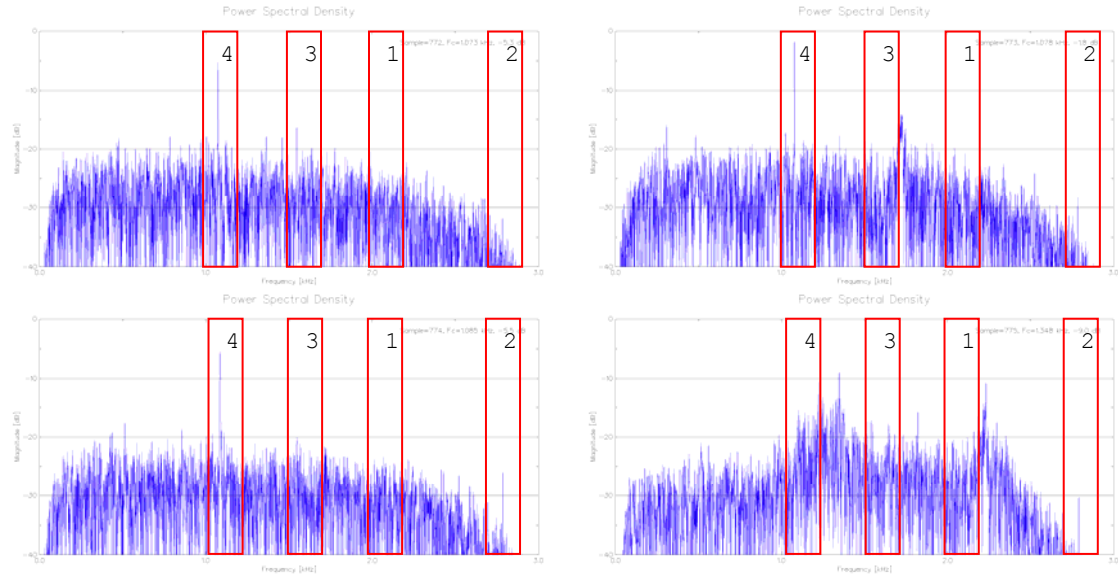


Figure 58. PSD-Plots for data records 772 to 775.

For this pass, a wide band interference signal appears, as seen in data record 775 and continues through data record 777 in Figure 59. This interference triggers the automatic gain control of the receiver and reduces the signals PSDs.

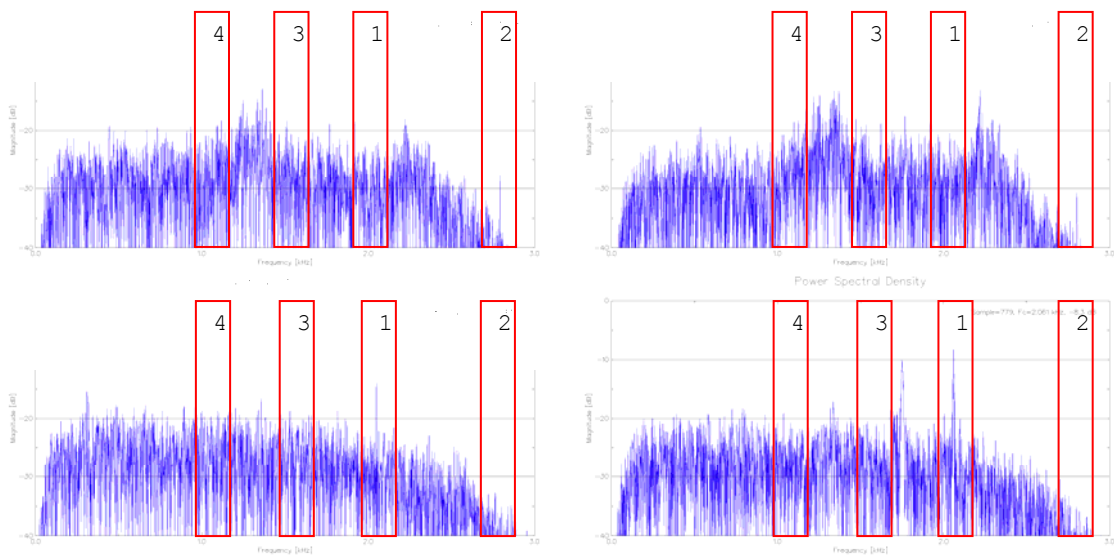


Figure 59. PSD-Plots for data records 776 to 779.

Data records 775 through 778 show simulated IED #2 gaining strength and peaking in data record 777. Simulated IED #1 begins to break out in data record 778 and is strong enough to lock the system. The system displayed the signal as having a center frequency of 2.05 kHz with a PSD of -14.1 dB. Data record 779 shows the TERN about to over fly the simulated IED #1.

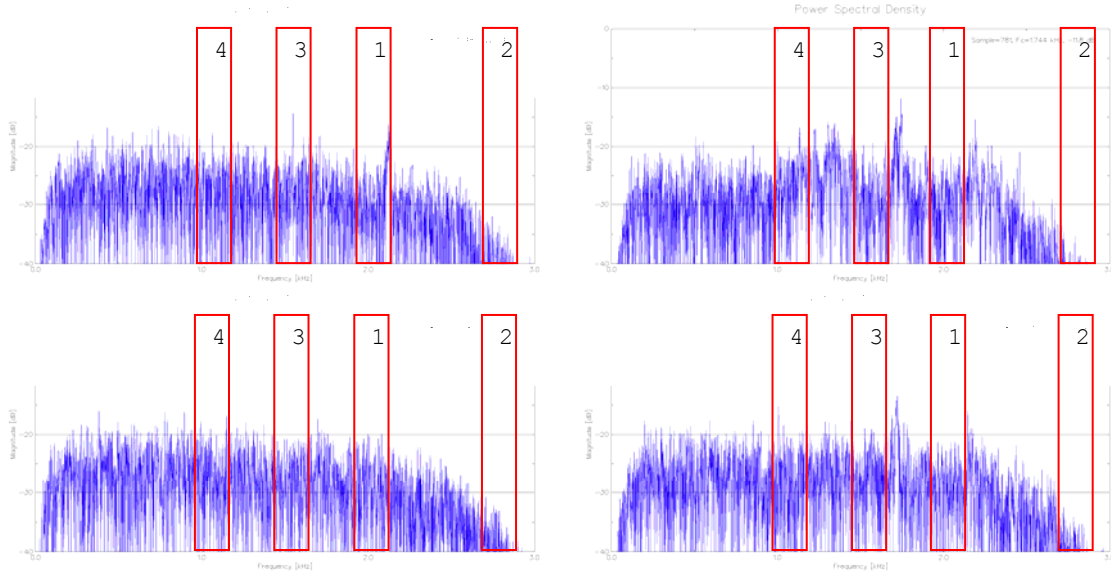


Figure 60. PSD-Plots for data records 780 to 783.

Figure 60 shows the last four PSD-plots of this area of interest. These data records are dominated by noise with no real signal present.

4. Multiple IEDs Conclusion

An interesting observation from this series of test is the effect of wind speed on detection range. The High Sensitivity RF Receiver's detection range is greater when flying into a headwind. This is logical as it decreases the groundspeed of the TERN allowing the system greater time to process the signal. The RF systems ability to pick up multiple signals is clearly displayed in this test series. Multiple detections are common and in some cases three signals are present for the highly successful test. Such a case is shown in data record number 708 which shows three signals on one plot.

This series also shows the importance of setting the bandwidth over which the system looks. Simulated IED #2 is never locked on by the RF system due to attenuation of that IED's signal at the edge of the bandwidth. Shifting the bandwidth up in frequency allows the system to lock this signal. It also shows the amount of drift within the system. Either the simulated IED's local oscillators are drifting or the receiver's local oscillators are drifting. Simulated IEDs are in direct sunlight for over an hour experiencing a significant temperature differential. The System's receiver portion is placed in a UAV and flown. The altitude at which the TERN flies does not experience low temperatures, but the system forces circulation of air from the TERN's forward motion. What ever the cause, the RF signals drift considerably.

G. POWER SPECTRAL FILTERING

The power of the target emitter is used to filter data prior to being displayed to the user. Setting a threshold that the signals power spectral density must meet prior to being displayed reduces the monitoring burden of the operator. This is a task that humans are not well suited to. As seen in the below graph, there is a large number of signals to be analyzed as the TERN collects data records.

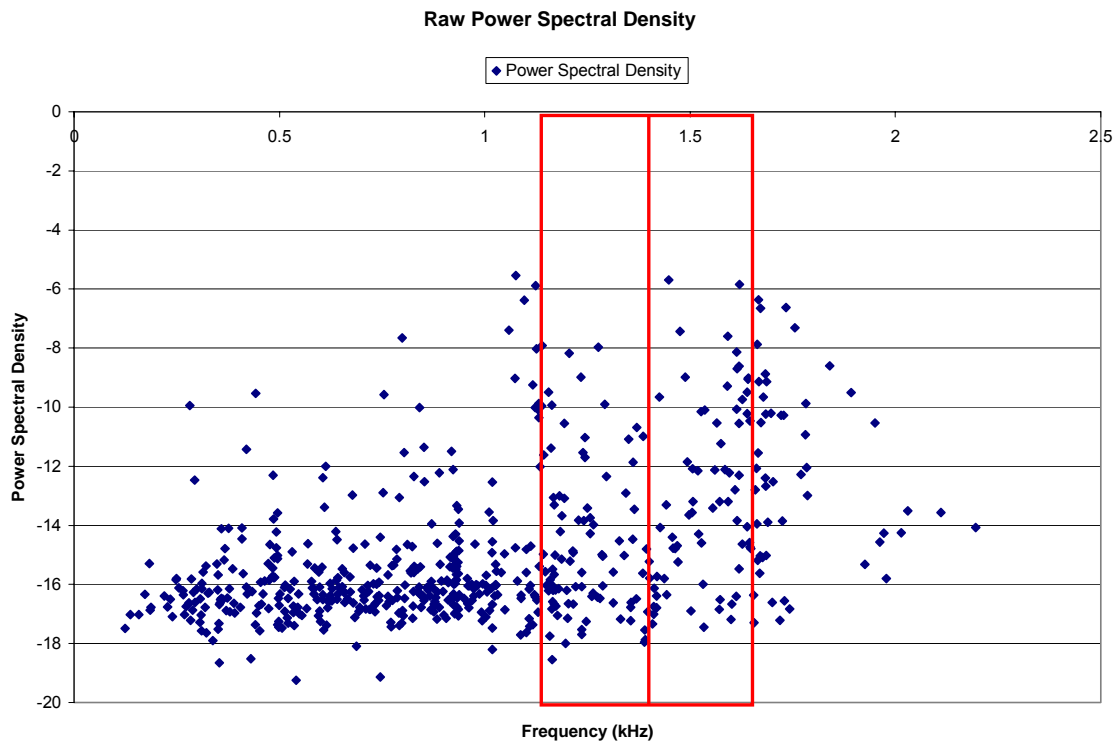


Figure 61. Unfiltered Power Spectral Density Plot.

With 595 data records, the operator has a hard time determining if there is a real emitter present. This is the idea behind the Tonal box in the ground station display discussed earlier. The plot below shows the same period covered, yet only displays the signals that are higher than -10dB.

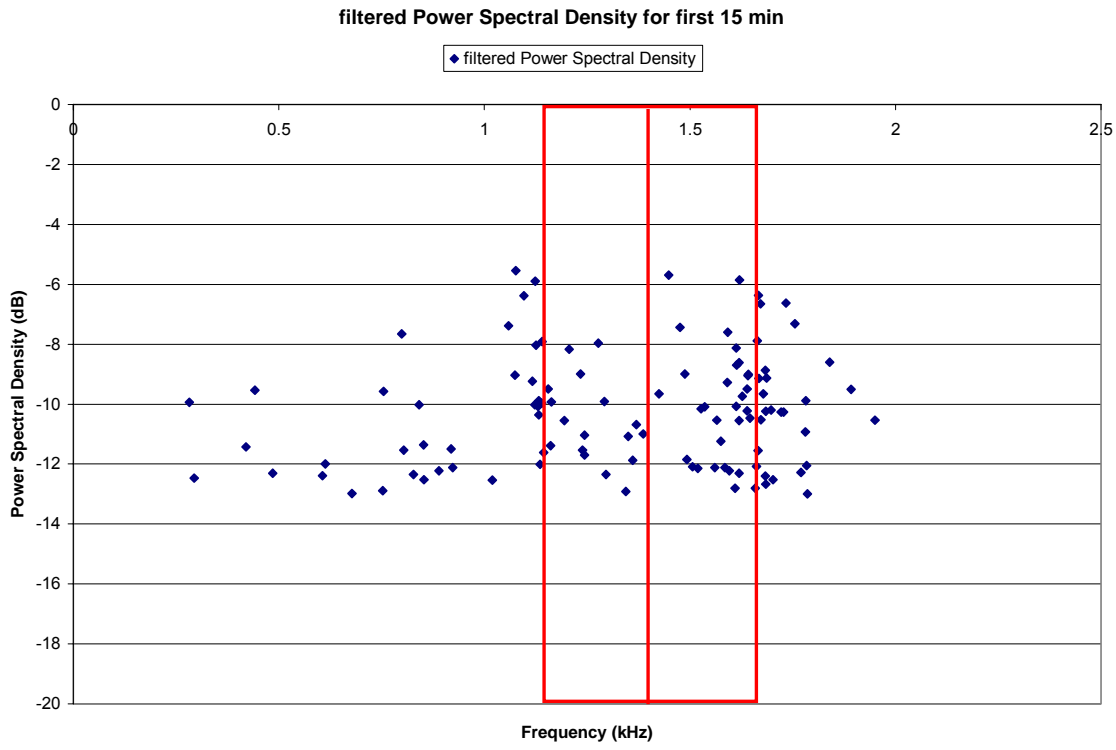


Figure 62. Filtered Power Spectral Density Plot.

This reduces the displayed data to 163 signals, a 72.6 percent reduction. This drastically reduces the number of false targets. The areas boxed in red indicate the center frequency of the emitter plus or minus 400 Hz. There is some drift in the emitter and the direction of drift is unknown. Simulated IEDs are powered up over an hour prior to testing in an effort to reduce warm up variations. There is a trade off when setting the threshold. By setting it high, the number of false targets decreases, yet the chance of missing a valid target increases. By setting it too low, the chance of missing a real target decreases, yet more false targets must be analyzed.

H. CONCLUSION

Both the single and multiple IED test are highly successful. The High Sensitivity RF Receiver performs better than expected and with further refinement, improvements in capabilities will be seen.

Signal detection requires careful analysis of the power spectral densities. By first determining areas of interest, post flight analysis of the large number of data records are efficiently accomplished. This is a procedure that is ideal for computers. Computational algorithms that analyze the signal's PSD are currently being developed and can soon be tested. This will greatly increase the effectiveness of the overall system by reducing the burden of the operator.

A wideband source is present during testing. Post flight analysis is able to localize the source north of the field. The wideband noise's shape is indicative of FM communications signals and demonstrates the High Sensitivity RF Receiver's ability to pick up varying types of signals.

This configuration of the High Sensitivity RF Receiver is demonstrating that the concepts upon which it is built are sound. However, this system is a test platform constructed from off the shelf equipment. As a test system, its continued development is limited to refining the system for small gains. This will do little in truly advancing the system's capabilities. To accomplish this, the High Sensitivity RF Receiver must be built from the ground up. Only this will truly define the limits of this type of system. The current RF system's detection range covers most

situations that combat troops are involved in. However, the enemy is ever changing and what is true today may not be true tomorrow.

VI. FUTURE DEVELOPMENT

The High Sensitivity RF Receiver is proven to work with these technical feasibility demonstrations and tests. By placing it on an UAV, the detection range is drastically increased. The UAV is not tied to ground troops, hence the detection range is realistically increased to that of the UAV's range capabilities. The field tests prove the RF system can be flown at higher altitudes.

Future development of the High Sensitivity RF Receiver should be developed along three paths. The first future development must take the existing High Sensitivity RF Receiver out of the TERN, reduce the payload dimensions and place it into a theater available UAV such as the Scan Eagle. This can and should be done first. Additionally, the System should be reconstructed into a cheap and easily produced hand held version for employment with front line troops down to the infantry platoon level. Lastly, an active detection system version should be developed to further increase the detection range of the system.

A. SCAN EAGLE

The TERN UAV is an ideal testing platform for many reasons. It is easily modified to accommodate the High Sensitivity RF Receiver system as a front end payload. It is capable of carrying over 25 lbs. This allows the design of the payload to not be streamlined for weight. Because of its size, it has stable flight characteristics allowing for the mounting of external antennas with minimal effects. However, the TERN UAV is a test platform, and as such, it is

not available to the troops on the front lines in the war on terror. These troops are the ones who can benefit from this high performance detection technology. UAV systems available include the Pioneer, Predator, Hunter and Dragon. However, the majority of UAVs, including the Hunter, Predator and Pioneer, are limited assets that are rarely used in support of small units outside of Special Forces. Other UAVs, such as the Dragon are too small to be realistically used by the High Sensitivity RF Receiver. The Dragon is almost solely used with small cameras that weigh ounces.

The best UAV option for use is the Scan Eagle. The Scan Eagle was a possible testing platform but was not selected because it required major modification to streamline the system. However, the RF detection system is proven to work in the TERN, and it can easily be streamlined for mass production. The Scan Eagle is quickly becoming an increasingly available asset in country. The Scan Eagle is currently deployed with the US Marine Corps in Iraq, where the system flew over 4000 hours by July of 2005¹⁹. These numbers will only increase as the demand for UAVs also increases. The Scan Eagle's follow-on model will employ the same designs, and increase the payload capabilities of the existing Scan Eagle. At the time of testing, both Scan Eagles on loan to the Naval Postgraduate School are damaged and in need of replacement. Figure 63 below shows a Scan Eagle before a mission in Iraq.

¹⁹ Online defense update magazine found at [<http://www.defense-update.com/products/s/scaneagle.htm>], September 2007.



Figure 63. Scan Eagle UAV. (From Boeing)

The NPS Scan Eagles are being replaced and will be operational for future testing and evaluation of the High Sensitivity RF Receiver. Further modification will only improve the system and increase reliability as drivers are updated. This allows for the system to streamline the boot up and operation of the system. As seen in the picture of the Scan Eagle, it is substantially smaller than the TERN yet, with modification, the High Sensitivity RF Receiver will be an important augment to the Scan Eagle's payloads.

B. TROOP PORTABLE UNIT

The second future development deals with a handheld version of the High Sensitivity RF Receiver. While there are systems in theater which may be capable of performing this mission, they are complex and require special training to operate. Additionally, their primary missions are Intelligence, Surveillance and Reconnaissance (ISR). These systems are not provided to a standard infantry platoon. The portable unit could be used by the troops. Because the

system only needs limited computing power, the onboard computer may be replaced by a palm pilot. The system can be repackaged into one unit and housed in a unit similar to that of the radar guns used by police to measure speed. With palm pilots capable of using SDRAM, area specific threat libraries can be installed. The figure below shows the Cross Match personal identity verification (PIV) system. This system is built around a palm pilot interface.



Figure 64. CrossMatch PIV system. (from CrossMatch Technologies)

The High Sensitivity RF Receiver System would have to be redesigned or repackaged to fit into a unit similar to the one in Figure 64. First the preamplifier, receiver and digitizer would have to be built instead of using commercial units. The original RF system is designed for long range detection. From the below figure showing characteristics of common rounds, the detection ranges needed are considerably less.

Caliber	60 mm	81 mm	105 mm (1)	155 mm	227 mm (1)	607 mm (1)
Model	M224	M252	M119A	M198	MLRS	ATACMS
Max Range (m)	3,500 (2)	5,600 (3)	11,500	18,300 22,000(4)	32,000 45,000 (5)	165,000 300,000(6)
Ammo	HE, WP, ILLUM	HE, WP, RP, ILLUM	HE, HC WP, ILLUM, APICM	HE, HC, WP, ILLUM, APICM, DPICM, M825 Smoke, FASCAM, CPHD	DPICM	APAM
Max Rate of Fire (RDS/Min)	30	35	10	4	12/40 Sec	2/20 Sec
Sustnd Rate of Fire (RDS/Min)	20	15	3	2	N/A	N/A
Range of RAP (m)	N/A	N/A	19,500	30,100	N/A	N/A
Range of DPICM	N/A	N/a	14,100	18,000 28,200 (7)	N/A	N/A
Min Range (m)	75	70	N/A	N/A	10,000 13,000	25,000 70,000
Fuzes	MO	MO	PD, VT, MT, MTSQ, CP, Delay	PD, VT, MT, MTSQ, Delay	ET	ET
ILLUM TIME (SEC)	25	60	75	120	N/A	N/A
HE BURST WIDTH (1 RND)	28	35	35	50	100	N/A
PPF	90 3 Tubes	35 1 Tube	210 6 Guns	300 with 6 Guns	N/A	N/A

NOTES:
 1.) U.S. Marine Corps units do not possess these weapons systems. However, Marine Corps units may operate with Army units equipped with these weapons. 2.) With M720 ammunition. 3.) With M821 ammunition. 4.) With M795 HE, M825 smoke ammunition. 5.) BBDPICM M864. 6.) ATACMS.

LEGEND: ATACMS = Army Tactical Missile System MT = Mechanical Time (Fuze)
 ET = Electronic Time MTSQ = Mechanical Time Superquick (Fuze)
 HC = High Capacity RAP = Rocket-Assisted Projectile
 ILLUM = Illumination MO = Multi-Option Fuze (VT, PD, Delay)

Figure 65. Characteristics of common Artillery rounds (from the USMC FAC Handbook).

Typical IEDs consist of 155mm artillery rounds. The high explosive burst width of a 155 mm artillery round is 50 meters (164 feet). With these ranges, the design purpose of a troop portable version of the High Sensitivity RF Receiver would be compactness and not detection range. The system can be reduced to a few pounds which can easily be carried by a member of an infantry platoon.

The primary use of a troop portable version would be in detecting RF IEDs at a safe distance. The High Sensitivity RF Receiver system provides this capability both easily and

cheaply. It is capable of determining the presence of RF emitters in a local area. In most instances, a reduced detection capability would not be a benefit. However in an environment of high RF activity, this provides an aspect of discrimination. The ability of the RF system to be directed at a suspected IED emplacement, than detect a passive RF emitter provides a great capability.

C. ACTIVE DETECTION

The High Sensitivity RF Receiver system is designed to be a passive system. An alternate way of increasing the detection range would be to implement an active detection portion to the system. This technique has been used in radar systems as well as sonar. In both cases, a portion of the system sends out a signal. The target reradiates the signal. A second portion of the system detects the reradiated signal. The strength of the return signal is diminished as a function of the square of the range. However, when dealing with passive emitters such as those associated with RF IEDs, the unintended emissions are incredibly low to begin with. This is why coherent integration is required to pull the threat signals out of the noise. By implementing an active component into the system, the front half of the IED receiver including the antenna acts as a reflector and reradiates the incoming signal. This pulse can be higher in power than the unintended emissions and if so will increase detection range. This is similar to the use of mirrors as safety devices for downed aviators. By reflecting sunlight, the downed aviator can be visually spotted at incredible ranges

by search aircraft. In this scenario, the IED itself becomes the mirror and the active RF signal becomes the sunlight.

An active component can easily be employed in either a vehicle mounted version or a UAV version of the RF system. For a vehicle mounted version, almost all the system components would be the same. The addition of a duplexer, transmitter and modulator as shown in the below figure would allow for an active component to be implemented into the High Sensitivity RF Receiver system. On a vehicle mounted system, the additional weight would add little to the overall package.

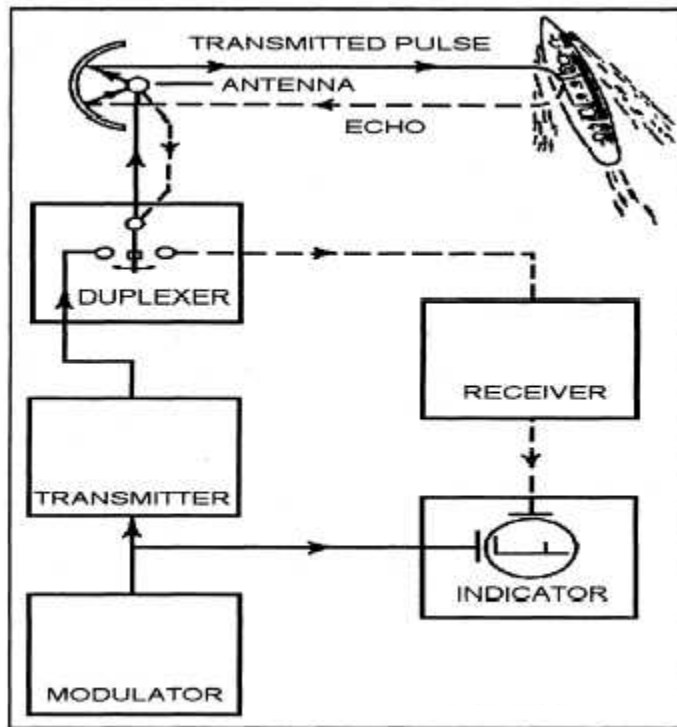


Figure 66. Standard Radar block diagram.

D. JAMMER INCORPORATION

Additional benefits not only include increased detection range but upon detection of a signal, the active component can switch to a jamming mode and block the detonation signal. Incorporating an active jammer into the system dramatically increases the overall systems capabilities. Marrying up the detection capabilities of the High Sensitivity RF Receiver System with a Smart Jammer creates several advantages for the overall system.

Knowing the frequency of the RF IED allows for smart jamming waveforms or spot jamming instead of wideband jamming. This increases the power of the jamming since it can concentrate at that frequency instead of spread out over a large frequency band. Because the jamming frequency is narrow, interference with communication units can be avoided.

An active jammer component implemented on UAVs provides interesting possibilities. With a single UAV, the RF system similar to a TERN can be used. The extra weigh reduces the possibility of using the current Scan Eagle. The follow on version of the Scan Eagle increases payload capabilities and can possible carry an active version of the High Sensitivity RF Receiver system.

Multiple UAVs working in a networked fashon create even more capabilities. Multiple Scan Eagles working together allow one to carry the passive components of the system. Additional Scan Eagles can carry the active components. By using multiple Scan Eagles, greater areas can be covered.

This can also be accomplished in a air to ground operation. The High Sensitivity RF Receiver can work in a passive mode in order to detect the emissions of an IED. Upon detection, it can pass this information over a network to ground based convoys employing jamming until they are either out of range of the UAV's signal or the blast range of the IED. The airborne system can perform additional actions to localize the IED and send a grid to Explosive Ordnance Disposal (EOD) units to remove it.

E. CONCLUSION

The High Sensitivity RF Receiver is proven to work in a ground based version. The technical results presented in this thesis prove the High Sensitivity RF Receiver works well from a UAV platform. With further modification and development, this RF detection system can provide a dramatic capability to the front line troops in the war on terror.

THIS PAGE INTENTIONALLY LEFT BLANK

APPENDIX A. ANTENNA LAB VOLT RESULTS

Results from Lab Volt Antenna Training and Measuring System							
Angle	LPY41		Dipole	Angle	LPY41		Dipole
	E	H	E		E	H	E
0	5.45	5.4	-0.12	180	-15.38	-17.5	-0.51
1	5.43	5.4	-0.11	181	-15.38	-17.5	-0.51
2	5.42	5.37	-0.12	182	-15.6	-17.17	-0.49
3	5.43	5.38	-0.13	183	-15.38	-17.17	-0.51
4	5.42	5.37	-0.13	184	-15.38	-17.17	-0.49
5	5.43	5.35	-0.12	185	-15.38	-17.17	-0.5
6	5.41	5.34	-0.13	186	-15.38	-17.17	-0.49
7	5.37	5.35	-0.16	187	-15.18	-16.87	-0.51
8	5.37	5.34	-0.19	188	-15.38	-17.17	-0.52
9	5.34	5.34	-0.22	189	-14.98	-16.58	-0.54
10	5.28	5.32	-0.27	190	-14.98	-16.58	-0.58
11	5.27	5.29	-0.31	191	-14.8	-16.32	-0.59
12	5.24	5.28	-0.34	192	-14.8	-16.32	-0.63
13	5.2	5.27	-0.41	193	-14.8	-16.06	-0.66
14	5.13	5.26	-0.48	194	-14.62	-16.32	-0.69
15	5.1	5.26	-0.54	195	-14.45	-16.06	-0.72
16	5.04	5.24	-0.61	196	-14.28	-16.58	-0.77
17	4.99	5.19	-0.69	197	-14.28	-15.83	-0.79
18	4.89	5.19	-0.74	198	-14.12	-15.6	-0.85
19	4.85	5.18	-0.83	199	-13.97	-15.6	-0.9
20	4.77	5.15	-0.91	200	-13.82	-15.38	-0.97
21	4.71	5.14	-1.03	201	-13.53	-14.98	-1.03
22	4.61	5.11	-1.13	202	-13.67	-14.98	-1.08
23	4.51	5.08	-1.24	203	-13.4	-14.8	-1.15
24	4.43	5.06	-1.38	204	-13.14	-14.45	-1.22
25	4.32	5.04	-1.47	205	-13.14	-14.28	-1.31
26	4.25	5	-1.6	206	-13.02	-14.28	-1.38
27	4.16	4.96	-1.73	207	-12.78	-13.97	-1.47
28	4.03	4.92	-1.85	208	-12.66	-13.82	-1.56
29	3.93	4.89	-1.96	209	-12.55	-13.53	-1.67
30	3.81	4.88	-2.11	210	-12.34	-13.4	-1.77
31	3.67	4.85	-2.24	211	-12.34	-13.14	-1.85
32	3.55	4.8	-2.38	212	-12.03	-12.89	-1.96
33	3.44	4.77	-2.54	213	-11.94	-12.66	-2.1
34	3.29	4.72	-2.73	214	-11.94	-12.44	-2.19
35	3.17	4.71	-2.86	215	-11.84	-12.23	-2.34
36	3.02	4.68	-3.05	216	-11.66	-12.03	-2.44
37	2.87	4.65	-3.22	217	-11.66	-11.84	-2.6
38	2.72	4.63	-3.4	218	-11.66	-11.57	-2.7
39	2.56	4.59	-3.62	219	-11.57	-11.4	-2.86
40	2.41	4.54	-3.82	220	-11.48	-11.07	-3.01
41	2.23	4.52	-4.04	221	-11.57	-10.84	-3.17

42	2.08	4.46	-4.22	222	-11.57	-10.62	-3.33
43	1.91	4.41	-4.46	223	-11.57	-10.28	-3.5
44	1.73	4.37	-4.64	224	-11.57	-10.02	-3.65
45	1.52	4.32	-4.83	225	-11.75	-9.78	-3.83
46	1.34	4.24	-5.07	226	-11.84	-9.5	-4.02
47	1.12	4.18	-5.24	227	-11.84	-9.23	-4.24
48	0.89	4.14	-5.48	228	-12.03	-8.93	-4.41
49	0.68	4.1	-5.71	229	-12.13	-8.64	-4.63
50	0.43	4.04	-5.98	230	-12.34	-8.29	-4.85
51	0.19	3.97	-6.18	231	-12.55	-7.97	-5.03
52	-0.02	3.89	-6.4	232	-12.78	-7.7	-5.26
53	-0.3	3.84	-6.68	233	-13.02	-7.41	-5.48
54	-0.57	3.75	-6.92	234	-13.27	-7.11	-5.73
55	-0.83	3.64	-7.15	235	-13.67	-6.77	-5.98
56	-1.13	3.53	-7.35	236	-13.97	-6.45	-6.21
57	-1.42	3.47	-7.56	237	-14.28	-6.18	-6.48
58	-1.74	3.4	-7.81	238	-14.62	-5.88	-6.77
59	-2.06	3.31	-7.97	239	-14.98	-5.64	-7.02
60	-2.4	3.32	-8.21	240	-15.38	-5.37	-7.31
61	-2.75	3.2	-8.46	241	-15.83	-5.11	-7.59
62	-3.09	3.14	-8.78	242	-16.06	-4.85	-7.93
63	-3.47	3.03	-9.02	243	-16.58	-4.61	-8.21
64	-3.86	2.93	-9.39	244	-17.5	-4.39	-8.55
65	-4.27	2.79	-9.61	245	-17.86	-4.14	-8.83
66	-4.68	2.64	-9.9	246	-18.68	-3.92	-9.18
67	-5.09	2.64	-10.09	247	-19.15	-3.75	-9.61
68	-5.5	2.53	-10.35	248	-19.69	-3.53	-9.96
69	-6.03	2.36	-10.55	249	-20.31	-3.36	-10.28
70	-6.54	2.28	-10.92	250	-21.03	-3.14	-10.77
71	-6.74	2.12	-11.23	251	-22	-3	-11.15
72	-7.31	1.96	-11.57	252	-22	-2.81	-11.57
73	-7.81	1.82	-11.94	253	-21.91	-2.64	-12.03
74	-8.29	1.69	-12.23	254	-22	-2.49	-12.34
75	-8.93	1.5	-12.78	255	-22	-2.34	-12.89
76	-9.44	1.33	-13.14	256	-22	-2.19	-13.27
77	-10.28	1.2	-13.53	257	-22	-2.04	-13.67
78	-10.92	1	-13.97	258	-22	-1.9	-13.97
79	-11.48	0.8	-14.45	259	-21.91	-1.77	-14.45
80	-12.13	0.65	-14.98	260	-19.69	-1.64	-14.8
81	-12.44	0.48	-15.38	261	-19.69	-1.49	-15.18
82	-13.14	0.32	-15.6	262	-19.15	-1.31	-15.83
83	-13.82	0.12	-16.06	263	-18.25	-1.18	-16.06
84	-14.28	-0.04	-16.58	264	-17.5	-1.03	-16.32
85	-14.12	-0.22	-17.17	265	-17.5	-0.87	-16.58
86	-14.45	-0.43	-17.5	266	-16.87	-0.73	-16.58
87	-15.18	-0.67	-18.68	267	-16.06	-0.58	-16.58
88	-15.18	-0.84	-18.68	268	-15.83	-0.41	-16.87
89	-15.6	-1.07	-19.69	269	-15.18	-0.29	-16.87
90	-15.83	-1.25	-20.31	270	-14.98	-0.12	-16.58

91	-15.38	-1.45	-21.03	271	-14.45	0.03	-16.87
92	-15.18	-1.65	-21.91	272	-13.97	0.21	-16.58
93	-14.62	-1.82	-21.91	273	-13.4	0.36	-16.32
94	-13.97	-2.07	-21.03	274	-13.02	0.51	-16.06
95	-13.67	-2.27	-21.91	275	-12.78	0.63	-16.06
96	-13.53	-2.49	-20.31	276	-12.23	0.76	-15.83
97	-13.27	-2.68	-20.31	277	-11.94	0.88	-15.6
98	-13.4	-2.85	-19.69	278	-11.57	1.06	-15.38
99	-12.89	-3.01	-19.15	279	-11.23	1.16	-14.8
100	-13.14	-3.2	-17.86	280	-10.77	1.3	-14.8
101	-13.02	-3.4	-17.17	281	-10.35	1.4	-13.97
102	-12.66	-3.6	-16.58	282	-9.96	1.51	-13.97
103	-12.55	-3.8	-15.6	283	-9.61	1.65	-13.82
104	-12.55	-3.99	-14.98	284	-9.18	1.77	-13.4
105	-12.03	-4.17	-14.45	285	-8.78	1.9	-13.4
106	-12.03	-4.32	-13.82	286	-8.38	2.02	-12.78
107	-11.94	-4.52	-13.27	287	-7.93	2.11	-13.67
108	-11.84	-4.64	-12.89	288	-7.45	2.2	-12.66
109	-11.84	-4.83	-12.34	289	-6.99	2.31	-12.34
110	-11.57	-4.99	-11.75	290	-6.54	2.43	-12.23
111	-11.48	-5.15	-11.23	291	-6.1	2.56	-11.4
112	-11.31	-5.28	-10.69	292	-5.66	2.67	-11.4
113	-11.31	-5.43	-10.28	293	-5.22	2.78	-11.75
114	-11.31	-5.62	-9.78	294	-4.81	2.86	-10.99
115	-10.99	-5.71	-9.44	295	-4.39	2.97	-10.55
116	-10.77	-5.88	-9.12	296	-4.04	3.05	-10.15
117	-10.77	-6.08	-8.74	297	-3.66	3.13	-9.84
118	-10.69	-6.21	-8.38	298	-3.29	3.24	-9.55
119	-10.55	-6.4	-8.05	299	-2.96	3.36	-9.39
120	-10.35	-6.51	-7.74	300	-2.64	3.42	-9.23
121	-10.28	-6.68	-7.41	301	-2.3	3.53	-8.64
122	-10.09	-6.86	-7.11	302	-2	3.6	-8.46
123	-9.9	-7.02	-6.8	303	-1.68	3.68	-8.46
124	-9.66	-7.18	-6.48	304	-1.39	3.79	-8.09
125	-9.5	-7.31	-6.23	305	-1.12	3.89	-7.89
126	-9.33	-7.41	-5.88	306	-0.86	3.97	-7.63
127	-9.18	-7.63	-5.71	307	-0.59	4.06	-7.38
128	-8.97	-7.74	-5.46	308	-0.32	4.11	-7.08
129	-8.97	-7.93	-5.24	309	-0.11	4.2	-6.86
130	-8.88	-8.09	-5.07	310	0.14	4.28	-6.54
131	-8.74	-8.29	-4.87	311	0.38	4.33	-6.26
132	-8.69	-8.46	-4.64	312	0.59	4.38	-5.9
133	-8.51	-8.64	-4.44	313	0.82	4.45	-5.66
134	-8.42	-8.74	-4.32	314	1.02	4.52	-5.55
135	-8.38	-8.93	-4.25	315	1.22	4.55	-5.39
136	-8.33	-9.02	-4.02	316	1.41	4.6	-5.15
137	-8.29	-9.28	-3.85	317	1.6	4.63	-4.93
138	-8.25	-9.55	-3.62	318	1.77	4.7	-4.76
139	-8.21	-9.78	-3.39	319	1.94	4.74	-4.59

140	-8.21	-10.09	-3.21	320	2.09	4.8	-4.32
141	-8.21	-10.15	-3.03	321	2.26	4.83	-4.24
142	-8.25	-10.48	-2.9	322	2.45	4.87	-4
143	-8.29	-10.84	-2.78	323	2.58	4.89	-3.85
144	-8.38	-10.99	-2.66	324	2.73	4.9	-3.65
145	-8.42	-11.23	-2.55	325	2.9	4.95	-3.46
146	-8.55	-11.23	-2.42	326	3.04	4.93	-3.29
147	-8.69	-11.48	-2.31	327	3.15	4.98	-3.09
148	-8.74	-11.57	-2.2	328	3.3	4.99	-2.91
149	-8.88	-11.75	-2.08	329	3.43	5.04	-2.76
150	-9.02	-12.03	-2.01	330	3.55	5.09	-2.61
151	-9.18	-12.34	-1.9	331	3.67	5.14	-2.5
152	-9.39	-12.44	-1.85	332	3.77	5.16	-2.34
153	-9.55	-12.66	-1.78	333	3.87	5.18	-2.22
154	-9.84	-12.89	-1.76	334	4	5.19	-2.08
155	-10.02	-13.27	-1.69	335	4.08	5.22	-1.95
156	-10.28	-13.4	-1.58	336	4.2	5.21	-1.8
157	-10.55	-13.82	-1.55	337	4.29	5.24	-1.7
158	-10.77	-13.82	-1.43	338	4.38	5.25	-1.58
159	-10.99	-14.28	-1.38	339	4.48	5.24	-1.46
160	-11.31	-14.62	-1.31	340	4.56	5.26	-1.38
161	-11.57	-14.8	-1.24	341	4.62	5.27	-1.25
162	-11.94	-14.98	-1.19	342	4.7	5.27	-1.16
163	-12.23	-15.38	-1.11	343	4.77	5.28	-1.07
164	-12.44	-15.38	-1.08	344	4.84	5.28	-0.96
165	-12.66	-15.83	-1.03	345	4.91	5.35	-0.89
166	-13.02	-16.06	-1.01	346	4.96	5.33	-0.81
167	-13.4	-16.06	-0.94	347	5.02	5.35	-0.75
168	-13.82	-16.06	-0.88	348	5.08	5.32	-0.66
169	-13.97	-16.58	-0.85	349	5.12	5.35	-0.57
170	-14.12	-16.32	-0.8	350	5.16	5.34	-0.52
171	-14.45	-16.58	-0.75	351	5.2	5.34	-0.46
172	-14.62	-16.58	-0.72	352	5.23	5.33	-0.38
173	-14.8	-16.87	-0.71	353	5.28	5.36	-0.35
174	-15.18	-16.58	-0.66	354	5.3	5.37	-0.3
175	-14.98	-17.17	-0.62	355	5.34	5.35	-0.27
176	-15.38	-17.17	-0.6	356	5.36	5.39	-0.23
177	-15.38	-17.17	-0.57	357	5.39	5.38	-0.23
178	-15.38	-17.86	-0.57	358	5.41	5.38	-0.18
179	-15.38	-17.86	-0.53	359	5.41	5.39	-0.14

APPENDIX B. TERN DATA

In the below data, a blank space indicates no data is received from the GPS onboard the TERN UAV.

Data Record #	Fc [kHz]	PSD Peak [dB]
0	0.742	-16.54
1	0.68	-16.62
2	0.932	-14.89
3	0.321	-15.38
4	0.931	-15.67
5	0.717	-16.24
6	1.39	-17.55
7	1.027	-16.03
8	0.932	-13.33
9	0.932	-16.76
10	0.933	-16.46
11	0.869	-16.86
12	0.521	-17.31
13	1.532	-15.99
14	1.412	-16.75
15	0.931	-15.84
16	0.932	-15.39
17	0.389	-16.64
18	0.792	-17.4
19	0.721	-15.35
20	0.994	-17.23
21	0.931	-14.9
22	0.929	-15.87
23	0.872	-16.82
24	1.236	-17.7
25	0.514	-16.02
26	0.928	-15.97
27	1.109	-17.42
28	0.927	-17
29	0.927	-14.34
30	1.331	-17.18
31	0.688	-18.09
32	0.925	-16
33	0.926	-15.92
34	1.355	-16.78
35	0.852	-16.54
36	0.925	-15.16

37	0.923	-12.11
38	0.924	-16.37
39	0.924	-15.07
40	0.923	-15.02
41	0.885	-16.25
42	0.819	-15.54
43	0.889	-16.77
44	1.656	-17.3
45	0.778	-15.35
46	0.329	-16.27
47	1.743	-16.83
48	0.924	-16.33
49	0.501	-16.33
50	0.923	-16.45
51	0.266	-16.35
52	0.386	-15.48
53	0.924	-16.69
54	0.957	-15.8
55	0.444	-16.97
56	0.497	-16.48
57	1.385	-15.63
58	0.881	-16.45
59	0.876	-16.93
60	1.088	-16.47
61	0.495	-15.13
62	0.495	-13.58
63	0.495	-15.02
64	0.867	-16.02
65	0.493	-14.23
66	0.493	-14.76
67	0.927	-15.33
68	0.928	-16.97
69	1.177	-17.05
70	0.929	-14.3
71	0.775	-16.55
72	0.719	-16.85
73	0.929	-14.93
74	0.35	-16.18
75	0.488	-15.1
76	0.93	-15.49
77	0.487	-15.78
78	0.486	-13.79
79	1.197	-18
80	0.485	-12.31
81	0.862	-16.19
82	0.484	-15.72
83	0.666	-16.49
84	0.306	-17.29

85	0.311	-15.97
86	0.365	-15.17
87	0.936	-15.64
88	0.935	-15.25
89	0.936	-13.46
90	0.937	-14.85
91	0.495	-17.36
92	1.166	-16.06
93	0.645	-16.1
94	0.379	-16.93
95	0.362	-16.5
96	0.938	-14.53
97	0.356	-16.62
98	0.938	-13.93
99	0.477	-14.65
100	0.938	-16.35
101	0.286	-15.82
102	0.475	-15.86
103	0.42	-16.09
104	0.474	-16.82
105	0.992	-16.94
106	0.473	-15.29
107	1.402	-15.79
108	1.448	-5.69
109	1.464	-14.79
110	1.469	-14.69
111	0.624	-16.38
112	1.413	-16.13
113	0.322	-17.64
114	1.571	-16.85
115	0.526	-16.16
116	0.85	-16.39
117	0.351	-17.52
118	1.14	-7.91
119	0.826	-16.24
120	1.13	-10.08
121	0.405	-16.78
122	1.123	-10.02
123	0.8	-16.88
124	1.135	-12.01
125	0.255	-16.12
126	1.144	-11.62
127	0.545	-16.78
128	1.155	-9.49
129	1.369	-16.49
130	1.163	-9.93
131	0.885	-14.61
132	1.161	-11.38

133	0.498	-17.25
134	1.167	-13.06
135	0.422	-16.32
136	1.169	-13.31
137	0.378	-16.14
138	1.184	-14.21
139	0.87	-15.9
140	1.389	-17.96
141	1.202	-17.15
142	0.615	-17.38
143	0.273	-16.75
144	0.915	-16.49
145	1.275	-16.44
146	0.239	-17.09
147	1.148	-15.57
148	0.54	-16.8
149	0.278	-16.68
150	0.76	-16.72
151	0.673	-16.26
152	0.969	-16.55
153	0.658	-15.6
154	0.536	-17.39
155	0.519	-17.13
156	0.891	-15.32
157	0.489	-15.76
158	0.464	-15.89
159	1.108	-17.16
160	0.973	-16.15
161	0.584	-16.33
162	0.353	-17.33
163	1.206	-8.17
164	1.13	-16.94
165	0.753	-12.89
166	0.919	-11.49
167	1.194	-13.08
168	0.922	-15.45
169	1.208	-15.21
170	0.791	-16.97
171	0.961	-16.79
172	0.771	-17.29
173	1.257	-14.28
174	1.409	-17.34
175	1.25	-13.41
176	0.265	-16.21
177	1.234	-8.99
178	0.973	-16.39
179	1.244	-11.7
180	0.45	-16.72

181	1.244	-11.03
182	1.391	-17.87
183	1.241	-13.84
184	1.497	-13.65
185	1.505	-13.56
186	0.746	-19.14
187	1.534	-17.45
188	0.598	-16.09
189	1.164	-18.55
190	0.877	-16.66
191	1.08	-15.89
192	0.31	-17.57
193	0.706	-16.53
194	0.359	-16.48
195	0.731	-16.71
196	0.513	-16.92
197	1.239	-11.54
198	0.841	-10.02
199	0.852	-11.36
200	0.871	-13.95
201	1.77	-12.28
202	0.889	-12.22
203	0.124	-17.49
204	0.137	-17.02
205	0.787	-16.45
206	1.026	-16.01
207	1.34	-15.02
208	0.249	-15.8
209	1.285	-14.99
210	1.18	-16.14
211	1.236	-16.08
212	0.298	-16.16
213	0.311	-16.14
214	1.555	-13.41
215	1.565	-10.53
216	1.613	-10.07
217	1.662	-12.07
218	1.67	-15.62
219	0.234	-16.5
220	0.348	-15.31
221	0.359	-14.12
222	0.37	-16.89
223	1.049	-16.86
224	1.296	-12.35
225	1.004	-15.69
226	1.277	-7.97
227	1.006	-16.25
228	1.292	-9.91

229	1.287	-16.05
230	1.228	-13.83
231	0.307	-16.49
232	0.878	-16.17
233	1.2	-16.2
234	1.394	-14.8
235	0.42	-11.43
236	1.37	-10.68
237	0.442	-9.54
238	1.781	-10.93
239	1.216	-14.92
240	1.786	-12.99
241	0.842	-16.33
242	1.35	-11.08
243	1.612	-16.4
244	1.361	-11.87
245	1.613	-8.13
246	1.62	-5.85
247	1.639	-9.49
248	0.531	-14.9
249	0.28	-16.63
250	1.364	-13.46
251	0.884	-17.18
252	0.787	-16.21
253	0.805	-16.48
254	0.962	-16.05
255	0.845	-16.77
256	0.936	-17.07
257	0.61	-13.39
258	1.019	-18.2
259	0.158	-17.03
260	0.43	-18.52
261	0.606	-12.38
262	0.613	-12
263	0.624	-16.45
264	0.976	-14.63
265	0.678	-12.98
266	0.916	-15.07
267	1.143	-14.98
268	1.003	-16.03
269	1.437	-15.8
270	0.746	-14.4
271	0.755	-9.58
272	0.764	-15.68
273	1.677	-15.09
274	1.683	-12.4
275	1.725	-13.86
276	1.782	-9.88

277	0.785	-14.81
278	0.854	-16.47
279	0.792	-13.06
280	1.419	-15.73
281	0.498	-17.45
282	1.442	-13.3
283	0.326	-16.29
284	1.425	-9.66
285	0.71	-16.83
286	1.386	-10.99
287	0.894	-15.88
288	1.012	-16.88
289	1.418	-16.79
290	1.493	-11.85
291	0.578	-15.9
292	0.859	-16.11
293	0.799	-7.65
294	0.804	-11.53
295	0.915	-15.4
296	1.457	-14.4
297	0.823	-14.72
298	0.826	-15.57
299	0.827	-12.34
300	1.028	-15.55
301	1.019	-12.54
302	1.728	-10.27
303	1.734	-6.62
304	1.755	-7.31
305	0.853	-12.52
306	1.048	-14.97
307	0.452	-17.57
308	0.409	-14.09
309	0.658	-16.26
310	0.183	-15.29
311	1.151	-16.04
312	1.127	-16.53
313	0.923	-14.37
314	0.911	-16.53
315	1.313	-16.63
316	1.158	-17.75
317	0.584	-16.14
318	0.319	-16.78
319	0.812	-14.65
320	0.269	-17.02
321	0.738	-16.42
322	0.284	-17.22
323	0.733	-16.93
324	0.705	-16.39

325	0.708	-14.64
326	0.456	-16.66
327	1.018	-14.92
328	1.011	-13.55
329	1.257	-13.75
330	1.784	-12.05
331	1.84	-8.6
332	1.892	-9.5
333	1.031	-16.35
334	1.121	-16.35
335	1.112	-14.71
336	1.101	-14.81
337	1.972	-14.26
338	1.962	-14.57
339	1.95	-10.53
340	1.074	-9.03
341	1.488	-8.99
342	1.059	-7.39
343	1.076	-5.54
344	1.096	-6.38
345	1.117	-9.24
346	1.126	-8.03
347	1.124	-5.89
348	1.019	-14.55
349	1.02	-13.84
350	1.026	-15.32
351	1.397	-16.93
352	0.484	-15.45
353	1.506	-12.09
354	0.772	-17.44
355	0.608	-17.55
356	1.476	-7.44
357	0.84	-16.09
358	1.507	-13.19
359	0.721	-16.84
360	1.527	-10.15
361	1.159	-15.84
362	1.56	-12.12
363	0.911	-15.94
364	1.355	-17.23
365	0.737	-15.45
366	1.6	-17.19
367	1.088	-16.36
368	1.171	-15.01
369	2.03	-13.51
370	1.132	-9.88
371	1.139	-9.96
372	0.357	-16.52

373	0.684	-17.12
374	0.639	-15.86
375	1.519	-12.15
376	0.827	-15.6
377	1.528	-14.59
378	1.132	-10.36
379	1.187	-15.14
380	1.182	-13
381	1.173	-16.74
382	1.165	-15.49
383	1.117	-17.36
384	1.169	-15.67
385	1.73	-16.56
386	0.672	-15.75
387	0.806	-16.02
388	0.454	-15.92
389	0.338	-17.9
390	0.774	-15.37
391	0.441	-17.36
392	0.839	-16.25
393	0.737	-16
394	1.133	-15.39
395	0.598	-16.9
396	0.376	-14.1
397	1.602	-16.66
398	1.401	-15.23
399	0.566	-16.82
400	0.767	-16.58
401	0.521	-16.47
402	0.659	-16.61
403	0.898	-16.24
404	1.019	-16.68
405	0.879	-16.59
406	1.596	-12.22
407	0.62	-16.58
408	1.573	-16.51
409	0.958	-16.65
410	0.968	-16
411	0.979	-16.01
412	1.521	-14.3
413	1.017	-16.13
414	1.536	-10.09
415	1.155	-16.22
416	2.014	-14.25
417	0.172	-16.34
418	1.188	-13.68
419	1.926	-15.32
420	1.627	-9.74

421	1.265	-13.98
422	0.743	-15.93
423	1.236	-15.6
424	1.659	-12.8
425	0.46	-16.33
426	1.641	-9.05
427	0.987	-16.33
428	1.614	-8.7
429	0.291	-16.27
430	1.591	-9.28
431	1.026	-16.02
432	1.585	-12.11
433	0.733	-16.65
434	1.572	-13.19
435	0.506	-17.48
436	1.123	-16.42
437	1.194	-10.55
438	1.619	-12.3
439	0.701	-16.18
440	1.648	-14.79
441	0.837	-15.48
442	1.04	-15.6
443	0.354	-16.68
444	0.58	-16.12
445	1.261	-16.41
446	1.087	-17.71
447	1.247	-17.25
448	0.695	-16.77
449	0.606	-16.35
450	0.842	-16.34
451	1.166	-16.2
452	0.657	-16.27
453	1.236	-17.53
454	0.715	-16.03
455	1.427	-14.08
456	0.68	-14.77
457	0.586	-15.45
458	0.64	-14.49
459	0.637	-14.21
460	1.344	-12.91
461	1.328	-14.53
462	1.108	-16.16
463	0.764	-16.41
464	0.534	-16.74
465	1.287	-15.05
466	0.248	-15.84
467	1.627	-14.64
468	0.314	-15.58

469	1.614	-13.84
470	0.743	-16.38
471	1.575	-11.24
472	0.908	-15.86
473	1.593	-13.19
474	1.221	-16.08
475	1.592	-7.6
476	1.216	-16.67
477	1.61	-12.8
478	0.367	-14.79
479	2.111	-13.56
480	1.075	-14.76
481	1.663	-13.95
482	0.541	-19.25
483	0.499	-16.71
484	0.373	-16.46
485	0.354	-18.66
486	0.309	-17.04
487	1.684	-10.23
488	0.653	-15.47
489	1.645	-14.58
490	1.169	-16.67
491	1.639	-14.04
492	0.825	-16.73
493	1.619	-10.55
494	0.627	-16.56
495	1.619	-8.61
496	1.215	-14.87
497	1.646	-10.46
498	0.409	-14.46
Data Record #	Fc [kHz]	PSD Peak [dB]
499	1.668	-9.14
500	0.606	-16.52
501	1.683	-8.87
502	0.936	-16.85
503	1.281	-16.47
504	0.624	-15.97
505	1.719	-17.22
506	0.534	-16.95
507	1.412	-17.01
508	0.653	-16.08
509	1.689	-13.9
510	1.418	-16.39
511	1.684	-12.67
512	0.412	-15.64
513	1.646	-14.73

514	1.024	-16.39
515	0.906	-17.14
516	0.595	-17.07
517	0.618	-16.79
518	0.843	-15.4
519	1.655	-16.37
520	0.604	-15.42
521	1.356	-16.61
522	1.471	-15.24
523	1.101	-17.63
524	0.6	-17.26
525	0.351	-15.68
526	0.568	-15.31
527	1.165	-16.59
528	0.22	-16.39
529	0.9	-17.04
530	1.163	-16.83
531	0.628	-16.14
532	0.282	-9.94
533	0.294	-12.47
534	0.512	-16.11
535	1.019	-17.48
536	0.64	-16.5
537	0.995	-15.98
538	0.433	-16.24
539	0.555	-17.05
540	1.671	-15.03
541	1.502	-16.9
542	1.264	-16.29
543	0.642	-15.77
544	1.459	-14.77
545	0.549	-16.99
546	0.828	-15.39
547	1.003	-17.11
548	1.702	-12.52
549	0.228	-16.76
550	1.204	-16.65
551	0.642	-16.32
552	0.802	-17.07
553	1.101	-15.59
554	0.592	-16.52
555	0.959	-16.05
556	1.619	-15.48
557	1.7	-16.61
558	1.665	-15.18
559	0.547	-16.33
560	1.685	-15.02
561	0.569	-14.62

562	0.596	-15.58
563	0.729	-15.98
564	0.867	-16.39
565	0.536	-15.9
566	1.978	-15.8
567	0.95	-16.48
568	1.36	-14.47
569	0.786	-15.15
570	1.697	-10.2
571	0.821	-15.61
572	1.642	-9.01
573	0.982	-16.04
574	1.313	-15.58
575	0.295	-16.61
576	1.639	-10.22
577	0.824	-17.14
578	1.664	-7.88
579	0.289	-16.87
580	1.672	-6.65
581	1.172	-16.18
582	1.673	-10.52
583	0.798	-17.31
584	1.667	-6.37
585	0.187	-16.78
586	1.666	-11.55
587	0.693	-16.92
588	1.678	-9.66
589	0.185	-16.87
590	1.686	-9.13
591	1.111	-16.04
592	2.196	-14.07
593	1.443	-16.35
594	1.722	-10.27
595	0.391	-16.97
596	1.749	-11.74
597	0.336	-16.82
598	1.375	-11.87
599	1.536	-15.79
600	1.788	-10.57
601	0.982	-16.31
602	1.738	-12.52
603	0.427	-16.41
604	1.766	-16.32
605	0.274	-16.59
606	1.758	-14.44
607	1.995	-12.27
608	2	-6.1
609	2.037	-10.44

610	2.664	-10.77
611	0.356	-15.33
612	1.76	-15.01
613	0.872	-9.38
614	0.844	-15.62
615	1.317	-15.63
616	1.075	-17.7
617	1.718	-14.99
618	0.692	-15.58
619	1.713	-13.09
620	0.841	-17.09
621	1.703	-13.29
622	1.345	-16.01
623	1.295	-15.27
624	0.49	-16.31
625	1.747	-15.76
626	1.135	-15.7
627	1.588	-16.35
628	0.7	-17.04
629	1.753	-8.22
630	1.372	-16.04
631	1.779	-15.77
632	0.312	-16.69
633	1.69	-9.7
634	0.84	-15.16
635	1.711	-8.56
636	1.038	-15.28
637	1.725	-15.1
638	0.901	-14.42
639	1.697	-10.87
640	0.903	-11.32
641	1.708	-10.45
642	0.909	-8.09
643	2.028	-13.86
644	0.852	-15.71
645	0.546	-15.43
646	1.673	-15.83
647	0.994	-16.99
648	1.708	-15.47
649	0.268	-15
650	1.706	-9.37
651	0.55	-15.68
652	1.737	-14.64
653	0.552	-15.6
654	1.757	-10.58
655	0.529	-15.93
656	1.776	-17.1
657	0.533	-16.95

658	1.792	-15.96
659	0.377	-16.41
660	1.873	-16.62
661	1.572	-13.79
662	1.8	-15.63
663	1.612	-15.61
664	0.417	-16.02
665	1.631	-14.88
666	1.762	-16.12
667	2.017	-15.68
668	2.019	-11.59
669	2.02	-6.34
670	2.041	-9.63
671	2.723	-14.23
672	0.677	-17.03
673	0.961	-13.47
674	0.967	-13.08
675	0.981	-16.22
676	1.037	-12.4
677	0.905	-15.35
678	0.699	-16.41
679	0.956	-13.93
680	1.064	-16.77
681	1.111	-15.2
682	0.704	-15.1
683	1.107	-16.37
684	1.54	-15.55
685	0.414	-16.48
686	0.328	-16.17
687	0.264	-16.71
688	0.971	-13.38
689	1.576	-16.36
690	1.252	-16
691	1.269	-15.73
692	0.298	-16.45
693	0.633	-14.73
694	0.611	-15.9
695	1.735	-10.4
696	0.279	-15.49
697	1.737	-9.21
698	0.553	-15.76
699	1.256	-18.59
700	0.988	-15.62
701	0.988	-16.16
702	0.986	-15.14
703	0.985	-9.39
704	0.988	-3.88
705	0.992	-4.18

706	1.031	-11.98
707	0.984	-16.79
708	1.545	-11.8
709	2.03	-12.14
710	2.034	-7.73
711	1.556	-14.81
712	0.998	-17.11
713	0.832	-16.23
714	0.612	-15.34
715	0.771	-17.02
716	0.222	-15.93
717	0.294	-15.82
718	1.701	-15.09
719	0.363	-17.1
720	1.709	-10.98
721	0.312	-16.26
722	1.739	-8.7
723	0.365	-16.42
724	1.751	-10.73
725	0.661	-15.46
726	1.768	-10.76
727	1.73	-16.44
728	1.414	-15.73
729	1.56	-16.56
730	1.81	-14.51
731	1.171	-16.84
732	1.747	-7.07
733	0.81	-16.44
734	1.79	-11.35
735	0.297	-15.75
736	1.732	-15.5
737	2.039	-12.63
738	2.041	-8.4
739	2.058	-7.81
740	1.795	-12.92
741	1.028	-14.18
742	1.034	-10.79
743	1.043	-7.55
744	1.808	-13.9
745	1.099	-14.04
746	1.791	-12.55
747	0.517	-14.75
748	1.792	-10.63
749	0.25	-15.46
750	0.729	-15.95
751	0.4	-13.99
752	1.769	-15.02
753	1.06	-16.47

754	1.772	-17.06
755	0.526	-16.09
756	0.254	-16.73
757	0.271	-16.4
758	0.638	-16.71
759	1.169	-16.84
760	0.352	-14.48
761	0.592	-13.69
762	1.551	-12.16
763	1.548	-14.71
764	1.437	-17.28
765	1.568	-15.46
766	0.241	-15.9
767	0.61	-14.21
768	1.075	-17.56
769	0.507	-14.64
770	1.073	-17.49
771	1.071	-9.59
772	1.073	-5.28
773	1.078	-1.8
774	1.085	-5.5
775	1.348	-9.03
776	1.364	-12.87
777	2.221	-13.15
778	2.05	-14.1
779	2.061	-8.26
780	1.548	-14.34
781	1.744	-11.79
782	0.38	-15.9
783	1.723	-13.42
784	0.669	-15.67
785	1.727	-12.42
786	0.785	-14.14
787	1.743	-8.13
788	0.834	-15.07
789	1.751	-15.23
790	0.533	-16.17
791	1.768	-9.36
792	0.968	-14.56
793	1.783	-12.62
794	0.803	-16.33
795	1.817	-14.35
796	1.263	-16.41
797	1.833	-15.24
798	0.286	-16.65
799	1.818	-15.49
800	0.378	-16.71
801	1.01	-16.5

802	1.245	-16.85
803	0.875	-16.89
804	2.056	-15.96
805	2.057	-13.69
806	2.064	-11.32
807	2.08	-10.21
808	0.905	-16.76
809	1.091	-15.99
810	1.092	-15.04
811	1.095	-13.98
812	1.122	-14.46
813	0.482	-16.69
814	0.702	-16.58
815	1.27	-17.43
816	1.181	-17.34
817	0.353	-16.41
818	1.318	-16.42
819	1.083	-16.47
820	0.248	-15.86
821	1.471	-16.32
822	0.557	-16.56
823	1.264	-17.17
824	0.832	-15.98
825	1.168	-16.68
826	1.718	-16.35
827	0.328	-16.62
828	1.756	-13.9
829	1.557	-15.51
830	1.715	-8.53
831	1.109	-16.75
832	1.687	-8.52
833	0.559	-15.08
834	1.703	-12.3
835	1.106	-9.58
836	1.754	-9.3
837	1.109	-6.05
838	1.752	-10.74
839	1.146	-15.34
840	1.762	-10.76
841	0.491	-15.26
842	1.722	-13.62
843	2.076	-10.37
844	1.762	-10.82
845	1.072	-16.61
846	1.746	-11.65
847	1.053	-17.78
848	1.732	-9.4
849	0.912	-17.28

850	1.734	-12.89
851	0.435	-16.67
852	1.744	-11.35
853	1.109	-16.22
854	1.75	-11.81
855	0.365	-17.4
856	1.775	-15.9
857	0.172	-16.08
858	1.405	-16.12
859	1.404	-15.43
860	1.428	-15.03
861	1.454	-13.63
862	0.243	-16.54
863	0.474	-17.79
864	0.356	-16.3
865	1.356	-12.28
866	1.344	-12.19
867	1.34	-12.95
868	1.344	-12.72
869	1.343	-16.48
870	1.341	-15.96
871	1.341	-15.14
872	2.064	-9.94
873	2.081	-10.81
874	0.848	-17.17
875	1.64	-16.27
876	1.145	-12.85
877	1.154	-9.6
878	0.502	-15.17
879	1.23	-13.18
880	0.61	-15.95
881	1.751	-12.56
882	0.42	-15.61
883	1.743	-10.66
884	0.775	-15.85
885	1.711	-8.92
886	0.566	-15.97
887	1.732	-12.23
888	0.665	-17.4
889	1.757	-13.82
890	0.459	-16.75
891	1.253	-14.99
892	0.309	-16.43
893	1.533	-15.54
894	1.536	-13.94
895	1.54	-15.63
896	1.548	-14.74
897	1.161	-14.4

898	1.164	-14.52
899	1.166	-12.67
900	1.166	-11.55
901	1.166	-11.5
902	1.168	-5.87
903	1.174	-8.86
904	1.722	-14.63
905	0.862	-17.58
906	1.719	-14.73
907	2.069	-14.68
908	0.517	-13.87
909	1.27	-16.67
910	1.719	-12.54
911	1.059	-16.63
912	1.692	-11.24
913	0.851	-16.58
914	1.679	-12.51
915	0.641	-16.11
916	1.691	-7.05
917	0.268	-16.81
918	1.701	-6.85
919	0.709	-15.76
920	1.73	-8.23
921	0.926	-16.75
922	1.764	-9.88
923	1.214	-16.73
924	1.422	-16.78
925	1.463	-11.81
926	1.476	-12.92
927	1.471	-7.9
928	1.432	-9.36
929	1.428	-8.68
930	1.836	-7.81
931	0.532	-16.62
932	1.777	-10.7
933	2.079	-14.44
934	1.763	-9.23
935	2.094	-8.9
936	1.792	-11.31
937	1.586	-16.14
938	1.764	-7.71
939	1.205	-12.93
940	1.77	-9.06
941	0.513	-16.21
942	1.748	-11.81
943	0.312	-15.93
944	1.762	-6.33
945	1.305	-15.76

946	1.74	-7.6
947	1.192	-15.54
948	1.747	-13.68
949	0.858	-14.96
950	1.756	-13.19
951	1.497	-15.43
952	1.791	-13.68
953	0.596	-16.33
954	0.461	-16.67
955	0.681	-16.01
956	1.825	-15.44
957	0.767	-16.64
958	1.798	-16.48
959	1.362	-16.64
960	0.313	-15.8
961	0.708	-15.12
962	0.644	-18.23
963	1.217	-15.75
964	1.219	-13.03
965	1.219	-12.5
966	1.223	-12.87
967	1.227	-8.69
968	1.23	-13.46
969	1.249	-12.48
970	1.266	-16.94
971	2.082	-15.93
972	0.529	-17.66
973	2.095	-12.91
974	0.561	-14.4
975	0.54	-17.98
976	0.539	-17.53
977	1.024	-16.56
978	0.549	-15.01
979	1.387	-16.55
980	0.951	-17.18
981	0.636	-14.92
982	0.596	-15.03
983	1.718	-15.25
984	0.865	-17.86
985	1.721	-14.19
986	0.677	-16.93
987	0.517	-15.63
988	1.495	-15.25
989	1.759	-8.57
990	0.343	-16.48
991	1.792	-9.56
992	0.328	-16.42
993	1.789	-14.28

994	1.073	-14.88
995	1.786	-10.1
996	0.39	-15.73
997	1.339	-11.54
Data Record #	Fc [kHz]	PSD Peak [dB]
998	0.847	-16.55
999	1.757	-9.85
1000	0.716	-16.74
1001	1.376	-11.38
1002	0.377	-15.3
1003	1.774	-11.65
1004	0.58	-15.2
1005	1.806	-14.95
1006	0.784	-16.71
1007	2.262	-10.61
1008	0.502	-14.97
1009	1.762	-11.02
1010	0.377	-15.72
1011	1.783	-6.53
1012	0.941	-17.99
1013	1.783	-8.91
1014	0.403	-16.02
1015	1.748	-11.56
1016	0.281	-15.85
1017	1.753	-8.56
1018	0.338	-16.04
1019	1.747	-10.16
1020	0.757	-16.15
1021	1.769	-15.5
1022	0.994	-16.22
1023	1.554	-16.33
1024	0.407	-15.5
1025	1.324	-15.77
1026	0.711	-13.86
1027	0.681	-16.38
1028	1.495	-15.14
1029	1.742	-13.1
1030	0.232	-16.09
1031	1.751	-17.9
1032	1.282	-14.33
1033	1.743	-12.06
1034	1.292	-10.15
1035	1.742	-11.96
1036	0.249	-14.45
1037	1.762	-18.31
1038	0.379	-16.19

1039	1.747	-18.32
1040	0.482	-16.4
1041	1.75	-17.33
1042	1.2	-16.12
1043	0.581	-18.42
1044	0.779	-16.26
1045	0.565	-17.8
1046	1.631	-16.94
1047	0.603	-17.74
1048	0.626	-17.24
1049	0.361	-16.8
1050	0.241	-17.93
1051	0.734	-17.67
1052	1.133	-16.77
1053	1.518	-17.17
1054	0.268	-16.29
1055	1.34	-16.61
1056	1.501	-16.43
1057	0.51	-17.11
1058	0.382	-16.23
1059	0.544	-16.57
1060	0.301	-17.57
1061	0.293	-16.27
1062	1.405	-16.13
1063	0.547	-15.82
1064	1.745	-13.34
1065	0.515	-15.09
1066	1.723	-12.67
1067	1.229	-16.28
1068	1.749	-12.13
1069	0.565	-15.69
1070	1.729	-11.34
1071	0.625	-15.91
1072	1.757	-10.92
1073	0.961	-16.48
1074	1.778	-14.07
1075	1.331	-17.1
1076	1.78	-6.33
1077	1.535	-16.24
1078	1.796	-11.95
1079	0.188	-16.7
1080	1.756	-4.99
1081	0.929	-16.46
1082	1.749	-7.44
1083	0.545	-16.94
1084	1.782	-14.99
1085	0.601	-15.75
1086	1.771	-12.62

1087	0.946	-14.66
1088	1.757	-11.62
1089	1.031	-15.76
1090	1.21	-19.4
1091	0.3	-16.79
1092	0.712	-13.53
1093	0.673	-15.82
1094	1.043	-16.44
1095	1.18	-14.36
1096	1.219	-14.73
1097	1.164	-14.48
1098	0.933	-15.6
1099	0.986	-15.91
1100	0.844	-16.02
1101	0.336	-16.4
1102	0.674	-15.37
1103	1.713	-13.58
1104	0.608	-14.94
1105	1.703	-13.9
1106	1.323	-14.82
1107	1.718	-10.95
1108	1.267	-15.99
1109	1.706	-6.28
1110	0.578	-15.73
1111	1.741	-13.12
1112	0.585	-16.49
1113	1.692	-9.72
1114	0.372	-13.59
1115	1.736	-11.56
1116	1.076	-16.52
1117	1.72	-8.61
1118	1.204	-15.72
1119	1.704	-9.89
1120	0.554	-13.75
1121	1.706	-11.06
1122	1.282	-15.4
1123	1.715	-11.38
1124	0.859	-14.81
1125	1.729	-9.04
1126	0.58	-16.39
1127	1.725	-10.82
1128	0.712	-16.32
1129	1.771	-12.39
1130	0.78	-16.95
1131	0.918	-15.67
1132	0.752	-16.68
1133	1.794	-17.36
1134	1.062	-17.58

1135	0.656	-17.56
1136	0.552	-16.09
1137	0.805	-17.76
1138	1.147	-16.95
1139	0.344	-18.72
1140	0.55	-15.84
1141	0.477	-17.19
1142	0.598	-16.98
1143	0.678	-17.72
1144	0.734	-17.01
1145	1.142	-19.32
1146	0.565	-16.21
1147	0.581	-20.51
1148	0.618	-17.73
1149	0.327	-17.65
1150	1.026	-16.98
1151	0.944	-16.25
1152	1.179	-16.89
1153	0.889	-16.76
1154	0.54	-16.85
1155	0.219	-17.49
1156	0.57	-16.12
1157	0.536	-18.14
1158	1.494	-16.36
1159	0.203	-14.75
1160	1.34	-15.9
1161	0.96	-16.35
1162	0.625	-15.29
1163	1.222	-15.07
1164	0.959	-16.15
1165	0.623	-16.19
1166	1.763	-13.04
1167	0.928	-15.77
1168	1.728	-11.11
1169	0.29	-16.04
1170	1.72	-10.86
1171	0.943	-17
1172	1.668	-5.72
1173	0.555	-15.91
1174	1.673	-7.63
1175	0.741	-15.71
1176	1.671	-4.89
1177	0.603	-17.2
1178	1.704	-6.26
1179	0.301	-15.16
1180	1.715	-5.36
1181	0.819	-16.77
1182	0.301	-15.47

1183	0.852	-15.79
1184	0.749	-15.95
1185	0.888	-15.81
1186	0.856	-16.82
1187	1.369	-16.39
1188	0.71	-16.2
1189	1.746	-12.79
1190	1.079	-15.62
1191	1.196	-14.54
1192	1.224	-15.32
1193	1.692	-12.86
1194	1.354	-15.73
1195	1.671	-10.41
1196	0.738	-15.24
1197	1.673	-6.55
1198	0.716	-14.69
1199	1.676	-8.03
1200	0.369	-15.49
1201	1.714	-10.7
1202	0.319	-16.12
1203	1.727	-13.35
1204	0.758	-15.07
1205	0.891	-16
1206	0.733	-15.97
1207	1.08	-15.3
1208	0.268	-15.77
1209	1.774	-12.19
1210	1.224	-17.07
1211	1.774	-7.2
1212	0.337	-16.3
1213	2.211	-14.24
1214	0.957	-15.3
1215	1.722	-7.96
1216	0.804	-17.03
1217	1.693	-8.63
1218	0.631	-15.22
1219	1.687	-8.47
1220	0.448	-16.34
1221	1.702	-12.13
1222	0.485	-15.7
1223	1.717	-11.12
1224	1.17	-14.74
1225	1.756	-13.07
1226	0.843	-16.73
1227	1.773	-15.89
1228	0.641	-16.66
1229	0.386	-17.25
1230	1.437	-16.04

1231	1.792	-13.87
1232	0.748	-16
1233	0.712	-15.45
1234	1.227	-17.09
1235	1.1	-16.95
1236	0.712	-17.06
1237	1.714	-17.22
1238	0.265	-6.89
1239	0.532	-5.41
1240	0.51	-9.57
1241	0.575	-14.26
1242	0.396	-16.73
1243	0.33	-17.71
1244	1.2	-15.43
1245	0.631	-15.55
1246	0.438	-15.63
1247	0.792	-15.64
1248	0.545	-16.41
1249	0.996	-15.68
1250	1.686	-15.86
1251	0.764	-16.45
1252	1.099	-15.33
1253	0.697	-15.1
1254	0.733	-14.67
1255	0.861	-18.95
1256	0.341	-15.91
1257	0.229	-15.33
1258	0.302	-15.08
1259	0.991	-17.38
1260	0.886	-16.82
1261	1.134	-17.91
1262	0.366	-15.79
1263	0.767	-17.41
1264	0.712	-14.83
1265	0.281	-16.39
1266	0.414	-15.62
1267	0.699	-16
1268	1.129	-16.2
1269	0.65	-14.67
1270	0.506	-15.37
1271	0.682	-16.98
1272	1.378	-16.1
1273	0.74	-15.66
1274	0.458	-14.7
1275	0.764	-13.2
1276	1.743	-13.43
1277	0.702	-14.71
1278	1.711	-13.69

1279	0.563	-16.18
1280	1.694	-14.64
1281	1.075	-16.07
1282	1.651	-6.46
1283	0.534	-16.23
1284	1.649	-4.83
1285	0.975	-16.21
1286	1.65	-4.3
1287	0.271	-18.39
1288	0.732	-17.65
1289	0.8	-15.44
1290	0.723	-16.22
1291	0.728	-15.44
1292	1.138	-15.95
1293	0.875	-16.26
1294	1.411	-17.53
1295	0.319	-16.74
1296	1.037	-16.91
1297	0.96	-16.35
1298	0.328	-15.72
1299	0.693	-16.19
1300	0.645	-17.62
1301	0.218	-16.12
1302	0.444	-17.33
1303	1.669	-6.39
1304	0.69	-16.44
1305	1.638	-4
1306	0.729	-15.66
1307	1.649	-11.26
1308	0.768	-15.76
1309	1.666	-6.15
1310	0.536	-17.18
1311	1.69	-9.08
1312	0.648	-15.2
1313	1.702	-10.68
1314	0.604	-17.38
1315	0.778	-16.22
1316	0.422	-15.1
1317	1.775	-15.44
1318	1.155	-15.59
1319	1.731	-8.57
1320	1.326	-16.39
1321	1.741	-10.5
1322	1.182	-16.83
1323	1.7	-7.95
1324	0.914	-16.38
1325	1.69	-8.65
1326	0.903	-15.17

1327	1.679	-9.01
1328	0.771	-15.66
1329	1.679	-7.62
1330	1.28	-17.17
1331	1.7	-10.46
1332	0.534	-16.07
1333	1.278	-16.18
1334	0.43	-16.48
1335	1.747	-10.43
1336	0.95	-15.97
1337	1.762	-16.75
1338	0.588	-17.44
1339	1.776	-16.82
1340	0.413	-15.56
1341	1.765	-10.89
1342	0.389	-13.96
1343	1.727	-15.31
1344	0.856	-14.47
1345	1.697	-11.82
1346	0.428	-15.37
1347	1.122	-16.37
1348	0.748	-15.5
1349	1.673	-16.39
1350	0.729	-16.68
1351	1.699	-17.95
1352	0.285	-15.35
1353	1.723	-17.57
1354	0.648	-15.52
1355	0.233	-15.59
1356	0.623	-15.55
1357	0.533	-15.6
1358	0.753	-18.2
1359	0.628	-16.74
1360	0.451	-17
1361	0.634	-17.53
1362	0.627	-15.54
1363	0.756	-17.6
1364	0.321	-15.17
1365	1.049	-15.18
1366	0.325	-15
1367	0.624	-15.76
1368	0.31	-16.13
1369	0.322	-15.65
1370	0.835	-15.7
1371	0.849	-18.37
1372	0.759	-17.26
1373	0.481	-17.61
1374	1.686	-15.33

1375	0.659	-16.82
1376	1.665	-7.04
1377	0.811	-15.73
1378	1.662	-9.1
1379	0.876	-17.98
1380	1.662	-7.17
1381	0.848	-16.78
1382	1.646	-9.51
1383	0.956	-17.6
1384	1.663	-7.25
1385	1.306	-16.05
1386	1.659	-6.74
1387	1.25	-16.62
1388	1.673	-5.88
1389	0.238	-15.8
1390	1.698	-10.31
1391	0.381	-18.04
1392	1.713	-6.5
1393	0.905	-17.43
1394	1.723	-16.06
1395	0.664	-16.71
1396	1.743	-11.76
1397	0.248	-17.35
1398	1.7	-13.19
1399	0.178	-18.01
1400	1.733	-14.89
1401	1.114	-18.97
1402	0.682	-19.22
1403	0.579	-17.68
1404	1.157	-16.69
1405	1.21	-17.42
1406	0.811	-17.2
1407	1.122	-18.02
1408	0.335	-16.48
1409	1.012	-16.47
1410	2.008	-14.95
1411	2.014	-14.1
1412	0.769	-16.53
1413	1.206	-15.49
1414	0.593	-16.67
1415	0.897	-16.28
1416	1.73	-17.17
1417	1.65	-16.19
1418	1.169	-16.69
1419	0.387	-16.26
1420	1.697	-15.62
1421	0.438	-16.46
1422	1.208	-16.89

1423	1.182	-15.86
1424	1.357	-15.92
1425	0.935	-16.67
1426	0.273	-15.26
1427	0.495	-17.85
1428	0.233	-18.15
1429	0.929	-15.79
1430	0.667	-15.51
1431	1.062	-16.38
1432	0.899	-17.14
1433	0.892	-16.75
1434	0.874	-16.55
1435	0.816	-16.5
1436	0.796	-15.71
1437	1.653	-16.45
1438	2.007	-15.38
1439	2.006	-12.14
1440	2.009	-8.15
1441	2.023	-11.09
1442	0.798	-18.33
1443	0.404	-14.89
1444	1.27	-14.56
1445	1.695	-15.57
1446	1.099	-11.19
1447	1.12	-13.2
1448	1.204	-14.78
1449	1.628	-13.05
1450	1.638	-10.53
1451	1.207	-10.39
1452	2.081	-10.18
1453	1.113	-9.42
1454	1.207	-11.15
1455	1.202	-10.8
1456	0.672	-17.02
1457	0.367	-14.18
1458	1.412	-15.2
1459	0.229	-17.72
1460	0.54	-17.21
1461	1.33	-13.57
1462	1.327	-11.78
1463	1.246	-15.82
1464	0.776	-15.95
1465	0.772	-16.4
1466	1.148	-16.33
1467	1.362	-15.64
1468	1.294	-11.56
1469	1.199	-17.41
1470	1.016	-16.46

1471	0.522	-16.77
1472	0.761	-17.6
1473	1.027	-16.18
1474	1.686	-17.01
1475	1.258	-13.69
1476	1.244	-15.03
1477	2.005	-14.38
1478	2.006	-15.87
1479	0.178	-16.6
1480	0.818	-17.57
1481	2.089	-14.66
1482	2.165	-13.1
1483	1.296	-8.65
1484	2.156	-11.37
1485	1.266	-10.17
1486	1.217	-10.63
1487	1.113	-13
1488	1.431	-15.81
1489	1.298	-15.68
1490	0.759	-16
1491	1.049	-16.48
1492	0.341	-14.41
1493	2.148	-15.32
1494	1.648	-14.83
1495	0.797	-15.18
1496	1.628	-10.75
Data Record #	Fc [kHz]	PSD Peak [dB]
1497	2.003	-15.77
1498	1.633	-5.47
1499	1.271	-12.62
1500	1.288	-9.94
1501	1.693	-11.39
1502	1.687	-11.48
1503	1.552	-15.97
1504	1.683	-12.58
1505	0.711	-18.8
1506	1.672	-17.93
1507	0.682	-14.37
1508	1.257	-18.3
1509	1.279	-15.44
1510	0.33	-17.7
1511	0.418	-15.75
1512	1.286	-10.89
1513	1.277	-8.46
1514	1.298	-9.13
1515	1.702	-8.68

1516	0.88	-17.62
1517	1.678	-10.3
1518	1.674	-16.24
1519	1.193	-14.29
1520	1.284	-12.7
1521	0.854	-15.66
1522	0.814	-14.96
1523	1.384	-14.96
1524	1.335	-12.23
1525	1.087	-15.17
1526	1.339	-15.94
1527	1.216	-14.32
1528	1.314	-10.73
1529	1.678	-17.55
1530	0.674	-16.72
1531	0.899	-17.46
1532	1.253	-17.17
1533	0.271	-16.85
1534	0.224	-17.11
1535	0.208	-17.91
1536	0.561	-14.48
1537	0.144	-17.78
1538	2.003	-15.49
1539	2.007	-13.01
1540	1.084	-17.2
1541	0.98	-17.01
1542	1.406	-15.45
1543	1.698	-11.72
1544	1.201	-17.11
1545	1.677	-13
1546	0.617	-16.98
1547	1.098	-16.7
1548	0.836	-16.71
1549	1.652	-11.26
1550	1.353	-16.96
1551	1.684	-14.49
1552	1.354	-16.23
1553	0.867	-17.18
1554	0.83	-16.46
1555	1.716	-14.44
1556	1.196	-14.15
1557	1.687	-11.32
1558	0.905	-16.95
1559	1.656	-13.6
1560	0.987	-18.25
1561	1.625	-14.29
1562	2.003	-14.15
1563	1.677	-9.55

1564	2.006	-9.52
1565	1.686	-9.51
1566	2.025	-12.84
1567	1.676	-15.87
1568	1.069	-16.66
1569	1.672	-17.06
1570	1.187	-13.49
1571	1.677	-11.49
1572	1.426	-18.65
1573	1.659	-16.73
1574	0.476	-16.67
1575	0.905	-15.51
1576	0.308	-16.5
1577	1.648	-16.18
1578	0.365	-17.16
1579	1.665	-13.67
1580	0.826	-15.76
1581	0.723	-16.9
1582	1.374	-16.89
1583	0.431	-17.92
1584	0.811	-15.44
1585	1.724	-14.55
1586	0.436	-18.4
1587	0.898	-16.87
1588	0.768	-16.02
1589	1.049	-17.37
1590	0.921	-17.35
1591	0.348	-17.55
1592	0.544	-15.93
1593	0.586	-16.2
1594	1.306	-16.91
1595	0.651	-17.91
1596	0.304	-14.94
1597	0.746	-17.74
1598	0.83	-16.92
1599	2.008	-13.29
1600	2.011	-13.93
1601	2.019	-13.63
1602	1.248	-17.12
1603	0.485	-16.14
1604	0.808	-15.83
1605	0.721	-16.24
1606	0.988	-16.62
1607	0.651	-17.23
1608	0.773	-15.78
1609	1.638	-9.4
1610	2.012	-12.92
1611	2.015	-10.55

1612	2.016	-6.29
1613	1.633	-15.1
1614	0.437	-15.94
1615	1.682	-10.86
1616	0.24	-17.59
1617	1.674	-10.68
1618	0.88	-15.82
1619	1.229	-15.03
1620	0.767	-15.36
1621	1.699	-14.17
1622	1.165	-17.73
1623	1.721	-11.17
1624	1.188	-16.38
1625	1.36	-16.37
1626	0.786	-15.59
1627	1.69	-13.16
1628	0.778	-15.19
1629	1.258	-10.42
1630	0.902	-18.56
1631	1.263	-13.65
1632	1.249	-15.51
1633	1.243	-14.71
1634	1.257	-15.48
1635	1.243	-15.74
1636	2.137	-12.17
1637	1.16	-15.75
1638	2.129	-11.79
1639	1.154	-12.62
1640	1.246	-14.74
1641	2.125	-13.34
1642	2.121	-13.28
1643	2.128	-13.22
1644	1.249	-11.41
1645	1.241	-11.61
1646	1.242	-12.8
1647	1.228	-13.74
1648	1.229	-12.46
1649	1.199	-13.32
1650	2.077	-9.97
1651	2.078	-10.71
1652	1.203	-16.89
1653	0.435	-15.2
1654	0.962	-15.95
1655	0.917	-14.08
1656	0.43	-17.27
1657	1.049	-15.68
1658	1.119	-16.53
1659	1.238	-13.06

1660	1.229	-12.43
1661	1.203	-14.08
1662	1.214	-14.41
1663	1.207	-12
1664	1.209	-10.8
1665	1.222	-11.18
1666	1.082	-10.85
1667	2.096	-10.06
1668	2.029	-13.35
1669	2.108	-13.98
1670	1.12	-17.23
1671	2.092	-13.58
1672	0.34	-17.84
1673	1.084	-17.4
1674	1.206	-15.26
1675	0.991	-18
1676	2.072	-16.16
1677	1.105	-15.31
1678	2.088	-12.12
1679	1.189	-11.99
1680	1.208	-11.86
1681	1.212	-10.28
1682	1.226	-10.23
1683	2.099	-14.63
1684	1.238	-10.87
1685	1.234	-13.79
1686	1.273	-15.17
1687	1.281	-15.5
1688	1.027	-14.21
1689	1.289	-13.88
1690	1.285	-10.22
1691	1.263	-14.53
1692	1.254	-15.13
1693	2.109	-15.19
1694	1.22	-14.63
1695	1.212	-14.45
1696	2.087	-15.31
1697	2.094	-13.55
1698	1.091	-15.88
1699	1.223	-9.87
1700	2.088	-11.08
1701	1.211	-12.37
1702	1.223	-13.35
1703	1.236	-12.48
1704	2.098	-12.41
1705	1.225	-15
1706	1.629	-7.26
1707	1.046	-14.84

1708	1.687	-10.13
1709	0.742	-15.66
1710	1.711	-11.3
1711	0.607	-18.25
1712	1.69	-11.6
1713	1.393	-18.93
1714	1.727	-12.77
1715	1.298	-18.17
1716	0.342	-17.17
1717	0.964	-18.51
1718	1.693	-13.4
1719	0.873	-18.85
1720	0.389	-15.58
1721	1.105	-16.72
1722	0.623	-18.97
1723	0.62	-16.53
1724	1.104	-17.11
1725	1.51	-19.46
1726	1.073	-18.83
1727	0.946	-17.26
1728	0.851	-15.41
1729	0.414	-16.83
1730	1.164	-15.28
1731	0.493	-16.07
1732	1.056	-17.66
1733	0.923	-15.98
1734	0.674	-17.01
1735	1.241	-15.85
1736	0.595	-17.02
1737	1.363	-17.6
1738	1.048	-17.74
1739	1.141	-16.74
1740	0.542	-15.68
1741	0.225	-16.07
1742	0.562	-15.65
1743	0.7	-16.2
1744	0.989	-16.39
1745	0.558	-16.13
1746	1.213	-15.87
1747	0.906	-16.24
1748	0.232	-16.78
1749	1.355	-14.75
1750	0.276	-15.2
1751	0.578	-15.95
1752	1.115	-16.11
1753	0.809	-17.35
1754	1.355	-15.82
1755	0.274	-16.2

1756	1.118	-17.08
1757	1.209	-16.83
1758	1.101	-16.32
1759	0.45	-17.06
1760	0.68	-16.34
1761	0.405	-16.19
1762	1.401	-16.56
1763	1.137	-16.28
1764	0.824	-14.97
1765	1.248	-15.95
1766	1.775	-16.36
1767	0.672	-15.93
1768	1.016	-15.89
1769	0.261	-16.7
1770	1.211	-16.58
1771	1.144	-16.62
1772	0.512	-17.45
1773	1.512	-16.15
1774	0.966	-16.43
1775	1.025	-15.67
1776	0.394	-16.02
1777	0.314	-17.14
1778	0.736	-15.74
1779	0.912	-16.47
1780	0.276	-16.09
1781	0.912	-15.92
1782	0.879	-16.55
1783	0.647	-16.4
1784	1.548	-17.23
1785	0.782	-16.4
1786	1.092	-15.26
1787	1.049	-14.21
1788	1.418	-16.57
1789	0.427	-17.61
1790	1.364	-16.19
1791	1.365	-16.19
1792	0.883	-14.89
1793	0.742	-16.78
1794	0.478	-16.3
1795	0.346	-15.52
1796	0.52	-16.48
1797	1.923	-16.36
1798	1.368	-14.24
1799	0.544	-16.17
1800	1.369	-15.97
1801	1.931	-15.58
1802	0.564	-16.66
1803	1.181	-17.17

1804	1.372	-17.52
1805	1.002	-11.22
1806	0.954	-14.72
1807	0.472	-15.74
1808	0.995	-14.05
1809	0.992	-11.72
1810	0.656	-15.82
1811	0.986	-13.72
1812	0.493	-16.74
1813	0.799	-16.78
1814	0.394	-16.66
1815	1.204	-16.92
1816	0.989	-17.16

THIS PAGE INTENTIONALLY LEFT BLANK

LIST OF REFERENCES

- Liotta, P. H. (2002). Chaos as strategy. *Parameters: Journal of the US Army War College*, 32, 47-56.
- Global war on terrorism casualty by reason*. Retrieved 6/27/2007, from
http://siadapp.dmdc.osd.mil/personnel/CASUALTY/gwot_reason.pdf.
- Improvised explosive devices (IEDs) / booby traps*. Retrieved 6/28/2007, from
<http://www.globalsecurity.org/military/intro/ied.htm>.
- Improvised explosive devices (IEDs) in Iraq: Effects and countermeasures*. Retrieved 6/28/2007, from
<http://www.history.navy.mil/library/online/ied.htm>.
- President requests boost for IED fund - the Boston Globe*. Retrieved 8/15/2007, from
http://www.boston.com/news/nation/washington/articles/2007/02/06/president_requests_boost_for_ied_fund/.
- RADAR BASICS*. Retrieved 7/08/2007, from
http://www.alphalpha.org/radar/intro_e.html#L'Equazione Radar.
- Stutzman, W. L., & Thiele, G. A. (1998). *Antenna theory and design* (2nd ed.). New York: J. Wiley.
- Antenna training and measuring system model 8092*. Retrieved 7/08/2007, from
<http://www.itp101.com/files/dsa8092.pdf>.
- Camp Roberts*. Retrieved 8/15/2007, from
<http://www.globalsecurity.org/military/facility/camp-roberts.htm>.
- GlobalSecurity.org - reliable military news and military information*. Retrieved 8/15/2007, from
<http://www.globalsecurity.org/military/facility/mcmillan.htm>.

Center for inter-disciplinary remotely piloted aircraft studies. Retrieved 8/15/2007, from
<http://www.cirpas.org/Facilities/McMillan>.

Instrumented UAV systems for earth science - Tern/Vehicle.
Retrieved 8/15/2007, from
<http://www.aeroconcepts.com/Tern/VehiclePage.html>.

AMS glossary. Retrieved 8/25/2007, from
<http://amsglossary.allenpress.com/glossary/browse?s=c&p=62>.

Skolnik, M. I. (2001). *Introduction to radar systems* (3rd ed.). Boston: McGraw Hill.

FCC: Wireless services: Family radio service: Family Home.
Retrieved 9/05/2007, from
http://wireless.fcc.gov/services/index.htm?job=service_home&id=family.

FCC: Wireless services: Family radio service: Band plan.
Retrieved 9/05/2007, from
http://wireless.fcc.gov/services/index.htm?job=service_bandplan&id=family.

Local oscillator: Definition and much more from answers.com.
Retrieved 9/05/2007, from
<http://www.answers.com/topic/local-oscillator-1?cat=technology>.

Scan eagle unmanned aerial system. Retrieved 9/05/2007, from
<http://www.defense-update.com/products/s/scaneagle.htm>.

INITIAL DISTRIBUTION LIST

1. Defense Technical Information Center
Ft. Belvoir, VA
2. Dudley Knox Library
Naval Postgraduate School
Monterey, CA
3. Marine Corps Representative
Naval Postgraduate School
Monterey, CA
4. Director, Training and Education, MCCDC, Code C46
Quantico, VA
5. Director, Marine Corps Research Center, MCCDC, Code C40RC
Quantico, VA
6. Marine Corps Tactical Systems Support Activity (Attn:
Operations Officer)
Camp Pendleton, CA
7. Lonnie Wilson (2 copies)
Naval Postgraduate School
Monterey, CA
8. David Netzer
Naval Postgraduate School
Monterey, CA
9. Dan Boger
Naval Postgraduate School
Monterey, CA
10. Chyau Shen
NAVAIR
Patuxent River, MD
11. Paul Morgan
USSOCOM
Tampa, FL

12. Erik Syvrud
USSOCOM
Tampa, FL
13. LCDR David Culpepper, USN
USSOCOM
Tampa, FL
14. CAPT David Balk, USN
NECC
Norfolk, VA
15. Ben Riley
OSD
Washington, D.C.
16. Peter Verga
OSD
Washington, D.C.
17. Ike Owens
NECC
San Diego, CA
18. CAPT Gregory Kniff, USN
NSWC
San Diego, CA
19. Ray Elliott
Naval Postgraduate School
Monterey, CA
20. Jim Horning
Naval Postgraduate School
Monterey, CA